UNIVERSITÀ
DEGLI STUDI
DI PADOVA

DIPARTIMENTO
DI INGEGNERIA
DELL'INFORMAZIONE

A Model of Beta-Cell Response to GLP-1 to Quantify Incretin Effect in Healthy and Prediabetic Subjects

Ph.D. Candidate
Ing. Francesco Micheletto

Advisor
Ing. Chiara Dalla Man

School director
Prof. Matteo Bertocco

Coordinator
Prof. Giovanni Sparacino

Department of Information Engineering
Ph.D. School in Information Engineering
XXV Serires

2013

A Model of Beta-Cell Response to GLP-1 to Quantify Incretin Effect in Healthy and Prediabetic Subjects

School director: *Ch.mo Prof. Matteo Bertocco*

Coordinator: *Prof. Giovanni Sparacino*

Advisor: *Ing. Chiara Dalla Man*

Ph.D. Candidate: *Ing. Francesco Micheletto*

2013

CONTENTS

ABSTRACT

English

Glucose regulation, in healthy subjects, relies on a complex control system that keeps blood glucose level within a narrow range around its basal value. Impairment of the glucose regulatory system is the cause of several metabolic derangements, including diabetes, which is characterized by chronic hyperglycemia which leads to severe micro and macro-vascular complications. Diabetes is generally classified into two categories, type 1 and type 2 diabetes. Both arise from complex interactions between genes and the environment, and are characterized by an absolute deficiency of insulin production (type 1) or a relative deficiency of the pancreas to produce insulin in amounts sufficient to meet the body needs (type 2). The prevalence of diabetes is increasing dramatically in populations of the world, and its global incidence has been increasing steadily in the past several years. Traditional medications for type 2 diabetes, including insulin, sulfonylureas, glitinides, acarbose, metformin, and thiazolidinediones, lower blood glucose through diverse mechanisms of action. However, many of the oral hypoglycemic agents lose their efficacy over time, resulting in progressive deterioration in β-cell function and loss of glycemic control due to progressive loss of β-cell mass. Consequently, there is an increasing interest in developing therapeutic agents that preserve or restore functional β-cells mass such as the incretin hormone Glucagon-Like Peptide-1 (GLP-1). It not only acutely lowers blood glucose by promoting insulin secretion and inhibiting glucagon release, but

also engages signaling pathways in the islet β-cells that leads to stimulation of β-cells proliferation and neo-genesis and inhibition of β-cell apoptosis.

Impairment of insulin secretion and glucagon suppression suggests that decreased β-cells responsiveness to GLP-1 is part of the pathogenesis of type 2 diabetes. Thus the ability to measure the effect of GLP-1 on insulin secretion can be useful to understand the pathogenesis of type 2 diabetes. Moreover it can be employed to optimized GLP-1 based therapy by determining those individuals who may benefit more from such therapy. However, a mechanistic model enabling direct quantitation of pancreatic response to GLP-1 has never been developed.

In this contribution a mathematical model which describes the mechanism of GLP-1 action on insulin secretion is proposed. It provides a direct measure of the β-cells responsivity indexes to glucose and GLP-1. Three databases were used to develop, test and validate the model.

Data of 88 healthy individuals, who underwent a hyperglycemic clamp with a concomitant GLP-1 intravenous infusion, were used for model formulation. A set of models of increasing complexity describing GLP-1 action on insulin secretion were tested. All models share the common assumption that insulin secretion is made up of two components, one proportional to glucose rate of change through dynamic responsivity, Φ_d, and one proportional to glucose through static responsivity, Φ_s, but differ in the modality of GLP-1 control on β-cells. For each model potentiation index Π was derived representing the percent increase in secretion due to 1 pmol/l of circulating GLP-1. All the models fit the data well, as confirmed by the run test, which supported randomness of residuals in 70% of the subjects and provide precise estimate of model parameters. Model selection was tackled using standard criteria (e.g. ability to describe the data, precision of parameter estimates, model parsimony, residual independence). The most parsimonious model in most subjects assumes that above-basal insulin secretion depends linearly on GLP-1 concentration and its rate of change.

However, the hyperglycemic clamp with concomitant intravenous infusion of GLP-1, is not physiological and easy to perfume in large scale studies. Thus data of 22 impairing fasting glucose (IFG) subjects, studied twice with a mixed meal,

were used to test the model performance in a more physiological condition. We found that during an oral test, a simpler model is sufficient to describe the data. Validation of the model was performed using both simulations and real data of 10 healthy subjects studied with an OGTT and matched intravenous glucose challenge (I-IVG). The protocol allows to calculate a model-independent index (PI) from the comparison of insulin secretion rate estimated in these two occasions. The comparison between model-derived Π and incretin potentiation index PI shows that they are very similar ($\Pi = 6.55$, CV = 65%; PI = 6.15 % per pmol/l). In addition in silico validation proved the ability of the model to single out the effect of GLP-1 on insulin secretion since it correctly estimated Π in the $93 \pm 1\%$ of the simulations.

Italiano

La regolazione della glicemia in soggetti sani, si basa su un complesso sistema di controllo che permette di mantenere il livello di glucosio nel sangue all'interno di un range ristretto che oscilla attorno al suo valore basale. Il mal funzionamento di tale sistema è la causa di patologie metaboliche, ad esempio il diabete. Questa patologia è caratterizzata da iperglicemia cronica che, se non curata, a lungo termine comporta gravi complicanze micro e marco vascolari. Il diabete è comunemente classificato in tipo 1 e tipo 2. Entrambi derivano da complesse interazioni tra ambiente e geni, e sono caratterizzati da una totale mancanza di produzione di insulina, nel tipo 1, o da una carenza da parte del pancreas nel produrre insulina in quantità sufficiente per soddisfare le necessità dell'organismo, nel tipo 2. La prevalenza del diabete è in costante aumento in tutto il mondo, così come la sua incidenza è in costante crescita negli ultimi anni. I farmaci tradizionali per la terapia del diabete di tipo 2, come l'insulina, sulfaniluree, metformina e tiazolidinedioni, riducono la glicemia attraverso diversi meccanismi di azione. Tuttavia, molti degli agenti ipoglicemizzanti assunti per via

orale, perdono di efficacia con il tempo causando un progressivo deterioramento della funzionalità e riduzione della massa delle β-cellule con conseguente riduzione del controllo glicemico. Di conseguenza vi è un crescente interesse nello sviluppo di nuovi agenti terapeutici che preservino la massa e ripristino la funzionalità delle β-cellule. Uno di questi è l'ormone Glucagon-Like Peptide-1 (GLP-1), che non solo riduce la glicemia aumentando la secrezione di insulina, ma agisce anche nel signaling nelle isole di Langherans stimolando la proliferazione e la neo-genesi delle β-cellule e inibendone l'apoptosi. La ridotta secrezione di insulina e la mancata soppressione del glucagone inducono ad ipotizzare che la diminuita risposata delle β-cellule al GLP-1 possa essere parte della patogenesi del diabete di tipo 2. Pertanto la capacità di misurare l'effetto del GLP-1 sulla secrezione dell'insulina è utile per studiare la patogenesi della malattia ed ottimizzare valutare l'efficacia delle terapie basate sul GLP-1. Infatti è cruciale determinare quali soggetti possono beneficiare maggiormente di tale terapia per ottimizzare le risorse. Tuttavia, non è ancora disponibile un modello che descriva l'azione del GLP-1 sulla secrezione di insulina e permetta di quantificarne l'entità.

In questo lavoro viene proposto un modello matematico che descrive i meccanismi di azione del GLP-1 sulla secrezione di insulina, fornendo una misura diretta dell'aumento della secrezione dell'insulina dovuto all'effetto del GLP-1. Sono stati utilizzati tre database per sviluppare, testare e validare i modelli proposti.

I dati di 88 soggetti sani sottoposti ad un clamp iperglicemico con contemporanea infusione intravenosa di GLP-1, sono stati utilizzati per lo sviluppo del modello. Sono stati testati una serie di modelli dell'azione del GLP-1 sulla secrezione di insulina di complessità crescente. Tutti i modelli si basano sulla comune assunzione che la secrezione di insulina è costituita da due componenti, una proporzionale alla concentrazione ed una alla velocità di variazione del glucosio plasmatico, modulate rispettivamente dalla responsività statica Φ_s e dalla responsività dinamica Φ_d. Ogni modello differisce dagli altri nella descrizione della modalità di azione del GLP-1. Per ciascun modello è stato derivato un indice di potenziamento, Π, che rappresenta l'aumento percentuale della secrezione di

insulina dovuta ad 1 pmol/l di GLP-1. I modelli predicono bene i dati (infatti il run test conferma la casualità dei residui nel 70% dei soggetti) e forniscono stime precise dei parametri . La selezione del modello ottimo è stata affrontata confrontando le prestazioni dei modelli sulla base di criteri standard (capacità di descrivere i dati, la precisione della stima dei parametri, la parsimonia, la casualità dei residui).

Il modello più parsimonioso ipotizza che la secrezione sopra basale di insulina dipenda linearmente sia dalla concentrazione di GLP-1 sia dalla sua variazione.

Tuttavia le condizioni sperimentali di tale protocollo non sono fisiologiche e applicabili su larga scala. Pertanto, i dati di 22 soggetti IFG (Impaired Fasting Glucose), studiati due volte con un pasto misto, sono stati utilizzati per testare il modello in una condizione sperimentale più vicina alla fisiologia. I risultati dimostrano che per descrivere i dati di un test orale, è sufficiente un modello più semplice.

La validazione del modello è stata effettuata sia in simulazione sia utilizzando i dati reali di 10 soggetti, studiati due volte: una prima volta utilizzando un test orale di tolleranza al glucosio (OGTT) e successivamente un test intravenoso di tolleranza al glucosio durante il quale il glucosio è stato infuso in modo tale da riprodurre la glicemia osservata durante l'OGTT. Questo protocollo permette di calcolare un indice di potenziamento (PI) modello-indipendente dal confronto tra la secrezione di insulina stimata nelle due occasioni. Il confronto tra il potenziamento stimato con il modello, Π, e l'indice di potenziamento PI mostra che i due indici sono molto simili (Π = 6.55, CV = 65%; PI = 6.15 % per pmol/l). Inoltre nel 93 $\pm$ 1% delle simulazioni effettuate il modello è in grado di quantificare correttamente l'effetto del GLP-1 sulla secrezione di insulina.

CHAPTER 1

INTRODUCTION

1.1 BACKGROUND

Glucose metabolism relies on complex internal feedback systems that keep blood glucose level within a narrow range around its basal value. The target blood glucose range is usually considered to be 70 to 180 mg/dl. Hypoglycemia is identified when plasma glucose concentration goes below 70 mg/dl, conversely hyperglycemia when glucose concentration raises over 180 mg/dl [92]. It is crucial that plasma glucose level does not decrease under 70 mg/dl since glucose is the predominant metabolic fuel for the brain which cannot store more than a few minutes supply as glycogen, or quickly increase its extraction of glucose from the circulation, the prevention of hypoglycemia is critical to survival. On the other hand the chronic hyperglycemia leads to micro-vascular and macro-vascular complications which include limb loss, blindness, ischemic heart disease, and end-stage renal disease [92], [93], [94].

Comprehension of the mechanisms that regulate plasma glucose have greatly evolved since the discovery in the 1920s of the peptide hormone insulin, which

was considered the principal, if not the only, actor of glucose homeostasis. Insulin is secreted by β-cells in response to high levels of plasma glucose and promotes glucose utilization by tissues and inhibit endogenous glucose production by the liver and kidney. In the 1950s pancreatic α-cells hormone glucagon was discovered leading to a bi-hormonal view of glucose regulation, where insulin was the key regulatory hormone of glucose disappearance, and glucagon the major regulator of glucose appearance; since it is secreted in response to a fall in plasma glucose concentration below the hypoglycemic threshold, and acts by stimulating hepatic glycogenolysis and gluconeogenesis, thus raising EGP which, results in an increase of plasma glucose concentration. Subsequently, the discovery of amylin, a secondary β-cell hormone, which has a complementary role to insulin delaying gastric emptying and thus slowing down postprandial glucose rate of appearance, leads to a view of glucose homeostasis involving multiple pancreatic hormones [57].

The intricacies of glucose homeostasis become clear when considering the role of gut hormones, identified in the 1960s, which are responsible for the, so called, incretin effect, i.e. ingested glucose potentiates insulin secretion compared to glucose infused intravenously. Several incretin hormones have been recognized, and a key role in glucose regulation is played by Glucagon-Like Peptide-1(GLP-1). GLP-1 is a 30–amino acid gut hormone produced by the enteroendocrine L-cells distributed in the region of terminal ileum and colon and is released into the portal circulation in response to meal ingestion [2]. It arises from the post-translational processing of proglucagon by prohormone-convertase- 1 (PC-1) in the enteroendocrine L-cells of the intestinal mucosa [40]. GLP-1 enhances insulin secretion and inhibits glucagon release in a glucose-dependent manner [40]. Active isoforms of GLP-1 include GLP-1(7-36) amide and GLP-1(7-37); after secretion GLP-1(7-36) amide is rapidly degraded by the enzyme dipeptidyl peptidase-4 (DPP-4) to its N-terminally truncated metabolite GLP-1(9-36), which does not interact with the known GLP-1 receptor (GLP1R) [2], [21], [24].

Impairment of the glucose regulatory system is the cause of several metabolic derangements, including diabetes, which is characterized by chronic

hyperglycemia. Diabetes is broadly classified into two categories, type 1 diabetes and type 2 diabetes. Both arise from complex interactions between genes and the environment, however their pathogenesis is distinct.

Type 1 diabetes is the result of immune-mediated destruction of the pancreatic β-cells in the islets of Langerhans, i.e. the site of insulin secretion and production. In general, the disease occurs in childhood and adolescence (although it can occur at all ages) and is characterized by absolute insulin deficiency. Consequently, affected individuals require, usually, insulin therapy to control hyperglycemia and sustain life. As a rule, obesity does not play a part in the pathogenesis of type 1 diabetes, although obesity in type 1 diabetes is associated with the development of cardiovascular complications.

Type 2 diabetes occurs because insulin secretion is inadequate and cannot overcome the prevailing defects in insulin action, resulting in hyperglycemia. Excess caloric intake, inactivity, and obesity all play parts in the pathogenesis of type 2 diabetes. In general, it is a disease that occurs with increasing frequency with increasing age and is uncommon before age 40 (although there are important exceptions). In addition, people with type 2 diabetes are more likely to have associated adverse cardiovascular risk factors such as dyslipidemia and hypertension. Prediabetes, i.e., impaired fasting glucose (IFG) and impaired glucose tolerance (IGT), is an intermediate condition in the transition between normality and diabetes. People with IGT or IFG are at high risk of progressing to type 2 diabetes, although this is not inevitable. Both type 2 diabetes and prediabetes are recognized risk factors for overt cardiovascular disease and related metabolic complications and are major components of health care spending [81]. Rapid urbanization and societal affluence of global migrating populations has been suggested as major risk factors for the observed exploding prevalence of prediabetes and type 2 diabetes with consequent rising trends in cardiovascular risks [95]. IFG is a rapidly emerging form of prediabetes with a 20%−30% risk of progression to diabetes over 5−10 years.
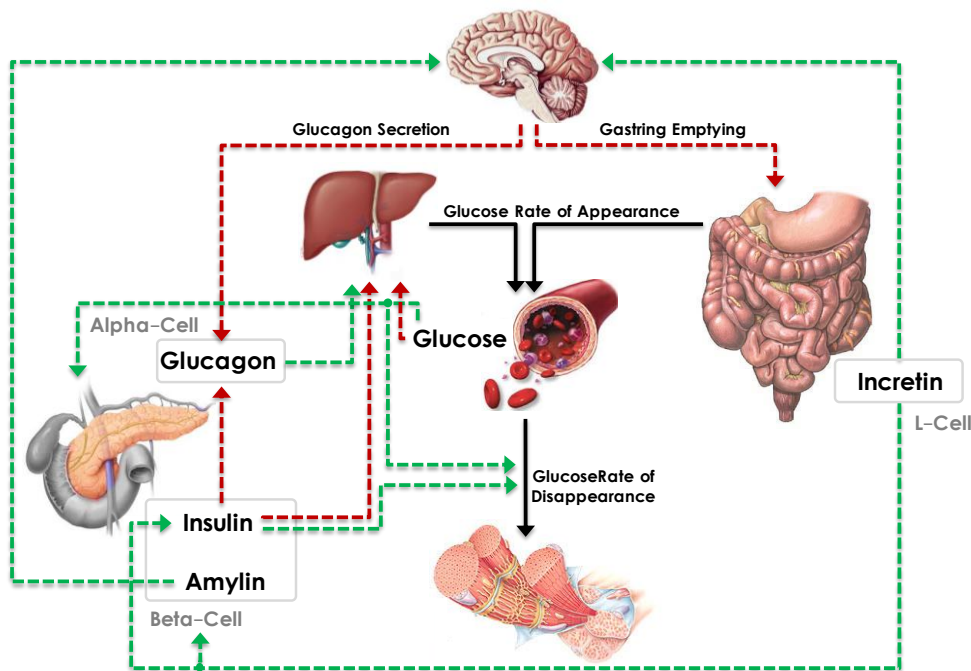
Figure 1. 1 – Glucose homeostasis in healthy individuals: roles of the major hormones. Black lines represent fluxes, red dotted lines represent inhibition control signals and green dotted lines represent promotion control signals

This risk is even greater if individuals have both IFG and IGT. Furthermore, both IFG and IGT are linked to increased risk for cardiovascular events [81] in the Caucasian population. Ninety percent of the world population with diabetes is type 2 with type 1 diabetes comprising between 5%–10%. It is plausible that the relative frequency of type 1 and type 2 diabetes will change with rising trends in the prevalence of type 2 diabetes, obesity, and prediabetes in the developing world. Over time, diabetes leads to complications, in particular: diabetic retinopathy, which leads to blindness; diabetic neuropathy, which increases of the risk of foot ulceration and limb loss; and diabetic nephropathy leading to kidney failure. In addition, there is an increased risk of heart disease and stroke with 50% of people with diabetes dying of cardiovascular disease and stroke. Finally, the overall risk of dying among people with diabetes is at least double the risk of their peers without diabetes.
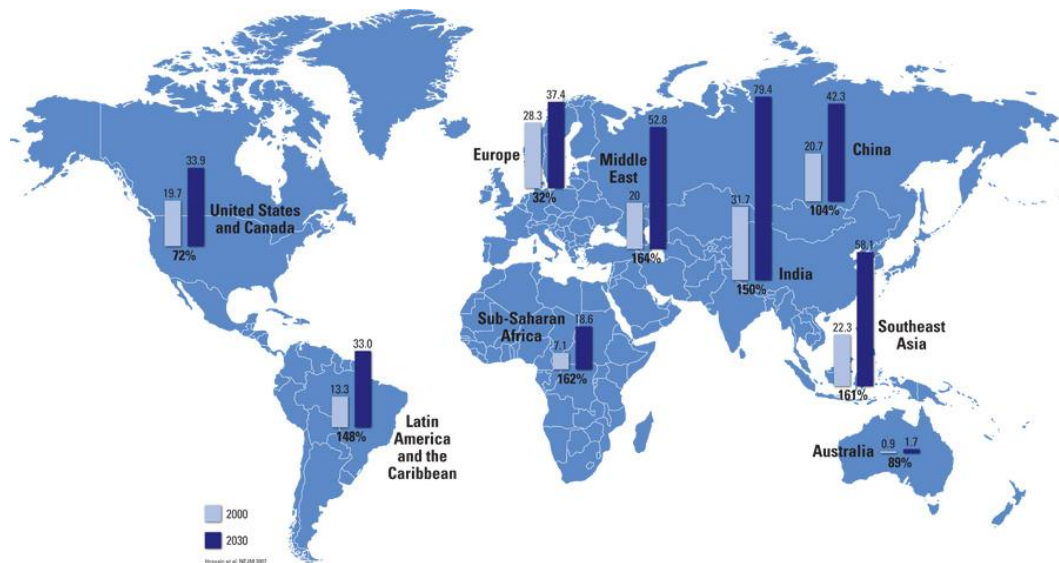
Figure 1. 2 – World diabetes forecast [94]

The World Health Organization (WHO) estimates than more than 180 million people worldwide had diabetes in 2000. This number is likely to more than double by 2030. In 2005, an estimated 1.1 million people died from diabetes. In Italy people with diabetes were estimated to be, 3 million (4.9% of the population) in 2011. When ranked by cause-specific mortality, diabetes is the fifth cause of death, after communicable diseases, cardiovascular diseases, cancer and injury [95]. Almost 80% of diabetes death occurs in low- and middle-income countries. WHO projects that diabetes deaths will increase by more than 50% in the next ten years without urgent action. Most notably, diabetes is projected to increase by over 80% in upper-middle income countries between 2006 and 2015. Diabetes and its complications impose significant economic consequences on individuals, families, health systems, and countries. WHO estimates that over the next ten years (2005–2015) China will lose $558 billion in national income due to heart disease, stroke, and diabetes alone.

Traditional medications for type 2 diabetes, including insulin, sulfonylureas, glitinides, acarbose, metformin, and thiazolidinediones, lower blood glucose through diverse mechanisms of action. Study such as the United Kingdom Prospective Diabetes Study (UKPDS) clearly illustrate that better glycemic

control achieved with some of these drugs can significantly reduce the development of diabetes associated secondary complications [85]. However, many of the oral hypoglycemic agents lose their efficacy over time, resulting in progressive deterioration in β-cell function and loss of glycemic control. The reason why current anti-diabetic agents become less effective over time are not well understood, but they appear to include progressive loss of β-cell mass. Autopsy studies demonstrate that β-cell mass is decreased in type 2 diabetes despite a normal capacity for β-cell replication and neo-genesis. β-cell mass is governed by a combination of factors: replication of existing β-cell, differentiation of new β-cell from ductal and extra-islet precursor cells (neo-genesis), and β-cell apoptosis. Reduced β-cell mass has been observed in both obese and lean type 2 diabetic humans [46]. Commonly observed in both human and rodent studies of type 2 diabetes is an increase in β-cell apoptosis; the mechanisms responsible include chronic hyperglycemia, dyslipidemia, endoplasmic reticulum and oxidative stress, islet amyloid deposition, and actions of inflammatory cytokines. Medications currently used to treat type 2 diabetes cannot prevent β-cell death or re-establish β-cell mass. Moreover, short term studies demonstrate that sulfonylureas can induce apoptosis in rodent β-cell or cultured human islet. Thus, sulfonylureas therapy could theoretically exacerbate β-cell loss in subjects with type 2 diabetes [23]. Consequently, there has been intense interest in the development of therapeutic agents that preserve or restore functional β-cell mass such as GLP-1.

GLP-1 based therapy for type 2 diabetes has required the development of GLP1R agonists that resist the action of DPP-4 [62] or compounds that inhibit DPP-4, thereby raising endogenous concentrations of GLP-1[19]. GLP1R is the principal site of action of GLP-1 and GLP1R agonists, however the gene coding for this receptor is highly polymorphic and contains numerous non-synonymous SNPs which could potentially alter response to endogenous GLP-1 and GLP1R agonists, thereby contribute to defects in incretin-induced insulin secretion may be associated with type 2 diabetes. Furthermore, since GLP-1 analogues that act as receptor agonists are being used to treat type 2 diabetes, such genetic variation

may alter response to such therapy. It has previously been suggested that genetic differences may explain some of the variation to GLP-1 response in prior studies [74]. Moreover administration of GLP-1 in pharmacological doses improve both insulin secretion and suppression of glucagon secretion [21], [70]. Because of these, numerous investigators have hypothesized that decreased GLP-1 secretion is part of the pathogenesis of type 2 diabetes. However, more recent evidence suggests that postprandial GLP-1 concentrations are not decreased across the spectrum of prediabetes and early type 2 diabetes i.e. glucose intolerance cannot be explained by decreased GLP-1 secretion [76]. Taken together these data suggest that decreased β-cell responsiveness to GLP-1 is part of the pathogenesis of type 2 diabetes [31]. Whether this is part of a global decrease in response to various secretagogues or an early specific defect remains uncertain. More recently it has been suggested that states associated with insulin resistance result in decreased incretin receptor expression on β-cells [54].

Several studies are available on GLP-1 action on insulin secretion [1], [2], [19], [26], [39], [56], however none of them has ever aimed to mechanistically model GLP-1 action on beta-cell. For instance, other investigators have previously utilized a hyperglycemic clamp to measure insulin secretion from deconvoluted C-peptide data. However such methodology does not take into account potential changes in glucose concentration during the hyperglycemic clamp or the changing GLP-1 concentrations prevailing during the experiment. The only model which indirectly accounts for a potentiation due to incretin is the one proposed by Mari and colleagues [55]. It introduced a potentiating factor, which modulates the dose-response relation between insulin secretion and plasma glucose, in order to better fit C-peptide data, but it did not explicitly describe incretin effect. Other studies, e.g. [1], also found a correlation between GLP-1 and the potentiating factor, or use the model to assess different hormone responses in morning vs afternoon [47]. However, in none of the above studies there was an attempt to mechanistically describe GLP-1 action on insulin secretion.

1.2 AIM

A methodology to accurately ascertain the contribution of GLP-1 to insulin secretion is a valuable tool to understand the pathogenesis of type 2 diabetes and to assess the efficacy of GLP-1 based therapy.

The aim of this contribution is to propose a whole-body mathematical model which describes the mechanism of GLP-1 action on insulin secretion, and thus allows a simultaneous estimate of both β-cells responsivity indexes to glucose together with the magnitude of GLP-1 mediated increase in insulin secretion.

1.3 OUTLINE OF THE THESIS

The thesis is articulated as follows. Chapter 2 presents history of the incretin effect, the discovery of the GLP-1, its metabolism and physiological actions. Chapter 3 describes the experimental protocol used to develop, test and validate the models. The models are presented in Chapter 4 and in Chapter 5; in Chapter 6 the numerical identification of the models is presented and their ability to describe the data and to measure the enhancement of insulin secretion due to plasma GLP-1 levels are compared. Model validation is tackled in Chapter 7 using both real and simulated data. Chapter 8 reports an example of application of the proposed models to assess the effect of DPP-4 inhibition on incretin secretion. The results obtained in this study as well as emerged open questions and future direction of research are discussed in Chapter 9.

CHAPTER 2

GLUCAGON-LIKE PEPTIDE-1

2.1 INTRODUCTION: THE INCRETIN CONCEPT

The firsts investigators of the incretin concept were Bayliss and Starling in 1902 who speculated that signals arising from the gut after ingestion of nutrients might elicit pancreatic endocrine response and affect the disposal of carbohydrates [5]. Subsequently in 1906 Moore et al. postulated that the duodenum produced a chemical excitant for pancreatic secretion and tried to treat diabetes by injecting gut extracts. Zunz and Labarre pursued this factor and prepared an intestinal extract free of secretin activity that was able to produce hypoglycemia in dogs. Thus Labarre first introduced the term incretin to describe the humoral activity of the gut that might enhance the endocrine secretion of the pancreas. interest in the incretin hormones was rekindled in the 1960s when a reliable RIA for insulin was developed by Yalow and Berson, which allowed the measurements of the circulating levels of this hormone renewing interest in the search for incretins due to demonstration of the incretin effect by means of this assay [14]. Immunoassay and bioassay demonstrated that the action of glucose on the pancreas could not

account completely for the insulin response observed in the blood. These reports demonstrated that intravenous glucose administration caused a lower plasma insulin response than when given by intrajejunal infusion, even though lower blood glucose levels were achieved by the later. Perley and Kipnis estimated the alimentary component to be close to 50% by subtracting from the insulin secretory response seen after oral glucose that insulin response obtained with the infusion of intravenous glucose, which duplicated the oral blood glucose profile [14].

In 1969, Unger and Eisentraut named the connection between the gut and the pancreatic islets the enteroinsular axis. Creutzfeldt suggested that this axis encompasses nutrient, neural, and hormonal signals from the gut to the islet cells secreting insulin, glucagon, somatostatin, or pancreatic polypeptide. Moreover, Creutzfeldt defined the criteria for fulfilment of the hormonal or incretin part of the enteroinsular axis as: it must be released by nutrients, particularly carbohydrates and at physiological levels, it must stimulate insulin secretion in the presence of elevated blood glucose levels [14].

2.2 GLP-1 DISCOVERY

Eating provokes the secretion of multiple gastrointestinal hormones involved in the regulation of gut motility, secretion of gastric acid and pancreatic enzymes, gall bladder contraction, and nutrient absorption. Furthermore gut hormones allows the disposal of absorbed glucose through the stimulation of insulin secretion from the endocrine pancreas. The observation that enteral nutrition provided a more potent insulinotropic stimulus compared with isoglycemic intravenous challenge led to the development of the incretin concept.1 The first incretin to be identified, glucose-dependent insulinotropic polypeptide (GIP), was purified from porcine intestinal extracts and had weak

effects on gastric acid secretion but more potent insulinotropic actions in human beings.

Still GIP does not explain the whole incretin effect on the insulin secretion. In the 1970s, with the advent of recombinant DNA technology, the tools to identify the missing incretin hormone were finally available.

In the early 1980s, the cloning of cDNAs encoding the preproglucagons from pancreata of the anglerfish was accomplished. The anglerfish was found to have two separate nonallelic preproglucagon genes, both encoding a glucagon and a glucagon-related peptide (GRP) (11) which bore a strong homology to the sequence of GIP [50], [51].

Thereby Lund et al. [51] proposed that the anglerfish GRP-1 may be an intestinal incretin hormone. In support of this supposition Lund et al. [49] showed that similar preproglucagon mRNAs were expressed in the anglerfish pancreas and intestine, a finding that strongly supported the prediction that GRP could be an incretin hormone.

Shortly after the discovery of anglerfish GRP, the preproglucagon cDNAs of mammals were cloned [48] as well as the human gene [7]. It became clear that the anglerfish GRP-I is a homolog of the GLP-1s encoded in the mammalian preproglucagons, which were subsequently proven to be potent insulinotropic incretins. There was, however, some uncertainty regarding the identification of the bioactive isoform of GLP-1 that had true insulinotropic actions. Based on the amino acid sequence of the mammalian preproglucagons, the sites that would be predicted for posttranslational processing into peptide hormones were somewhat ambiguous. At the time it was generally believed that the yet-to be-identified prohormone convertases (PCs) that enzymatically split prohormones into bioactive peptides required two adjacent basic amino acids, combinations of arginine, and lysine. The GLP-1 sequence begins with a histidine as the amino-terminal residue, as do most of the peptide hormones in the glucagon-related superfamily of hormones. In the preproglucagon sequence, the first histidine is preceded by two basic amino acids, Lys-Arg, followed by four residues, another single basic residue, arginine, and a second histidine. The thinking at that time

was that the putative bioactive peptide that would theoretically be cleaved from the preproglucagon during posttranslational processing would be at the Lys-Arg yielding a peptide of 37 or 36 amino acids, depending on whether the C-terminal glycine was present or absent and whether the penultimate C-terminal arginine was amidated in the absence of the C-terminal glycine. Thus, the 1-37 and 1-36 GLP-1 peptide isoforms were the first to be synthesized and tested for biological activity.

The results of the experimental testing were disappointing. In 1986 it was discovered that GLP-1 was further N-terminally truncated by posttranslational processing in the intestinal L cells [18]. In contrast to GLP-1(1-37), GLP-1(7-37) and (7-36)amide were found to be potent insulinotropic hormones in the isolated perfused pancreas [40].

At present it is well established that the GLP-1 isoforms GLP-1(7-37) and GLP-1(7-36)amide are the bioactive insulinotropic peptides derived from preproglucagon in the intestine and the hind brain [40].

2.3 GLP-1 SECRETION

The possibility of studying the GLP-1 release at the cellular level in vitro has enabled the analysis of intracellular signal pathways that regulate GLP-1 secretion and expression. Studies with intestinal cell cultures and the L cell line, which are distributed in the region of terminal ileum and colon, GLUTag, indicate that the activation of protein kinase A stimulates both GLP-1 release and synthesis [40]. In contrast, activation of protein kinase C results in an increased secretion of GLP-1 in intestinal cell cultures, but does not appear to increase transcription of the proglucagon gene [24]. Treatment with the phospholipase C activator α-ketoisocaproic acid does not enhance GLP-1 secretion by either fetal rat intestinal cultures or GLUTag cells. Inhibition of GLP-1 secretion by a calcium channel

blocker (CoCl2) and stimulation of GLP-1 release by increasing intracellular calcium concentrations indicate a primary role of calcium in basal secretion by the L cell [10].

Thus there may be multiple signals involved in the L cell response that are perhaps important in allowing for an integrated response to a variety of different L cell effectors.

GLP-1 is released into the circulation after a meal [40]. Significantly more GLP-1 is released after a liquid meal than a solid meal of identical composition. The majority of GLP-1 released appears to be in the form of GLP-1 (7-36 amide) with levels reaching approximately 50 pmol/l, whereas GLP-1 (7-37) rises to 10 pmol/l. The oral intake of glucose alone stimulates GLP-1 release whilst elevation of plasma glucose by the administration of glucose systemically does not stimulate GLP-1 secretion, indicating the glucose sensing machinery is distributed on the luminal side of the intestine [24]. Infusion of glucose into the intestinal lumen stimulates GLP-1 release [43]. These observations are consistent with the role of GLP-1 as an important incretin hormone acting on the pancreatic β-cells to stimulate appropriate insulin release after glucose absorption.

The release of GLP-1 from the isolated perfused ileum requires sodium, implicating the brush-border sodium/glucose cotransporter in the glucose effect. Consistent with these findings, other sugars that utilize this cotransporter for absorption across the intestinal epithelium, e.g., galactose, also stimulate GLP-1 release. Nontransportable sugars, e g., 2-deoxyglucose, or sugars using a different mechanism of transport, e.g., fructose and lactose, do not stimulate the release of GLP-1 [24]. In addition to glucose, fats appear to stimulate the release of proglucagon-derived peptides, perhaps related to the roles of both oxyntomodulin and GLP-1 as enterogastrones, or inhibitors of gastric function [24]. The secretion of GLP-1 is increased by ingestion of mixed fats or triglycerides in humans and dogs and by placement of mixed fats directly into the intestinal lumen of rats and pigs [24]. Interestingly, Roberge and Brubaker [67] discovered that placement of fat in the duodenum of rats stimulates GLP-1 secretion independently of the contact of nutrients with the distal L cells. Furthermore, duodenal fat increased the

secretion of GLP-1 into the circulation to the same extent as was observed after the direct administration of fat into the ileum [67], [68]. These observations suggest the existence of a proximal-distal loop regulating the L cell response to ingested nutrients [67]. Such a mechanism could contribute to the significant increase in circulating GLP-1 levels observed within 5-10 min of ingesting a meal, before contact of nutrients with the L cells [59].

The observation of fatty acid-induced GLP-1 release from isolated intestinal cell cultures suggests that fatty acids can act directly on the L cell [24]. Interestingly, bile acids appear to increase the secretion of proglucagon-derived peptides suggesting that the arrival of bile into the ileum may play an important feedback message for the release of GLP-1. Results obtained with fatty acids indicate that both the chain length and degree of saturation of the fatty acids affect the ability of fats to stimulate GLP-1 secretion. Monounsaturated longchain fatty acids (5C16) are preferred over short-chain or medium-chain, polyunsaturated or saturated fatty acids [24]. However, long-term exposure of rats to short-chain fatty acids derived from a diet containing readily fermentable fibers increases proglucagon mRNA levels and secretion of GLP-1 in response to a glucose challenge [66].

Moreover GLP-1 secretion is increased in humans by a protein-containing mixed meal. However, either amino acids or protein alone did not consistently increase GLP-1 release in in vivo studies [24].

Conversely to nutrients, GLP-1 seems to be counterregulated by insulin. Indeed insulin has been reported to inhibit GLP-1 release both in vitro and in vivo, acting as part of a feedback loop [40].

2.4 GLP-1 METABOLISM

Plasma levels of GLP-1 are low in the fasted state in a range of 5 – 10 pmol/l, and increase rapidly after eating reaching 15 – 50 pmol/l. The circulating levels of intact GLP-1 decrease quickly because of, at least, three different processes that eliminate the bioactive form of the GLP-1 from the circulation: renal clearance, hepatic clearance and degradation in circulation by enzymatic inactivation. In support of an important role for the kidneys in the clearance of GLP-1 the levels of immunoreactive GLP-1 are significantly elevated in uremic patients [24], [40]. Although no net extraction of endogenous GLP-1 across the liver has been detected, significant hepatic extraction of GLP-1 during a systemic infusion was identified in anesthetized pigs [24], [40]. The MCR, or least amount of plasma totally cleared of GLP-1 per unit of time, in humans is approximately 10 ml/Kg/min [24]. In accordance with this MCR, GLP-1 is eliminated relatively rapidly from plasma, with a half-life of approximately 5 minutes in humans [24], [40]. It is noteworthy that, because postsecretory degradation of the GLP hormones in the circulation may generate products that are immunoreactive in assays but are no longer biologically active, these assay values of circulating levels of GLP-1 may overestimate the true biological half-life of the hormone. Indeed, as described below, the biological half-life of GLPs appears to be in the range of 1-2 min. Degradation of GLP-1 in the circulation appears to occur initially by dipeptidyl peptidase IV (DPP IV) cleavage at the amino terminus (histidine-alanine), resulting in GLP-1 (9-36)amide and GLP-1 (9-37). These truncated forms of GLP-1 have been demonstrated to be the major metabolites of GLP-1 formed in human [24], [40].

In in vivo studies with rats, it was estimated that DPP IV cleaved 50% of a bolus GLP-1 infusion within 2 min. In contrast, GLP-1 remained intact for at least 10 min in rats that were DPP IV-deficient. Thirty minutes after subcutaneous GLP-1 administration to healthy humans, GLP-1(9-36)amide accounted for approximately 78% of immunoreactive GLP-1 [24], [40]. It is likely that there is

subsequent enzymatic degradation of GLP-1 after cleavage by DPP IV by other enzymes. In pigs, inhibition of DPP IV activity potentiates the insulin response to GLP-1, indicating that the intact N terminus of GLP-1 is important for its insulinotropic activity. Furthermore, the oral administration of a DPP IV inhibitor to Zucker fatty rats improves glucose tolerance by increasing the circulating half-lives of the endogenously released incretins GIP and, particularly, GLP-1 [63]. It remains possible, however, that the metabolic products of GLP-1 have important biological actions different from those of the parent peptides. Receptor-binding studies suggest that the DPP IV metabolite GLP-1(9-36)amide can bind to the pancreatic GLP-1 receptor, albeit with only 1% the affinity of native GLP-1 [41]. Further, GLP-1 (9-36)amide can antagonize the ability of native GLP-1 to generate adenyl cyclase activity by the pancreatic GLP-1 receptor [41].

Recently, it was shown that GLP-1(9-36)amide could antagonize the inhibitory effect of GLP-1(7-36)amide on antral motility in anesthetized pigs [24]. Whether sufficient quantities of this metabolite GLP-1(9-36)amide exist in vivo to act as an antagonist of GLP-1, or possibly to mediate other biological activities, remains to be determined.

Thus for estimation of L-cell secretion it is best to measure the sum of the intact hormone and the primary metabolite. In humans, this can be accomplished with assays for the amidated COOH terminus of the molecule, which is common to the intact hormone and the metabolite, because in humans, all of the GLP-1 released from the gut is amidated. Such assays are frequently designated "total" GLP-1 assays. Clearly, for estimation of the impact of circulating intact GLP-1 for insulin secretion via the endocrine route, it is necessary to measure the concentration of the intact hormone, which may be accomplished with sandwich assays as mentioned (often designated "active GLP-1 assays"). However, this is unlikely to reflect to total influence of L-cell secretion on insulin secretion.

2.5 GLP-1 PHYSIOLOGICAL ACTIONS

GLP-1 generates several different physiological actions which are correlated to the organs in which specific GLP-1 receptors are expressed. These organs include the pancreatic islets, stomach, lung, brain, kidney, pituitary gland, cardiovascular system, and small intestine.

2.5.1 Pancreatic islets

The earliest discovered biological actions of GLP-1 were on the pancreatic β-cells, in which GLP-1(7-37) and GLP-1(7-36)amide were shown to be highly equipotent secretagogues for glucose-dependent insulin secretion . It is important to point out that the [14] insulinotropic action of GLP-1 is attenuated if ambient glucose levels fall; in that way the glucose dependent nature of the incretin hormones like GLP-1 is an efficient protective measure against hypoglycemia.

The glucose competence concept has been used to describe the mutual interdependence between glucose metabolism and GLP-1 actions on β-cells, glucose is required for GLP-1 action, and GLP-1 is required to render β-cells competent to respond to glucose [24]. Thus the β-cells responsivity to glucose in subjects with impaired glucose tolerance is enhanced. Moreover not only GLP-1 stimulates insulin secretion, but it also stimulates transcription 1 is not an absolute requirement for the maintenance of normal proinsulin gene transcription, nevertheless, these properties clearly distinguish GLP-1 from those of the sulfonylurea class of hypoglycemic drugs that effectively stimulate insulin secretion but do not stimulate biosynthesis of proinsulin . Recent evidence indicates that GLP-1 may stimulate the proliferation and neogenesis of β-cells from ductal epithelium of mice and rats [24].
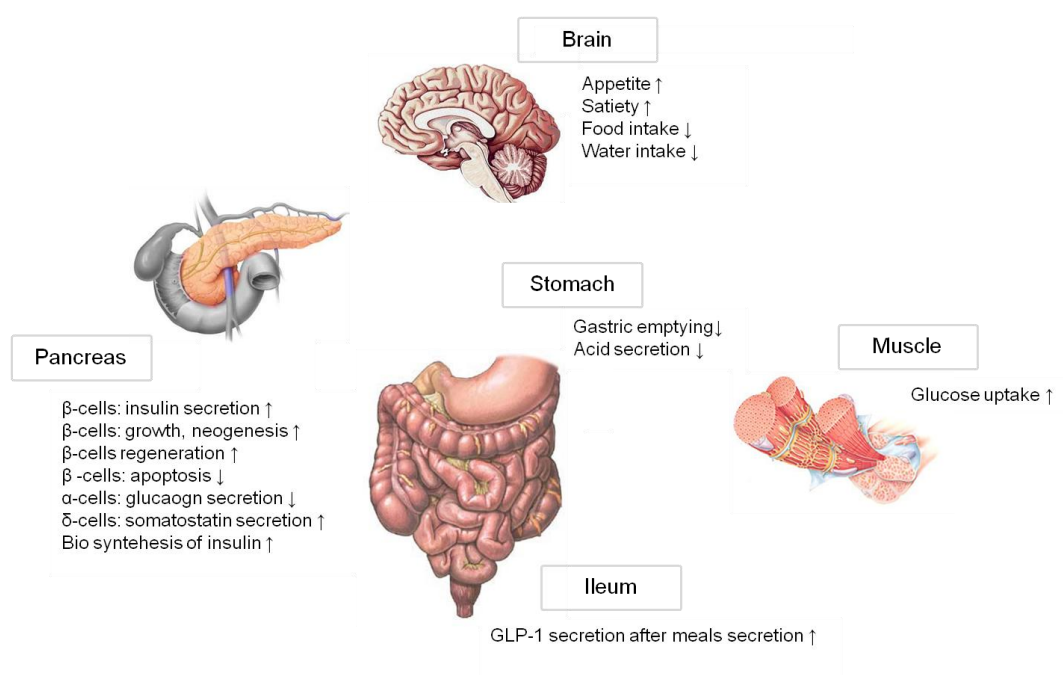
Figure 2. 1 – GLP-1 physiological actions

In the β-cell line INS-1, GLP-1 synergizes with glucose to activate expression of immediate early response genes coding for transcription factors implicated in cell proliferation and differentiation (c-fos, c-jun, junB, zif-268, nur-77). Moreover, administration of GLP-1 to aged rats that characteristically develop glucose intolerance between 18 and 20 months of age reverses the glucose intolerance. Thus GLP-1 may have potent pleiotropic actions on both mature β-cells and duct cells that are progenitors of β-cells. Receptors for GLP-1 have been detected also on α-cells and δ-cells [24]. The secretion of somatostatin increases in response to GLP-1 in rat islets and in isolated perfused rat and canine pancreases. Although GLP-1 appears to inhibit glucagon secretion in vivo, it stimulates glucagon release in vitro. We speculated that the small amounts of biologically active GLP-1 produced in islets during the fasting state might exert autocrine/paracrine effects on a subset of a-cells containing GLP-1 receptors to increase glucagon biosynthesis via the cAMP pathway. During feeding, such an effect would be

overcome by the combination of elevated insulin, somatostatin, and glucose, which collectively inhibit glucagon secretion. Thus the suppression of glucagon release observed in vivo may be indirectly attributable to the paracrine actions of the intraislet release of insulin and somatostatin. However, maintenance of glucagon secretion does not appear to be dependent upon functional GLP-1 signaling [24].

2.5.2 Stomach:

The distal portion of the small intestine regulates gastric function in humans, diversion of chyme from the ileum reduces the gastric secretory response compared with exposure of chyme to the entire small intestine. The presence of chyme or partially digested fat in the ileum of humans inhibits gastric emptying and jejunal motility – the so-called 'ileal brake'. As reviewed earlier, chyme and fats are potent stimulators of GLP-1, indicating GLP-1 may be a candidate hormone for regulating gastric function. Indeed, GLP-1 inhibits gastric acid secretion and gastric emptying when infused in quantities that result in plasma concentrations similar to those observed after meals. The inhibitory effect of GLP-1 on upper gastric functions could involve receptors located either in the central nervous system or associated with afferent pathways to the brain stem. These possibilities are supported by the observations that the inhibitory effect of GLP-1 on gastric emptying requires intact vagal enervation Therefore, despite the known insulinotropic actions of GLP-1, the net effect of administering GLP-1 with a meal in healthy humans is a reduction in meal-related integrated incremental glucose and insulin responses . This observation supports the concept that the primary physiological role of GLP-1 may be as a mediator of ileal brake mechanisms, rather than as a incretin hormone. The actions of GLP-1 to delay gastric emptying are under investigation as an aspect of therapy for diabetes to attenuate the postprandial glucose excursion [60], [61], [71], [72], [90].

2.5.3 Lung:

The unusually high abundance of receptors in the lung suggests important actions of GLP-1 in pulmonary physiology, but its physiological role remains uncertain. It is difficult to envision how GLP-1 actions on the lung would relate to the release of GLP-1 from the intestine in response to meals. One possibility is the local production of proglucagon and GLP-1 within the lung to establish a paracrine loop, but proglucagon expression has not yet been detected in the lung [24].

2.5.4 Brain:

Recently it has been discovered that GLP-1 acts on the hypothalamus to inhibit food and water intake, thus making the GLP-1 seems to be an anorexigenic hormone. The discovery of these actions on the promotion of satiety and the suppression of the energy intake are recent and are somewhat controversial. The expression of GLP-1 receptors in the brain was confirmed by RT-PCR cloning of the GLP-1 receptor from mRNA prepared from rat brain. It was also shown in earlier studies that proglucagon and proglucagon-derived peptides are produced locally in the brain. High densities of GLP-1-immunoreactive nerve fibers are present in paraventricular nucleus, dorsomedial hypothalamic nucleus, and the subfornical organ. There are at least two mechanisms by which GLP-1 may gain access to the appetite control centers located in the hypothalamus: local production of GLP-1 within the brain and uptake of intestinally derived GLP-1 in the circulation. Compelling experimental evidence has been presented in support of both mechanisms, and they are not mutually exclusive. The proglucagon gene is expressed in the nucleus of the solitary tract, which is the nucleus of the vagus nerve that regulates the autonomic functions of the gut. Furthermore, proglucagon produced in the nucleus tractus solitarius is processed to GLPs. Thus, an attractive mechanism for the exertion of GLP-1 actions to inhibit feeding behavior would be the activation of GLP-1 production in the nucleus tractus solitarius via afferent

enervation from the vagus nerve. Oral nutrients would then signal to the brain through the autonomic nervous system. It is tempting to speculate that this may constitute a prandial satiety signal generated during feeding, a signal to cease food consumption because enough has already been consumed. However, if an axonal transport of GLP-1 from the hindbrain to the hypothalamus is required, it may not be rapid enough to account for meal-induced satiety (20-30 min). Perhaps the more plausible mechanism is the uptake by brain of GLP-1 in the circulation released from the intestines in response to a meal. Remarkably, 125I-labeled GLP-1 injected into rats localizes to the subfornical organ and the area postrema of the brain within 5 min after the injection [89]. These regions of the circumventricular organ are known sites where blood-borne macromolecules can pass across the blood-brain barrier. The satiety-inducing obesity hormone leptin in the circulation is believed to gain access to the satiety centers in the hypothalamus via the circumventricular organ that contains a high concentration of leptin receptors, so called short-form receptors that have high affinity for leptin, but are defective in their signal transduction [91]. The model proposed for leptin transport into the brain is that the receptors extract leptin from the plasma and transport the leptin into the hypothalamus. Thus, in analogy with the mechanism of transport of leptin from the circulation to the brain, it seems reasonable to propose that GLP-1 released into the circulation in response to meals is similarly transported to the brain. The timing of GLP-1 release after a meal (15-30 min) and the demonstrated rapid uptake of GLP-1 by the circumventricular organ (2, 5 min) would be consistent with the development of satiety invoked by GLP-1 during the course of a meal [28].

2.5.5 *Cardiovascular system:*

GLP-1 receptor agonists have been reported to have cardiac and vascular actions in rodents and humans that include effects on contractility, blood pressure, cardiac output, and cardioprotection. Although GLP-1R is expressed in cells and throughout the gut, lung, kidney, heart, and central nervous system, including

autonomic nuclei that control cardiovascular functions, the specific cellular localization, relative abundance, and functional importance of the GLP-1R in cardiovascular tissues have not been fully defined.

Currently there are some studies that are trying to prove cardioprotective and vasodilatory actions of GLP-1(7-36) independently from the known GLP-1R and mediated, at least in part, by its metabolite GLP-1(9-36), suggesting the existence of an alternative signaling mechanism for GLP-1 and its metabolite in the cardiovascular system, and leading to the assumption that drugs targeting GLP-1R activation (GLP-1R agonists) versus GLP-1 degradation (DPP-4 inhibitors) for the treatment of diabetes may have different cardiovascular consequences [3].

2.6 GLP-1 RECEPTOR

The receptor for GLP-1 (GLP1R) is a member of the Family B (II) Glucagon-Secretin G Protein-Coupled Receptor (GPCR) superfamily and is distributed among several different tissues like: brain, lung, pancreatic islets, stomach, hypothalamus, heart, intestine, kidney [40], and, although most reports indicate that do not express the known GLP-1 receptor, investigators have reported binding and in vitro and in vivo effects of GLP-1 in liver, muscle, and adipose tissues. The gene for the human GLP-1 receptor is localized to chromosome 6p21 [79] and it consists of 463 amino acids containing eight hydrophobic segments. The N-terminal hydrophobic segment is probably a signal sequence, while the others are membrane-spanning hydrophobic motifs. Ligand-binding analysis of the recombinant receptors expressed in and assembled on the surface of β-cells show that the selectivity for the binding of GLP-1 is approximately 1 nm, whereas all of the other peptides of the glucagon superfamily bind poorly or not at all with the exception of glucagon, which is a weak, full agonist with a binding affinity of 100 – 1,000-fold less that of GLP-1 [79].

The GLP-1R binding site is an high affinity binding with a Michaelis-Menten kinetic. After the identification of GLP-1, the GLP-1 actions are mediated trough adenylate cyclase. Within β-cells, cAMP potentiates glucose-induced closure of ATP-sensitive K+ channels [40], thereby generating cellular depolarization, activation of voltage-dependent Ca2+ channel, and influx of Ca2+. The GLP-1 induced rise of Ca2+ serves as an important trigger for exocytosis of insulin. Thus the GLP-1R leads to insulin exocytosis in a glucose dependent manner.

Moreover the receptor signalling is associated with activation of protein kinase A, induction gene transcription, enhanced levels of insulin biosynthesis and stimulation of β-cells proliferation [21].

2.7 GENETIC ROLE IN DIABETES ONSET: GLP1R POLYMORPHISMS

Diabetes arises from a complex interaction between multiple genes and the environment. Until less than a century ago, the greatest selective pressures on human survival arose from infection and famine. It is conceivable that genetic variation conferring a survival advantage in responding to infection may predispose individuals to developing autoimmune disease. Similarly, variation that allowed more efficient conservation of energy in situations of lack of food may predispose individuals to obesity and type 2 diabetes when calories are abundant and physical exertion is optional. In the past 2 years, several studies have enhanced the understanding of the genetic predisposition to these common metabolic diseases.

Diabetes prevalence differs between races; concordance rates are higher in monozygotic, as compared to dizygotic twins and the sibling risk ratio (λs) of 5 [85]. All of these observations support a genetic contribution to the disease. A few, commonly encountered polymorphisms have been associated with an

increased risk of type 2 diabetes. Variation in three genes: TCF7L2, KCNJ11 and PPARG [34], [35], independently and interactively increase risk of progression from impaired fasting glucose and impaired glucose tolerance to overt diabetes [52]. Florez et al. [30] reported that two single nucleotide polymorphisms (SNPs) in TCF7L2 (rs7903146 and rs12255372) predicted the progression to diabetes of persons with impaired glucose tolerance who were enrolled in the Diabetes Prevention Program. Over the 3-year period of observation, participants homozygous for the risk-conferring allele were more likely to develop diabetes. Numerous studies have since shown that greater diabetes risk is conferred by the T allele of rs7903146 than the T allele of rs12255372 [30].

The metabolic effects of disease-associated polymorphisms in type 2 diabetes have been partly characterized for KCNJ11, PPARG and TCF7L2. The demonstration of a reproducible association of these loci with disease led to studies of their effects on glucose metabolism [52]. PPARG and KCNJ11 are the sites of action for thiazolidinediones and sulfonylureas, respectively; this has aroused interest in the effect of these variants on response to oral therapy for type 2 diabetes. A genetic defect producing a global impairment in insulin secretion, in addition to a predisposition to diabetes, will likely alter the response to insulin secretagogues. Since variation in KCNJ11 alters glucose-induced insulin secretion, it follows that the secretory response to sulfonylureas is also impaired, leading to failure of sulfonylurea therapy [73], however, this has not been true in all studies [33]. In the Diabetes Prevention Program, the same polymorphism also altered response to metformin monotherapy [29], and the mechanism of this alteration in response is unclear given the current understanding of the mechanism of action of metformin.

The product of TCF7L2 is a member of the TCF (transcription factor) family and is therefore an important constituent of the Wnt signaling pathway. This pathway regulates gene expression, cell–cell adhesion and cell cycle control and is initiated when Wnt binds the transmembrane, cysteine-rich Frizzled family of receptors. The resulting receptor kinase action ultimately allows β-catenin, the main effector of the signaling pathway, to accumulate in the cytoplasm and nucleoplasm. Within

the nucleus, β-catenin heterodimerizes with one of four TCFs, including TCF7L2 to mediate its regulatory role [58]. The incretin hormone GLP-1 results from post-translational processing of the glucagon gene (GCG) product. In the pancreatic α cells, prohormone Convertase-1 (PC-1) catalyzes the synthesis of glucagon, whereas in intestinal L cells and in the brain, PC-2 leads to the synthesis of GLP-1 and GLP-2. It has been shown that the β-catenin– TCF7L2 heterodimer regulates GCG expression in the intestinal L cells but not in pancreatic α cells. This led to the suggestion that the disease-associated alleles lead to defects in the incretin system and subsequently diabetes [35]. As expected, the disease-associated decrease in insulin secretion impairs the response to glucose, sulfonylureas and other secretagogues [53]. Polymorphisms in TCF7L2 do not alter response to interventions that improve insulin action in glucose-intolerant, obese patients [30]. A polymorphism in the GLP-1 receptor has been shown to alter response to GLP-1 in vitro [6]. To date, variation in GLP1R has not been associated with predisposition to type 2 diabetes. With the availability of GLP-1-based treatment of diabetes, it is relevant to understand whether polymorphisms in GLP1R alter response to GLP-1 receptor agonists or DPP-4 inhibitors, and such studies are awaited.

CHAPTER 3

DATA AND PROTOCOLS

3.1 INTRODUCTION

In this chapter all the experimental protocols used to develop and validate the models are described in detail. First a hyperglycemic clamp with concomitant GLP-1 intravenous infusion is presented; it is used to develop the model of GLP-1 action on insulin secretion. In fact, thanks to the fact that glucose is maintained almost constant, it was possible to single out the effect of GLP-1 on C-peptide secretion rate. However, this was a very unphysiological condition since, in normal life, glucose, C-peptide and GLP-1 concentrations vary in time. The second protocol of a mixed meal originally designed to assess the effect of DPP-4 inhibition on incretin secretion and glucose turnover and used to test the model performance to quantify the effect of GLP-1 on insulin secretion in a more physiological condition. The third, and last, protocol is used for model validation by comparing model ability to simultaneously quantify the enhancement of insulin secretion due to GLP-1 and β-cells responsivity indexes against those provided by

a model-independent technique, which employs OGTT and matched intravenous glucose challenge (I-IVG) data of 10 healthy subjects.

3.2 DATABASE 1: HYPERGLYCEMIC CLAMP WITH CONCOMITANT GLP-1 INTRAVENOUS INFUSION

3.2.1 Subjects

The study cohort is composed by 88 healthy individuals, 36 males and 52 females, aged between 18 and 40 (average 26 ± 6 yr) who do not have a diagnosis of diabetes and have a fasting glucose concentration of less than 95 mg/dl. Individuals with a BMI < 19 or > 40 kg/m^2 are excluded from the study in order to avoid potential confounding effects that may result from extreme leanness or obesity. Healthy indicates that the participant has no known systemic illness, is not on any medication that can alter gastric emptying, insulin secretion and action, and has no history of abdominal surgery.

3.2.2 Screening visit

To ensure subjects are healthy, following written, informed consent, subjects underwent a history and physical examination; blood has been collected for complete blood count and chemistry group; urine has been collected to ensure there is no evidence of infection, proteinuria or pregnancy. Subjects participating in this protocol have been at a stable weight and have not been engaging in regular vigorous physical exercise.

3.2.3 Experimental design

Subjects were admitted to the Mayo Clinic General Clinical Research Center at 18.00 hours the evening before the study. Following ingestion of a standard 10 Kcal/kg meal (55% carbohydrate, 30% fat, and 15% protein), subjects fasted until the end of the study. On the morning of the study at 06.00 hours (−60 min), an 18-gauge cannula was inserted into the non-dominant forearm to allow for hormone and dextrose infusion during the study. At 06.15 hours (−45 min), an 18-gauge cannula has been inserted in a retrograde fashion into a dorsal hand vein. The hand has then been placed in a heated box in order to obtain arterialized venous blood samples. At 07.00 hours (0 min), glucose has been infused intravenously in amounts sufficient to maintain plasma glucose concentration at 150 mg/dl.

This continued till the end of the study and adjusted as necessary. At 09.00 hours (120 min) an intravenous infusion of GLP-1 (BaChem, San Diego, CA) commenced at a rate of 0.75 pmol/kg/min from 121–180 min and subsequently increased to 1.5 pmol/kg/min from 181–240 min. The glucose infusion rate has been adjusted as necessary to maintain target glucose concentrations of 150 mg/dl. Blood has been drawn at -30, -15, 0, 2, 4, 6, 8, 10, 20, 30, 40, 50, 60, 75, 90, 105, 120, 122, 124, 126, 128, 130, 140, 150, 160, 180, 182, 184, 186, 188, 190, 210, 220, 230, 240 minutes. After the last blood draw all infusions has been discontinued. Figure 3. 1 shows the scheme of the experimental design.

Both hyperglycemia and GLP-1 are potent stimuli of insulin secretion. A glucose clamp at 150 mg/dl has been chosen in order to minimize the effect of glucose on insulin secretion, yet still providing the glycemic stimulus necessary for GLP-1 to enhance glucose-induced insulin secretion. However, it is possible that a subtle defect in the response to GLP-1 could be missed. In an effort to minimize this possibility, the GLP-1 infusion has been performed in two rates: one that results in a half-maximal (0.75 pmol/kg/min) and one that results in a near-maximal stimulation of insulin secretion (1.5 pmol/kg/min).

This was useful for the modeling point of view since it allowed us to test possible non-linearity in β-cells response to GLP-1, which would have been almost impossible if a single step infusion was used.

3.2.4 Analytic techniques:

All analytic techniques described in this and subsequent protocols are either established in the applicant's laboratory or are routinely performed in the Mayo GCRC Mass Spectrometry or Immunochemical Core laboratories. All blood has been immediately placed on ice, centrifuged at $4^{o}C$, separated and stored at -$80^{o}C$ until assay. Glucose concentrations have been measured using a Yellow Springs glucose analyzer. C-peptide and glucagon concentrations have been measured using reagents purchased from Linco Research Inc., St. Louis, MO. Insulin has been measured using a chemiluminescence assay with reagents obtained from Beckman (Access Assay, Beckman, Chaska, MN). GLP-1 hormone concentrations have been measured: blood has been collected in ice-cooled EDTA-plasma tubes. Immediately after collection a dipeptidyl peptidase-IV (DPP-IV) inhibitor, Aprotinin (Linco Research, St. Charles, MO) has been added to the sample tube to prevent DPP-IV mediated degradation of intact GLP-1. All blood has been immediately placed on ice, centrifuged at $4^{o}C$, separated and stored at -$80^{o}C$ until assay. body composition has been measured prior to participation using dual-energy X-ray absorptiometry (DPX-IQ scanner; Hologic, Waltham, MA).

Plasma glucose, C-peptide and GLP-1 concentrations are shown in Figure 3. 2 Figure 3. 3 Figure 3. 4, respectively. Basal plasma C-peptide concentration was 578.3±23.1 pmol/l; at 120 minutes, before the intravenous infusion of GLP-1 was started, C-peptide concentration was 1852.0±62.8 pmol/l, due to the rise in glucose concentration, and plasma GLP-1 was 4.4 ±0.8 pmol/l. After the GLP-1 infusion, plasma GLP-1 concentration increased to 23.9 ±1.6 pmol/l at 180 minutes and to 42.2 ± 2.1 pmol/l at 240 minutes (all differences were statistically significant, $p<0.0001$), and consequently C-peptide concentration rose to

4272.2±176.4 and 6995.8±323.5 pmol/l at 180 and 240 minutes, respectively (all differences were statistically significant, p<0.0001). The ratio between above-basal C-peptide and above-basal GLP-1 concentrations was 266.4±19.8 and 196.6±11.1 pmol/l at 180 and 240 minutes, respectively, and the difference was statistically significant (p<0.0001). Therefore this result supports the hypothesis that GLP-1 may act nonlinearly on C-peptide secretion.
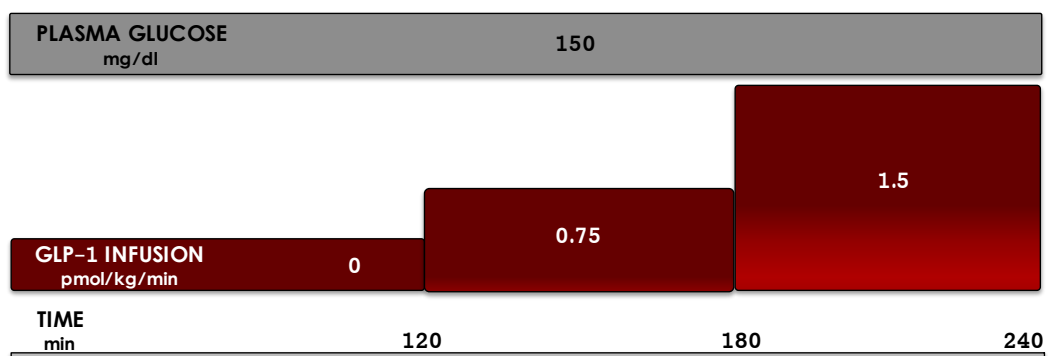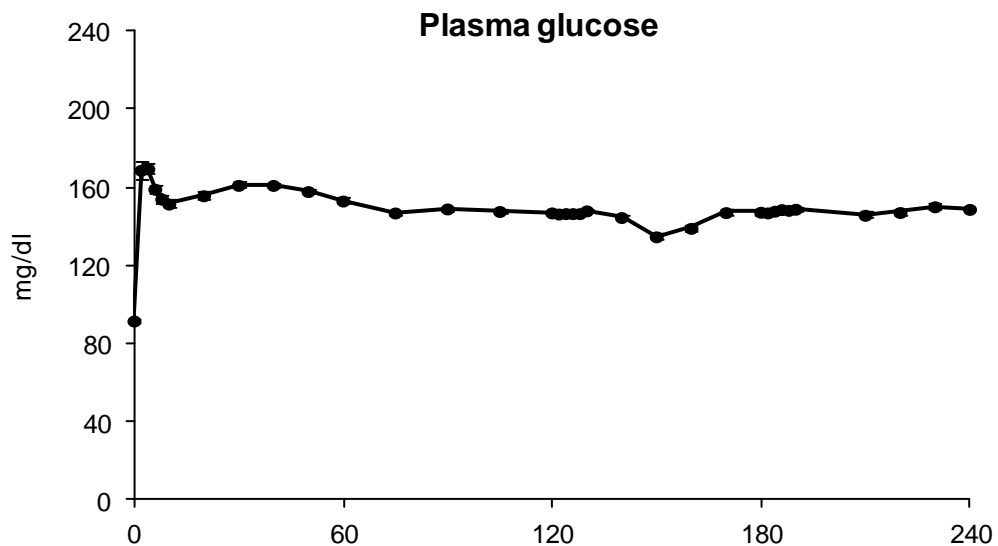

Figure 3. 1 – Experimental design scheme

Figure 3. 2 – Average plasma glucose concentration. Vertical error bars represent SE
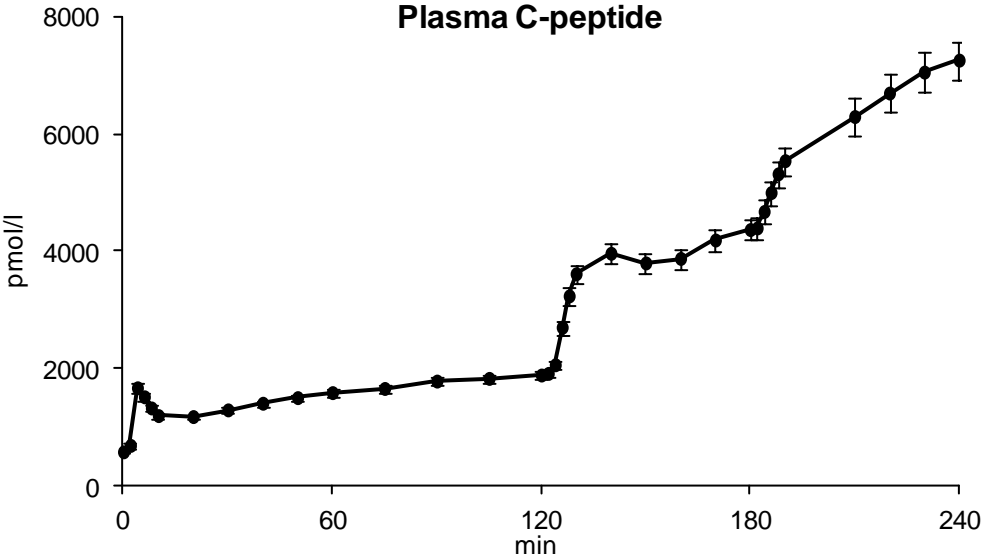
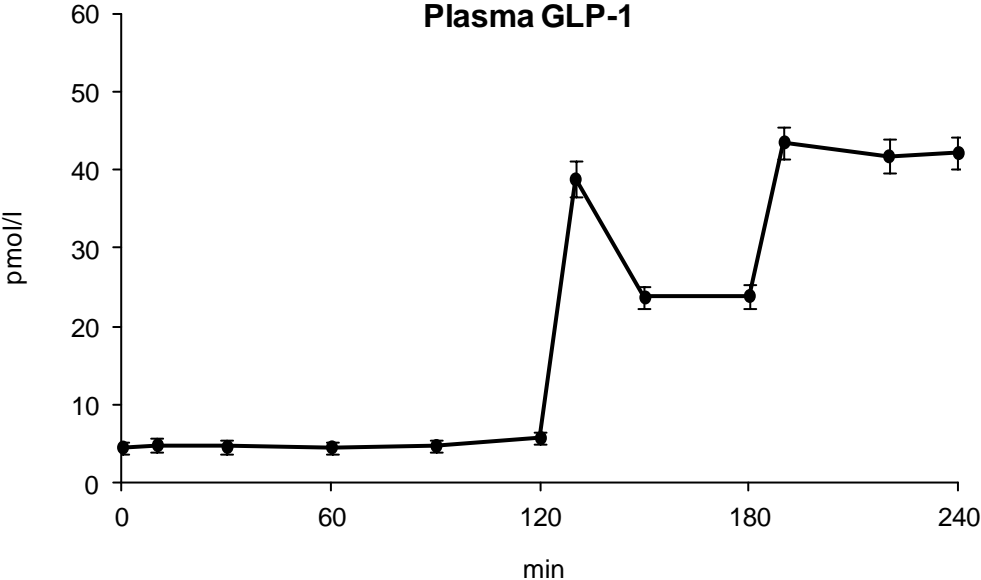**Figure 3. 3 – Average plasma C-peptide concentration. Vertical error bars represent SE**

Figure 3. 4 – Average plasma GLP-1 concentration. Vertical error bars represent SE

3.3 DATABASE 2: MIXED MEAL

3.3.1 Subjects

After obtaining approval from the Mayo Institutional Review Board, 22 subjects (age 54.7±1.8 years, BMI 32.9±1.2 kg/m^2) with a fasting glucose >99 mg/dl but < 125 mg/dl on two or more occasions gave written informed consent to participate in the study.

3.3.2 Screening visit

At screening visit, subjects were in good health, at stable weight and did not engage in regular vigorous exercise. Subjects had no history of diabetes or of prior therapy with antidiabetic medication. All subjects were instructed to follow a weight maintenance diet containing approximately 55% carbohydrate, 30% fat and 15% protein for the period of study. Body composition was measured using dual-energy X-ray absorptiometry (DPX scanner; Lunar, Madison, WI, USA).

3.3.3 Experimental design

A randomized, double-blinded, placebo-controlled, parallel-group design were adopted. After a baseline meal study, subjects were divided into two groups of 11 individuals, which received either sitagliptin 100 mg or an identical placebo taken before breakfast over an 8-week treatment period. Participants underwent a second meal study at the end of the treatment period (when they received study medication prior to meal ingestion). Participants were assessed in the Clinical Research Unit (CRU) 4 weeks after the first study when compliance was assessed by counting remaining medication.

Subjects were admitted to the CRU at 1700 on the evening prior to the meal study. Subsequently, they consumed a standard 10 cal/kg meal (55% carbohydrate, 30% fat and 15% protein) after which they fasted overnight. At 0630 (-210 min), a forearm vein was cannulated with an 18-g needle to allow infusions to be performed. An 18-g cannula was inserted retrogradely into a vein of the dorsum of the contralateral hand. This was placed in a heated Plexiglas box maintained at 55 °C to allow sampling of arterialized venous blood. At -180 min, a primed (12 mg/kg) continuous (0.12 mg/kg per min) infusion of $[6,6\text{-}^2H_2]$ glucose was initiated. Study medication was administered at -30 min on the second study day.

At time 0, subjects consumed a meal consisting of three scrambled eggs, 55 g of Canadian bacon, 240 ml of water and Jell-O containing 75 g of glucose labelled with $[1\text{-}^{13}C]$ glucose (4% enrichment). The meal provided 510 kcal (61% carbohydrate, 19% protein and 21% fat). An infusion of $[6\text{-}^3H]$ glucose was started at this time, and the infusion rate varied to mimic the anticipated appearance of meal $[1\text{-}^{13}C]$ glucose. The rate of infusion of the $[6,6\text{-}^2H_2]$ glucose was altered to approximate the anticipated fall in endogenous glucose production (EGP).

Blood samples were collected at time 0, 5, 10, 15, 20, 30, 40, 50, 60, 75, 90, 120, 150, 180, 210, 240, 270, 300, 330, and 360 min.

3.3.4 Analytical techniques

Plasma samples were placed on ice, centrifuged at 4 °C, separated and stored at -20 °C until assayed. Glucose concentrations were measured using a glucose oxidase method (Yellow Springs Instruments, Yellow Springs, OH, USA). Plasma insulin was measured using a chemiluminescence assay (Access Assay; Beckman, Chaska, MN, USA). Plasma glucagon and C-peptide were measured by Radio-Immunoassay (Linco Research, St. Louis, MO, USA). Collection tubes for Glucose-dependent Insulinotropic Polypeptide (GIP) and GLP-1 had 100 lm of DPP-4 inhibitor (Linco Research) added. Total and intact GLP-1 and GIP concentrations were measured using C-terminal and N-terminal

assays. Plasma [6,6-^{2}H$_2$] glucose and [1-^{13}C] glucose enrichments were measured using gas chromatographic mass spectrometry (Thermoquest, San Jose, CA, USA) to simultaneously monitor the C-1 and C-2 and C-3 to C-6 fragments. In addition, [6-^{3}H] glucose-specific activity was measured by liquid scintillation counting following deproteinization and passage over anion and cation exchange columns. Figure 3. 5 shows plasma glucose (A), C-peptide (B) and total GLP-1 (C) for baseline and sitagliptin mixed meal study.

3.4 DATABASE 3: OGTT AND MATCHED INTRAVENOUS GLUCOSE

3.4.1 Subjects

Study cohort is composed by 10 individuals aged 18 - 45 years (average ± SE age = 29 ± 9 years) who are otherwise healthy and have had stable weight (average ± SE BMI = 27 ± 5 kg/m^2) or > 6 months. Healthy status indicates that the participant has no known active systemic illness and no history of microvascular or macrovascular disease.

3.4.2 Screening visit

Subjects provided written informed consent at the time of the screening visit. After an overnight fast they were asked to report to the CRU the next morning. To ensure they are healthy, subjects underwent a history and physical examination, vital signs, height, weight; blood collection for complete blood count, chemistry group and glucose; ECG and urine collection to exclude infection, proteinuria or pregnancy.
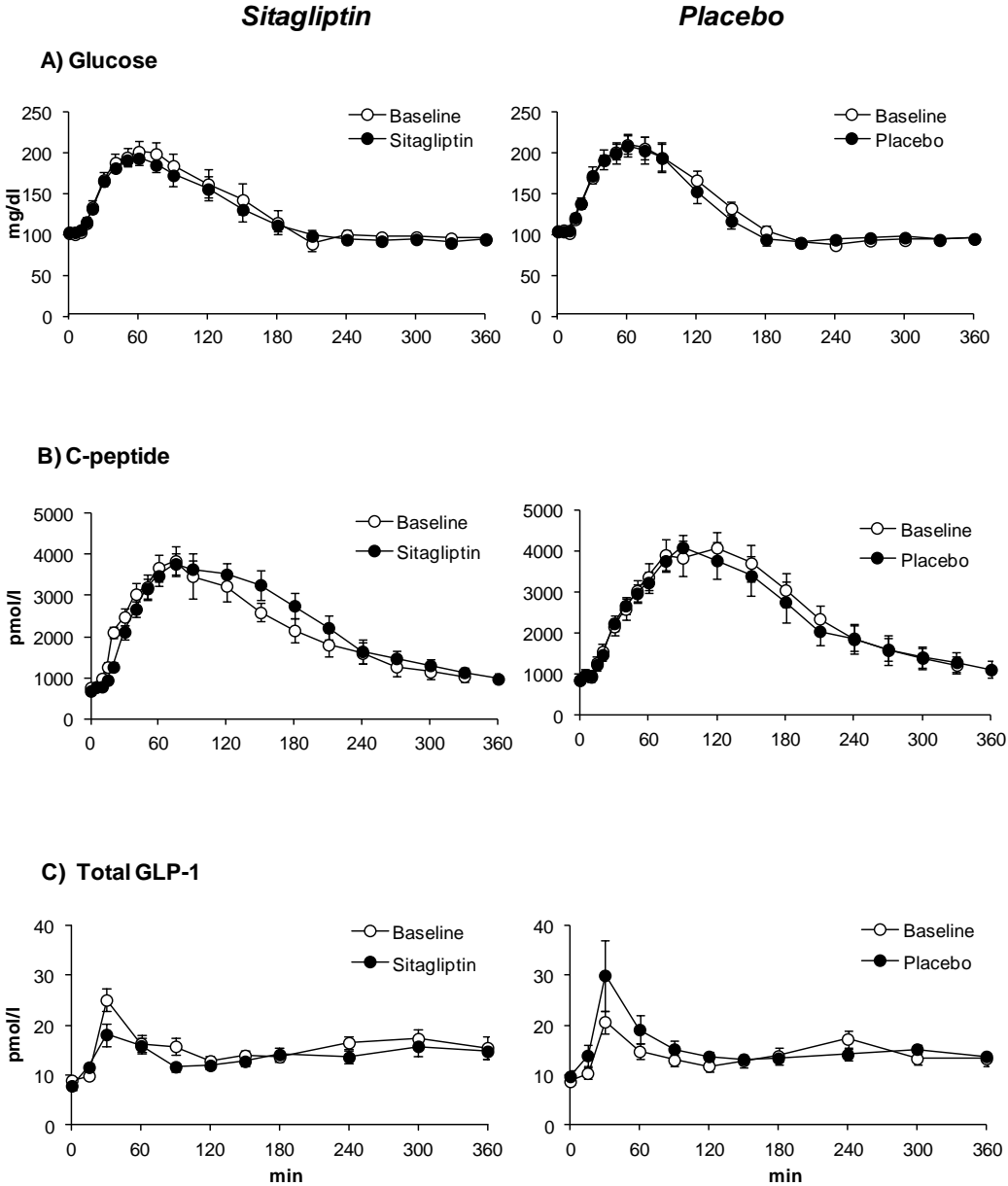
Figure 3. 5 – Average (N=22) measured concentrations of plasma glucose (A), C-peptide (B) and total GLP-1 (C) for baseline (white dots) and sitagliptin (black dots) mixed meal study. Vertical bars represents SE.

Subjects participating in this and subsequent protocols were not engaging in regular vigorous physical exercise. All participants underwent tests of body composition using dual-energy X-ray absorptiometry (iDXA scanner; GE, Wauwatosa, WI). Subjects were instructed by the CRU dietician to maintain their usual diet throughout the duration of the study.

3.4.3 Experimental design

Subjects participated in a total of 2 protocols (A, B) performed at least a week apart.

Protocol A – Oral Glucose Tolerance Test (OGTT):

Volunteers were admitted to the CRU the morning of the study after an overnight fast. An 18 g cannula was inserted retrogradely into a vein of the dorsum of the non-dominant hand which was placed in a heated Plexiglas box maintained at 55°C to allow sampling of arterialized venous blood. At time point (0), subjects ingested a glucose drink:1g per kg body weight.

Protocol B – Isoglycemic Intravenous Glucose Test (I-IVG):

Volunteers were admitted to the CRU the morning of the study after an overnight fast. An 18 g cannula was inserted retrogradely into a vein of the dorsum of the non-dominant hand which was placed in a heated Plexiglas box maintained at 55°C to allow sampling of arterialized venous blood. In addition, an 18g cannula was placed in the contralateral arm to allow intravenous infusion. At time point (0), glucose (Dextrose 20%) was infused via this latter cannula in amounts sufficient to match the glucose concentrations observed during the Oral Glucose Tolerance Test obtained during *Protocol A* as previously described.

Blood samples were collected for hormones concentrations on all protocols, at -30, -15, 0, 5, 10, 15, 20, 25, 30, 60, 90, 120, 150, 180, 210 and 240

minutes and glucose concentrations were measured from plasma every 10 minutes after time 0 to allow matching of glucose concentrations between study protocols.

3.4.4 Analytical techniques

Arterialized venous plasma samples will be placed in ice, centrifuged at 4°C, separated and stored at -20°C until assay. C-peptide and glucagon concentrations will be measured in the Mayo immunochemical core using reagents purchased from Linco Research Inc., St. Louis, MO. Insulin will be measured using a chemiluminescence assay with reagents obtained from Beckman (Access Assay, Beckman, Chaska, MN). Glucose concentrations will be measured using a Yellow Springs glucose analyzer.

Figure 3. 6 shows plasma C-peptide, glucose and total GLP-1 concentration for *Protocol A* and *Protocol B*.
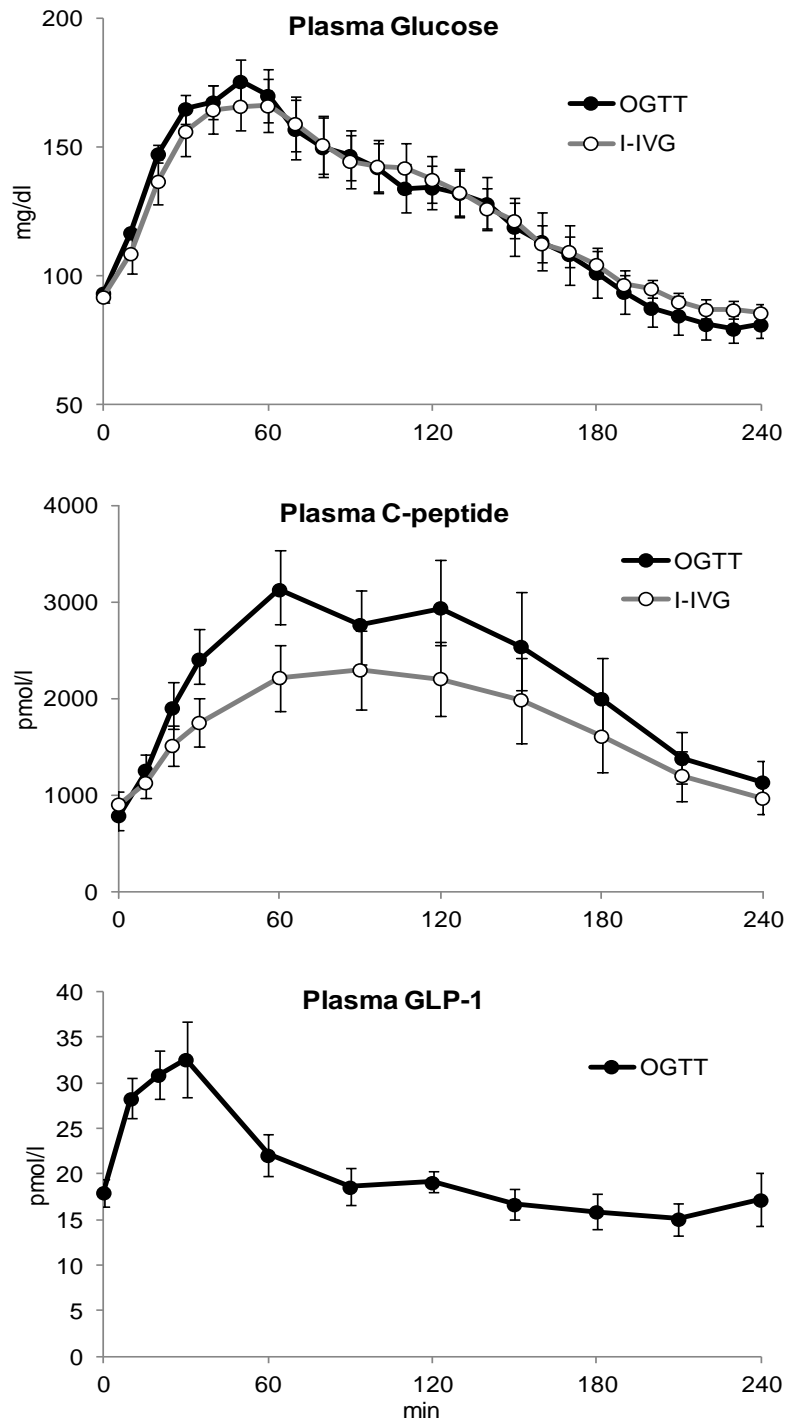
Figure 3. 6 – Plasma C-peptide, glucose and total GLP-1 in OGTT and I-IVG study. Vertical bars represent SE

CHAPTER 4

MODELS TO ASSESS INSULIN SECRETION AND INCRETIN EFFECT

4.1 INTRODUCTION

Insulin is the primary regulator of glucose homeostasis, hence the ability to evaluate the pancreatic insulin secretion rate, SR, is essential for a quantitative understanding of the glucose regulation system, and, in this specific study, of the GLP-1 action on insulin secretion. SR cannot be directly measured, since insulin is secreted by pancreatic β-cells into the portal vein which is not accessible *in vivo*. Before reaching the systemic circulation, insulin passes through the liver, where approximately 50% is degraded. Insulin level in plasma is a function of three processes: insulin secretion by the pancreas, hepatic insulin extraction, and insulin kinetics; however it is only measurable the effect of insulin secretion in circulation, since the best measure of insulin, or at least the simplest, are peripheral insulin concentrations, unless very invasive and complex experimental protocol are performed [36], [22], [82], [83], [84], [86].

The presence of the liver that extracts insulin to a large and variable extent is the crucial problem in using plasma insulin concentrations in order to assess insulin secretion rate. This problem can be bypassed if plasma C-peptide concentration instead of insulin is used. In fact, C-peptide is equimolarly secreted with insulin but it is not extracted significantly by the human liver, and its kinetics have been shown to be linear and time-invariant for a large range of C-peptide concentrations [9], [82], [83], [84], [86]. In addition, evidence exists that the inhibition effect of C-peptide on its own secretion appears to be, if any, very small [65], [27], and that C-peptide kinetics are linear and time invariant also in the presence of glucose and insulin concentrations that vary in time, like during a meal, IVGTT or OGTT, [45], [75]. Hence, it is possible to reconstruct post-hepatic C-peptide rate of appearance (Ra); and since the liver dynamics are very rapid, C-peptide Ra is a good measure of pre-hepatic C-peptide secretion, and thus of SR.

4.2 C-PEPTIDE MODEL

The problem of estimating the insulin secretion profile in vivo during perturbation from plasma concentration measurements is a classic input estimation problem for which deconvolution offers the classic solution [77], [64]. Since there is solid evidence that C-peptide kinetics are linear in a wide range of concentration, the relationship between above basal pancreatic secretion (SR, the input), and the above basal C-peptide concentration measurements (C, the output) is the convolution integral:

$$Cp(t) = \int_0^\infty h(t-\tau) \cdot SR(t) \cdot d\tau \qquad\qquad 4.1$$

where $h(t)$ is the impulse response of the system. $SR(t)$ profile during a perturbation can be reconstructed by deconvolution given $Cp(t)$ and $h(t)$. The knowledge of the impulse response is thus needed. It is usually approximated as a sum of two exponentials, or with a two compartmental model as proposed by Eaton et al. [22]. Parameters can be fixed at standard values using the method proposed in [86].

The model assumes that C-peptide is secreted in a accessible compartment, $Cp_1(t)$, representing plasma and rapidly equilibrating tissues, from which it distributes into a peripheral extravascular compartment, $Cp_2(t)$, representative of tissues in slow exchange with plasma. Model equations are:

$$\dot{Cp}_1(t) = -(k_{01} + k_{21}) \cdot Cp_1(t) + k_{12} \cdot Cp_2(t) + SR(t) \quad Cp_1(0) = Cp_{1b}$$

$$\dot{Cp}_2(t) = k_{21} \cdot Cp_1(t) - k_{12} \cdot Cp_2(t) \qquad\qquad Cp_2(0) = Cp_{2b} = \frac{Cp_{1b} \cdot k}{k_{12}} \qquad 4.2$$

where $Cp_1(t)$ and $Cp_2(t)$ are C-peptide concentrations in the accessible and peripheral compartments (pmol/l). The overdot indicates time derivative; $Cp_1(t)$ is plasma C-peptide concentration in compartment 1; $Cp_2(t)$ is the equivalent concentration in compartment 2, equal to the C-peptide mass in compartment 2 divided by the volume of the accessible compartment; k_{12} and k_{21} (min^{-1}) are transfer rate parameters between compartments; k_{01} (min^{-1}) is the irreversible loss; $SR(t)$ (pmol/l per min^{-1}) is the pancreatic secretion entering the accessible compartment. Deconvolution allows us to measure in a virtually model-independent way insulin secretion after a glucose stimulus. However, using a mechanistic description of pancreatic insulin secretion as a function of plasma

glucose concentration has the advantage to provide quantitative indexes of beta-cell function.

The functional relationship between insulin secretion and plasma glucose concentration was firstly described by Grodsky et al. [36], it is based on the packet storage hypothesis of insulin secretion. Based on that Toffolo et al. proposed a minimal model which assumes that the pancreatic insulin secretion as function of glucose and glucose rate of change for intravenous glucose graded infusion [82], and then also during an oral test [9] (Figure 4. 1).
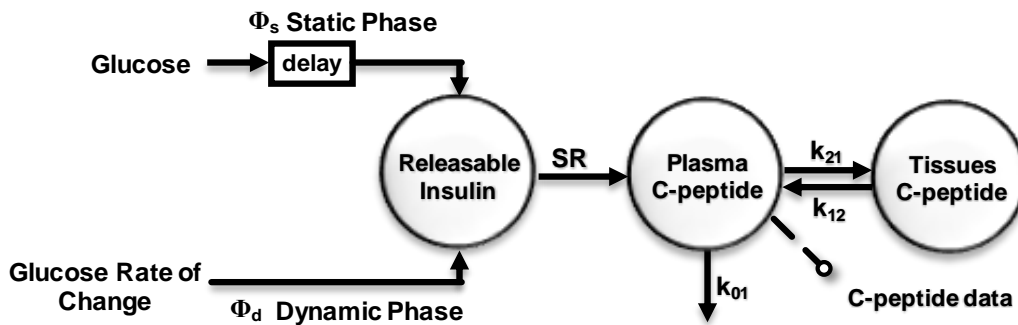
Figure 4. 1 – Graphic representation of the C-peptide model [82]

Hence SR(t) is described as the sum of three components:

$$SR(t) = SR_s(t) + SR_d(t) + SR_b \qquad 4.3$$

where SR_b is the insulin secretion rate at steady state, $SR_s(t)$ is the static secretion modulated by plasma glucose concentration (static glucose control); and $SR_d(t)$ is the dynamic secretion controlled by the rate of change of plasma glucose concentration (dynamic glucose control).

Over basal insulin secretion is given by the sum of the static and dynamic secretion components:

$$\Delta SR(t) = SR_s(t) + SR_d(t) \qquad\qquad 4.4$$

$SR_s(t)$ is assumed to be equal to the provision of new insulin in the β-cells, controlled by glucose concentration above a threshold level h:

$$\dot{SR}_s = -\alpha \cdot \left[SR_s(t) - \beta \cdot (G(t) - h) \right] \qquad\qquad 4.5$$

In response to an elevated glucose level, $SR_s(t)$ tends with a time constant $1/\alpha$ (min) toward a steady-state value linearly related via parameter β (min^{-1}) to glucose concentration G(t) (mg/dl) above the threshold h. Parameter β quantifies the static control of glucose on β-cells.

$SR_d(t)$ is assumed to represent the secretion of insulin stored in the β-cells in a promptly releasable form (labile insulin). The concept was introduced by Grodsky [36]. The idea is that labile insulin is not homogeneous with respect to the glucose stimulus: for a given glucose step, only a fraction of labile insulin is mobilized, so that more insulin can be rapidly released in response to a subsequent more elevated glucose step. In [36], it is assumed that the amount of released insulin, dQ(t), in response to a glucose increase from G(t) to G(t) + dG(t) is proportional to the glucose increase dG(t):

$$dQ(t) = K \cdot dG(t) \qquad\qquad 4.6$$

Toffolo thus assumed that one component of SR, $SR_d(t)$, is proportional to the derivative of glucose:

$$SR_d(t) = \begin{cases} \dfrac{dQ(t)}{dt} = K \cdot \dfrac{dG(t)}{dt} & \text{if} \quad \dfrac{dG(t)}{dt} > 0 \quad \text{and} \quad G(t) > G_b \\ 0 & \text{otherwise} \end{cases} \qquad\qquad 4.7$$

Parameter K quantifies the dynamic control of glucose on insulin secretion, i.e., the effect of the rate of change of glucose on insulin secretion when glucose concentration is increasing (positive $\dfrac{dG(t)}{dt}$).

From model parameters, β-cell static and dynamic responsivity indexes can be defined:

- the static sensitivity index to glucose, Φ_s ($10^{-9} \cdot min^{-1}$), measures the stimulatory effect of a glucose stimulus on β-cell secretion at steady state and it is defined as the ratio between SR and glucose concentration above the threshold h:

$$\Phi_s = \frac{\int_0^\infty SR_s(t) \cdot dt}{\int_0^\infty [G(t) - h] \cdot dt} = \beta \qquad 4.8$$

- the dynamic sensitivity index to glucose, Φ_d (10^{-9}), measures the stimulatory effect of the rate of change of glucose on secretion of stored insulin, it is defined as the amount of insulin released in response to the maximum excursion of plasma glucose above basal concentration:

$$\Phi_d = \frac{\int_0^\infty SR_d(t) \cdot dt}{\int_0^\infty \frac{dG(t)}{dt} \cdot dt} = \frac{\int_{G_b}^{G_{max}} K \cdot dG}{G_{max} - G_b} = K \qquad 4.9$$

4.3 GOLD STANDARD METHOD TO QUANTIFY INCRETIN EFFECT

Incretin effect potentiates β-cell responsivity to glucose thus enhancing insulin secretion. Campioni et al. [11] proposed a method to quantify both insulin potentiation and β-cells responsivity to glucose by using C-peptide model [9]. Each subject is studied twice, first with an OGTT, and second with an isoglycemic intravenous glucose infusion (I-IVG). On the first occasion glucose is administered orally at time 0 min whereas on the second occasion a glucose infusion is initiated at 0 and given in amounts sufficient to match the glucose concentrations observed on the first occasion. Plasma glucose, C-peptide, and incretin hormone concentrations are then frequently measured. A mandatory condition to successfully quantify incretin effect with such methodology is that plasma glucose concentration during OGTT and I-IVG are virtually superimposable.

C-peptide model is identified on both data of OGTT and I-IVG allowing to reconstruct insulin secretion profiles during the oral (SR^{OGTT}) and the i.v. matched (SR^{I-IVG}) test. It is then possible to define the time course of the incretin potentiation as [11]:

$$P(t) = \frac{SR^{OGTT}(t) - SR^{I-IVG}(t)}{SR^{I-IVG}(t)} \qquad 4.10$$

Similarly, percent increases of the static and dynamic responsivity indexes can be derived as:

$$P_s = \frac{\Phi_s^{\,OGTT} - \Phi_s^{\,I\text{-}IVG}}{\Phi_s^{\,I\text{-}IVG}}$$

$$P_d = \frac{\Phi_d^{\,OGTT} - \Phi_d^{\,I\text{-}IVG}}{\Phi_d^{\,I\text{-}IVG}}$$

4.11

Finally, in order to compare results of the gold standard method with the potentiation index Π, which will be defined in Chapter 5, paragraph 5.5.1 as the percent increase of insulin secretion due to 1 pmol/l of circulating GLP-1, the average of over basal potentiation $P(t)$ is normalized by plasma GLP-1 concentration:

$$PI = \frac{\int_0^\infty \dfrac{\Delta SR^{\,OGTT}(t) - \Delta SR^{\,I\text{-}IVG}(t)}{\Delta SR^{\,I\text{-}IVG}(t)}}{\int_0^\infty GLP1(t)\cdot dt} \cdot 100$$

4.12

CHAPTER 5

MODELS OF GLP-1 ACTION ON INSULIN SECRETION

5.1 MODELING GLP-1 ACTION ON STATIC β-CELL RESPONSIVITY TO GLUCOSE

The identification results of C-peptide minimal model shown in Chapter 6, demonstrate that the C-peptide model is unable to fit plasma C-peptide concentration data in presence of GLP-1, since incretin effect is not taken in account in the model. Hence, a model that incorporates a mathematical description of the GLP-1 action on insulin secretion is required to properly reconstruct the insulin secretion rate profile from plasma C-peptide data in presence of GLP-1 stimuli.

Previous studies have suggested that incretins enhance both static and dynamic insulin secretion through a potentiation factor [11]. However the first set of models of GLP-1 action on insulin secretion proposed here, only consider a GLP-1 effect which acts on the static phase. This choice has been made due to protocol

design, described in detail in Chapter 3 paragraph 3.2, in which plasma glucose concentration is maintained almost constant around 150 mg/dl when GLP-1 is infused intravenously, resulting in a negligible dynamic insulin secretion. Four models of increasing complexity have been tested. Each assume a different description of potentiation effect of the plasma GLP-1 concentration on static β-cells sensitivity to glucose Φ_s:

- *Model 1: proportional*
- *Model 2: proportional plus derivative*
- *Model 3: non-linear (Michaelis-Menten)*
- *Model 4: non-linear (Michaelis-Menten) plus derivative.*

Model 1:

Model 1 assumes a proportional action of GLP-1 on static β-cell responsivity (Figure 5. 1):

$$\Phi_s^{GLP1} = \Phi_s \cdot \left(a \cdot GLPl(t) + 1\right) \qquad\qquad 5.1$$

with Φ_s being the static β-cell responsivity to glucose before GLP-1 infusion, GLP1 the over-basal GLP-1 concentration, and a model parameter.

Model 2:

Model 2 assumes a proportional plus a derivative action of GLP-1 on static β-cell responsivity (Figure 5. 2):

$$\Phi_s^{GLP1} = \begin{cases} \Phi_s \cdot \left(a \cdot GLP1(t) + b \cdot \dfrac{dGLP1(t)}{dt} + 1 \right) & \text{if} \quad \dfrac{dGLP1(t)}{dt} \geq 0 \\ \Phi_s \cdot \left(a \cdot GLP1(t) + 1 \right) & \text{otherwise} \end{cases} \qquad 5.2$$

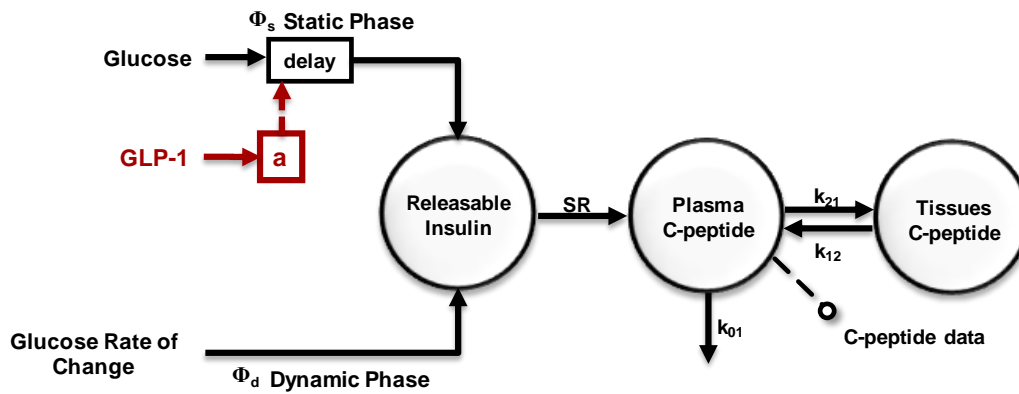with *a* and *b* model parameters representing the percentage increase of Φ_s due to the GLP-1 and GLP-1 rate of change respectively.

Model 3:

Model 3 assumes a nonlinear (Michaelis-Menten) action of GLP-1 on static β-cell responsivity (Figure 5. 3):

$$\Phi_s^{GLP1} = \Phi_s \cdot \left(\frac{c \cdot GLP1(t)}{d + GLP1(t)} + 1 \right) \qquad 5.3$$

with *c* and *d* model parameters representing respectively the maximum percentage increase of Φ_s due to GLP-1 and the value of the above basal GLP-1 concentration at which the half-maximum percentage increase is obtained, respectively:

$$\Phi_s^{GLP1}(\infty) = \Phi_s \cdot (c+1)$$

$$\frac{\Phi_s^{GLP1}(\infty) - \Phi_s(0)}{\Phi_s(0)} = \frac{\Phi_s \cdot (c+1) - \Phi_s}{\Phi_s} = c \qquad 5.4$$

$$\Phi_s^{GLP1}(d) = \Phi_s \cdot \left(\frac{c}{2} + 1 \right)$$

$$\frac{\Phi_s^{GLP1}(d) - \Phi_s(0)}{\Phi_s(0)} = \frac{\Phi_s \cdot \left(\dfrac{c}{2} + 1 \right) - \Phi_s}{\Phi_s} = \frac{c}{2} \qquad 5.5$$

Model 4:

Model 4 assumes a nonlinear (Michaelis-Menten) and derivative action of GLP-1 on static β-cell responsivity (Figure 5. 4):

$$\Phi_s^{GLP1} = \begin{cases} \Phi_s \cdot \left(1 + \dfrac{c \cdot GLPl(t)}{d + GLPl(t)} + b \cdot \dfrac{dGLPl(t)}{dt}\right) & \text{if } \dfrac{dGLPl(t)}{dt} \geq 0 \\[4ex] \Phi_s \cdot \left(1 + \dfrac{c \cdot GLPl(t)}{d + GLPl(t)}\right) & \text{otherwise} \end{cases} \qquad 5.6$$
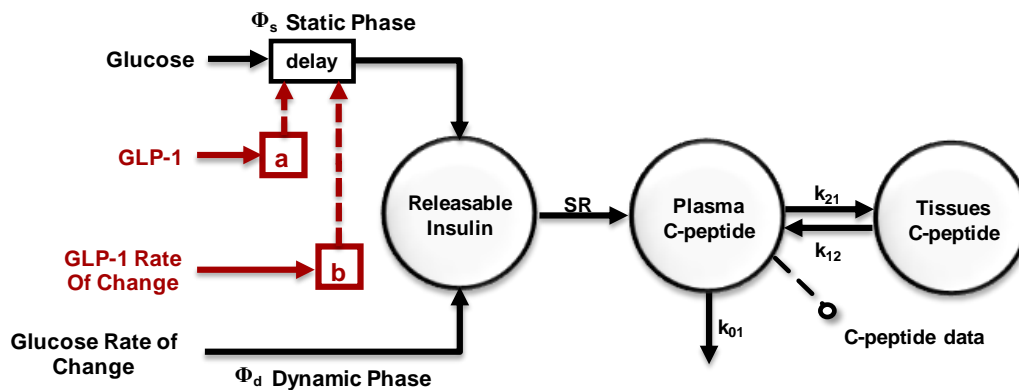

Figure 5. 1 – *Model 1* graphic representation

Figure 5. 2 – *Model 2* graphic representation
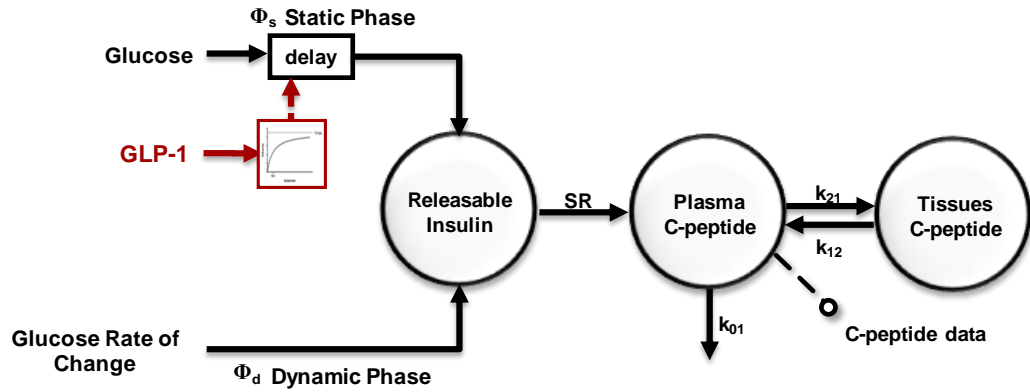
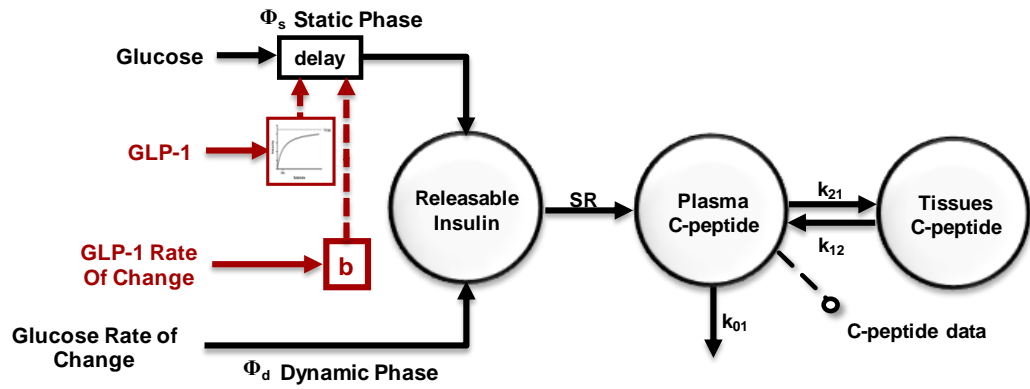**Figure 5. 3 –** *Model 3* **graphic representation**

Figure 5. 4 – *Model 4* **graphic representation**

5.1.1 GLP-1 potentiation index

It is useful to quantify the ability of GLP-1 to control insulin secretion through a potentiation index: Π. The index can be defined as the ratio between the average percentage increase of Φ_s and average plasma GLP-1 concentration. It represents the percent increase of the static responsivity index to glucose, due to 1 pmol/l of circulating GLP-1.

With this definition, Π (% per pmol/l) can be derived for all the above models.

Model 1 potentiation index:

In *Model 1*, Φ_s depends from the over basal GLP-1 concentration following the equation 5.1; with the definition reported above, Π is:

$$
\Pi = \frac{\int_0^\infty \dfrac{\Phi_s^{GLP1}(t) - \Phi_s}{\Phi_s} \cdot dt}{\int_0^\infty GLP1(t) \cdot dt} \cdot 100 = \frac{\int_0^\infty \dfrac{\Phi_s \cdot \left(a \cdot GLP1(t) + 1\right) - \Phi_s}{\Phi_s} \cdot dt}{\int_0^\infty GLP1(t) \cdot dt} \cdot 100 =
$$

$$
= \frac{\int_0^\infty \dfrac{\Phi_s \cdot \left(a \cdot GLP1(t) + 1 - 1\right)}{\Phi_s} \cdot dt}{\int_0^\infty GLP1(t) \cdot dt} \cdot 100 = \frac{\int_0^\infty a \cdot GLP1(t) \cdot dt}{\int_0^\infty GLP1(t) \cdot dt} \cdot 100 \qquad 5.7
$$

$$
= \frac{a \cdot \int_0^\infty GLP1(t) \cdot dt}{\int_0^\infty GLP1(t) \cdot dt} \cdot 100 = a \cdot 100
$$

Model 2 potentiation index:

In *Model 2*, Φ_s depends from the over basal GLP-1 concentration following the equation 5.2, thus the potentiation index Π is:

$$\Pi = \frac{\int_0^\infty \frac{\Phi_s^{GLP1}(t) - \Phi_s}{\Phi_s} \cdot dt}{\int_0^\infty GLP1(t) \cdot dt} \cdot 100 =$$

$$= \frac{\int_0^\infty \frac{\Phi_s \cdot \left(a \cdot GLP1(t) + b \cdot \frac{dGLP1(t)}{dt} + 1 \right) - \Phi_s}{\Phi_s} \cdot dt}{\int_0^\infty GLP1(t) \cdot dt} \cdot 100 =$$

$$= \frac{\int_0^\infty a \cdot GLP1(t) + b \cdot \frac{dGLP1(t)}{dt} \cdot dt}{\int_0^\infty GLP1(t) \cdot dt} \cdot 100 =$$

$$= \left(\frac{\int_0^\infty a \cdot GLP1(t) \cdot dt}{\int_0^\infty GLP1(t) \cdot dt} + \frac{\int_0^\infty b \cdot \frac{dGLP1(t)}{dt} \cdot dt}{\int_0^\infty GLP1(t) \cdot dt} \right) \cdot 100 =$$

$$= \left(a + b \cdot \frac{\int_0^\infty \frac{dGLP1(t)}{dt} \cdot dt}{\int_0^\infty GLP1(t) \cdot dt} \right) \cdot 100 =$$

5.8

then

$$\Pi = \left(a + b \cdot \frac{GLP1_{max}}{AUC[GLP1(t)]} \right) \cdot 100$$

with AUC, area under the curve and $GLP1_{max}$ the peak value of over-basal GLP-1 concentration.

Model 3 potentiation index:

In *Model 3*, Φ_s depends from the over basal GLP-1 concentration following the equation 4.17. Given the nonlinearity of *Model 3*, two potentiation indexes, at physiological Π_p and supra-physiological Π_{sp} GLP-1 levels, can be defined:

$$\Pi = \frac{\int_0^\infty \dfrac{\Phi_s^{GLP1}(t) - \Phi_s}{\Phi_s} \cdot dt}{\int_0^\infty GLP1(t) \cdot dt} \cdot 100 = \frac{\int_0^\infty \dfrac{\Phi_s \cdot \left(\dfrac{c \cdot GLP1(t)}{d + GLP1(t)} + 1\right) - \Phi_s}{\Phi_s} \cdot dt}{\int_0^\infty GLP1(t) \cdot dt} \cdot 100 =$$

$$= \frac{\int_0^\infty \dfrac{c \cdot GLP1(t)}{d + GLP1(t)} \cdot dt}{\int_0^\infty GLP1(t) \cdot dt} \cdot 100$$

5.9

The argument of the integral at the numerator of equation 5.9 can be approximated with its Taylor series development stopped at the first term, in the closeness of the operating point GLP1*:

$$f(GLP1) \cong f(GLP1^*) + \frac{df(GLP1)}{dGLP1}\bigg|_{GLP1=GLP1^*} \cdot \left(GLP1 - GLP1^*\right) =$$

$$= \frac{c \cdot GLP1^*}{d + GLP1^*} + \frac{c \cdot d}{\left(d + GLP1^*\right)^2} \cdot \left(GLP1 - GLP1^*\right)$$

5.10

thus

$$\int_{Ti}^{Tj} f(GLP1) \cdot dt \cong$$

$$\cong \frac{c \cdot GLP1^*}{d + GLP1^*} \cdot \left(T_j - T_i\right) - \frac{c \cdot d \cdot GLP1^*}{\left(d + GLP1^*\right)^2} \cdot \left(T_j - T_i\right) + \frac{c \cdot d}{\left(d + GLP1^*\right)^2} \cdot AUC\left[GLP1(t)\right]_{Ti}^{Tj} =$$

$$= \frac{c \cdot GLP1^{*2}}{\left(d + GLP1^*\right)^2} \cdot \left(T_j - T_i\right) + \frac{c \cdot d}{\left(d + GLP1^*\right)^2} \cdot AUC\left[GLP1(t)\right]_{Ti}^{Tj}$$

5.11

Considering that f(GLP1) is zero before t=120 min, and approximating the integral in [0 ∞] with the integral in the observation period, the potentiation depends from GLP1* and the integration interval.

In the present experimental condition, two potentiation indexes can be defined.

For t < 180 min, where GLP-1 is infused to achieve physiological over basal GLP-1 concentrations (GLP1$_p$), one has:

$$
\Pi_p = \frac{\int_0^{180} f(GLP1) \cdot dt}{\int_0^{180} GLP1 \cdot dt} \cdot 100 \cong
$$

$$
\cong \frac{\dfrac{c \cdot GLP1_p^2}{\left(d + GLP1_p\right)^2} \cdot (180 - 120) + \dfrac{c \cdot d}{\left(d + GLP1_p\right)^2} \cdot AUC[GLP1(t)]_{120}^{180}}{AUC[GLP1(t)]} \cdot 100 =
$$

$$
= \left(\frac{c \cdot GLP1_p^2 \cdot (180 - 120)}{\left(d + GLP1_p\right)^2 \cdot AUC[GLP1(t)]_{120}^{180}} + \frac{c \cdot d}{\left(d + GLP1_p\right)^2} \right) \cdot 100
$$

5.12

For $180 < t < 240$ min, where GLP-1 is infused to achieve supra-physiological plasma GLP-1 concentrations (GLP1$_{sp}$), one has:

$$
\Pi_{sp} = \frac{\Pi_p \cdot AUC[GLP1(t)]_{120}^{180}}{AUC[GLP1(t)]_{120}^{240}} \cdot 100 +
$$

$$
+ \frac{\dfrac{c \cdot GLP1_{sp}^2 \cdot (240 - 180)}{(d + GLP1s_{op})^2} + \dfrac{c \cdot d}{(d + GLP1_{sp})^2} \cdot AUC[GLP1(t)]_{180}^{240}}{\cdot AUC[GLP1(t)]_{120}^{240}} \cdot 100
$$

5.13

with GLP1$_p$ the average over-basal GLP-1 concentration between 120 and 180 minutes and GLP1$_{sp}$ the average over-basal GLP-1 concentration between 180 and 240 minutes.

Model 4 potentiation index:

Similarly to *Model* 3, potentiation indexes can be derived from equation 5.6 for *Model 4*:

$$\Pi_p = \frac{c \cdot GLP1_p^2 \cdot (180 - 120)}{\left(d + GLP1_p\right)^2 \cdot AUC\left[GLP1(t)\right]_{120}^{180}} \cdot 100 +$$

$$+ \frac{c \cdot d}{\left(d + GLP1_p\right)^2} \cdot 100 + \qquad 5.14$$

$$+ b \cdot \frac{GLP1_{MAX}}{AUC\left[GLP1(t)\right]}$$

and

$$\Pi_{sp} = \frac{\Pi_p \cdot AUC\left[GLP1(t)\right]_{120}^{180}}{AUC\left[GLP1(t)\right]_{120}^{240}} \cdot 100 +$$

$$+ \frac{\dfrac{c \cdot GLP1_{sp}^2 \cdot (240 - 180)}{(d + GLP1_{sp})^2} + \dfrac{c \cdot d}{(d + GLP1_{sp})^2} \cdot AUC\left[GLP1(t)\right]_{180}^{240}}{\cdot AUC\left[GLP1(t)\right]_{120}^{240}} \cdot 100 + \qquad 5.15$$

$$+ b \cdot \frac{GLP1_{MAX}}{AUC\left[GLP1(t)\right]} \cdot 100$$

5.2 MODELING GLP-1 ACTION ON STATIC AND DYNAMIC β-CELL RESPONSIVITY TO GLUCOSE

Several study which investigated the incretin effect on insulin secretion, comparing OGTT against I-IVG data, reported that the presence of GLP-1 could induce a modification of the dynamic, which is related to exocytosis of readily releasable pool of docked granules, and static, which requires a replacement of the released docked granules from a large reserve pool to the plasma membrane followed by docking and preparation for release, insulin secretion due to a variation of β-cells responsivity to the glucose levels [1], [2], [19], [26], [32], [37], [39], [42], [47].

From literature it is known that GLP-1 only acts on the above-basal insulin secretion rate, while it has no effect on basal secretion, i.e. if glucose is at basal level an increase in plasma GLP-1 does not produce an increase in insulin secretion. For this reason models presented in the previous paragraph were modified to account for the insulin secretagogue effect of GLP-1 on both static and dynamic responsivity indexes, Φ_s and Φ_d respectively. In other words, GLP-1 potentiates the above basal insulin secretion rate, causing an increment in beta-cell responsivity indexes.

The assumption that both Φ_d and Φ_s are modulated by GLP-1 relies in particular on the evidence provided by Campioni et al. in [11], which demonstrates that both static and dynamic phase of insulin secretion are increased by incretins. As already stated here, the particular protocol design did not allow to verify this assumption. In fact, when GLP-1 is infused, glucose is approximately constant and dynamic insulin secretion is virtually absent. This makes it impossible to separately assess GLP-1 potentiation on Φ_d. However, we believe that, in light of the applicability of the model to different protocol designs, the GLP-1 action on dynamic insulin secretion, i.e. Φ_d, has to be included in the model.

Hence four models of GLP-1 action on static and dynamic β-cell insulin secretion are proposed and tested.

Model 5:

Model 5 assumes a proportional action of GLP-1 on static, Φ_s, and dynamic, Φ_d, β-cell responsivity. In principle one should assume a different effect of GLP-1 on static and dynamic components (Figure 5. 5):

$$\Phi_s^{GLP1} = \Phi_s \cdot \left(a_s \cdot GLP1(t) + 1\right)$$
$$\Phi_d^{GLP1} = \Phi_d \cdot \left(a_d \cdot GLP1(t) + 1\right)$$

5.16

with Φ_s and Φ_d respectively the static and dynamic beta-cell responsivity to glucose before GLP-1 infusion, GLP1 the over-basal GLP-1 concentration, a_s and a_d model parameters.

However, due to the protocol design, parameter a_d cannot be indentified with precision. Thus the following model, as all the models presented in this paragraph, will assume that the parameter which modulates the effect of GLP-1 on dynamic β-cells responsivity to glucose is equal to the static one; thus for *Model 5* one has: $a_s = a_d = a$.

Model 6:

Model 6 assumes a proportional plus derivative action of GLP-1 on Φ_s and Φ_d (Figure 5. 6):

$$\Phi_s^{GLP1} = \begin{cases} \Phi_s \cdot \left(a \cdot GLP1(t) + b \cdot \dfrac{dGLP1(t)}{dt} + 1 \right) & \text{if} \quad \dfrac{dGLP1(t)}{dt} \geq 0 \\ \Phi_s \cdot \left(a \cdot GLP1(t) + 1 \right) & \text{otherwise} \end{cases}$$

$$\Phi_d^{GLP1} = \begin{cases} \Phi_d \cdot \left(a \cdot GLP1(t) + b \cdot \dfrac{dGLP1(t)}{dt} + 1 \right) & \text{if} \quad \dfrac{dGLP1(t)}{dt} \geq 0 \\ \Phi_d \cdot \left(a \cdot GLP1(t) + 1 \right) & \text{otherwise} \end{cases}$$

5.17

with a and b model parameters representing the percentage increase of Φ_s and Φ_d due to the GLP-1 and GLP-1 rate of change respectively.

Model 7:

Model 7 assumes a nonlinear (Michaelis-Menten) action of GLP-1 on static, Φ_s and dynamic Φ_d β-cell responsivity (Figure 5. 7):

$$\Phi_s^{\text{GLP1}} = \Phi_s \cdot \left(\frac{c \cdot \text{GLP1(t)}}{d + \text{GLP1(t)}} + 1 \right)$$

$$\Phi_d^{\text{GLP1}} = \Phi_d \cdot \left(\frac{c \cdot \text{GLP1(t)}}{d + \text{GLP1(t)}} + 1 \right)$$

5.18

with c and d model parameters representing respectively the maximum percentage increase of Φ_s and Φ_d due to GLP-1 and the value of the above basal GLP-1 concentration at which the half-maximum percentage increase is obtained.

Model 8:

Model 8 assumes a nonlinear (Michaelis-Menten) and derivative action of GLP-1 on static, Φ_s β-cell responsivity (Figure 5. 8):

$$\Phi_s^{\text{GLP1}} = \begin{cases} \Phi_s \cdot \left(1 + \dfrac{c \cdot \text{GLP1(t)}}{d + \text{GLP1(t)}} + b \cdot \dfrac{d\text{GLP1(t)}}{dt} \right) & \text{if } \dfrac{d\text{GLP1(t)}}{dt} \geq 0 \\[4mm] \Phi_s \cdot \left(1 + \dfrac{c \cdot \text{GLP1(t)}}{d + \text{GLP1(t)}} \right) & \text{otherwise} \end{cases}$$

$$\Phi_d^{\text{GLP1}} = \begin{cases} \Phi_d \cdot \left(1 + \dfrac{c \cdot \text{GLP1(t)}}{d + \text{GLP1(t)}} + b \cdot \dfrac{d\text{GLP1(t)}}{dt} \right) & \text{if } \dfrac{d\text{GLP1(t)}}{dt} \geq 0 \\[4mm] \Phi_d \cdot \left(1 + \dfrac{c \cdot \text{GLP1(t)}}{d + \text{GLP1(t)}} \right) & \text{otherwise} \end{cases}$$

5.19

with b, c and d model parameters respectively the percentage increase of Φ_s and Φ_d due to GLP-1 rate of change respectively, the maximum percentage increase of Φ_s and Φ_d due to GLP-1 and the value of the above basal GLP-1 concentration at which the half-maximum percentage increase is obtained.
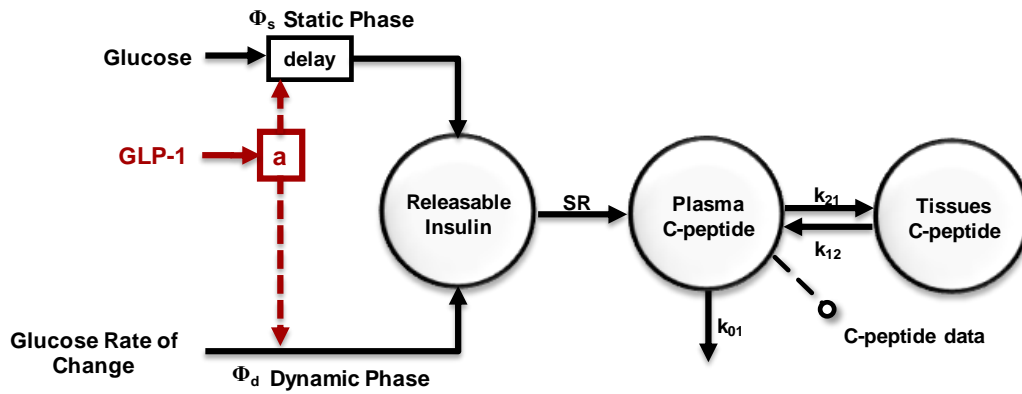
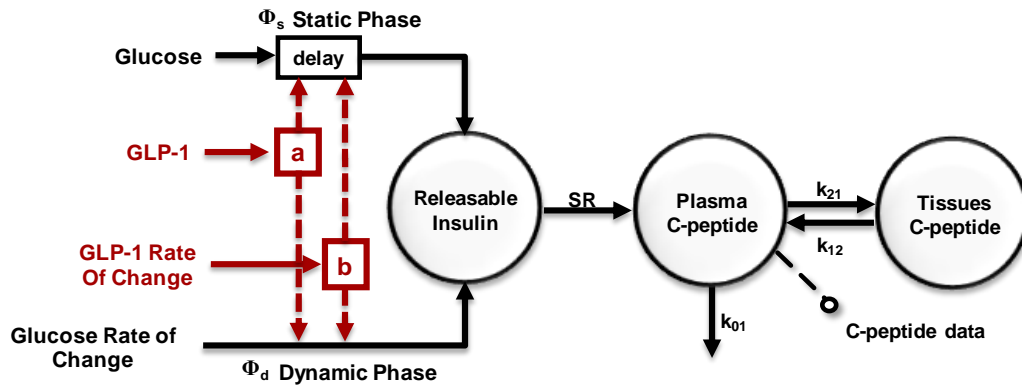**Figure 5. 5 –** *Model 5* **graphic representation**

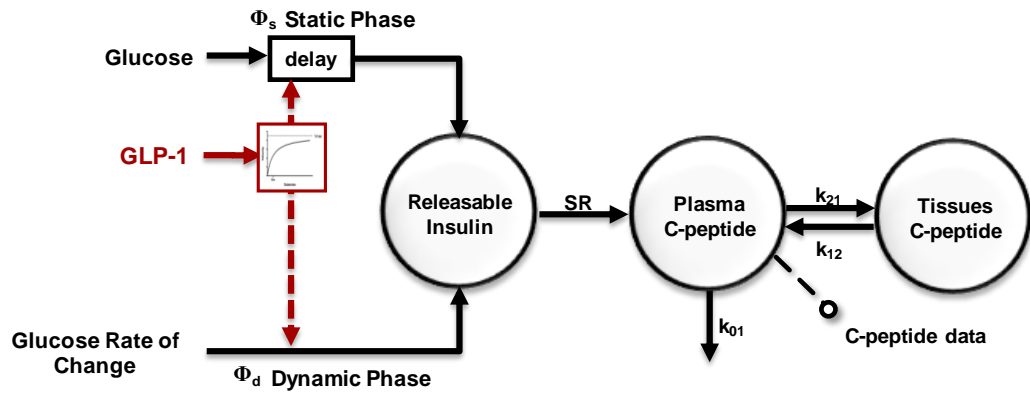**Figure 5. 6 –** *Model 6* **graphic representation**

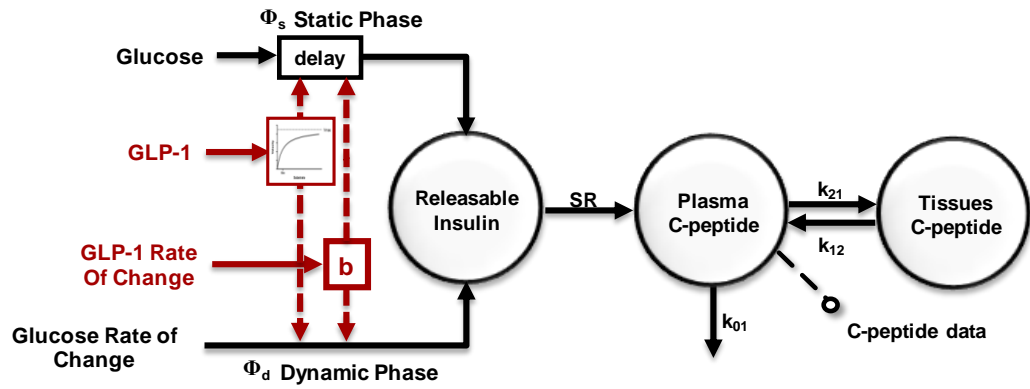**Figure 5. 7 –** *Model 7* **graphic representation**

Figure 5. 8 – *Model 8* **graphic representation**

5.2.1 Model reformulation

Given the formulation of the C-peptide secretion model, described in detail in Chapter 4, it is possible to demonstrate that describing GLP-1 action on Φ_s and Φ_d, it is equivalent to describe GLP-1 action on the above-basal insulin secretion rate.

In fact:

$$\Delta SR(t) = SR_s(t) + SR_d(t) \qquad\qquad 5.20$$

where

$$\dot{SR}_s(t) = -\alpha \cdot \left\{ SR_s(t) - \left[\beta \cdot \left(G(t) - h \right) \right] \right\} \qquad\qquad 5.21$$

or equivalently

$$
\begin{aligned}
SR(t) &= \beta \cdot Y(t) \\
\dot{Y}(t) &= -\alpha \cdot \left\{ Y(t) - \left[\left(G(t) - h \right) \right] \right\}
\end{aligned}
\qquad\qquad 5.22
$$

and

$$
SR_d(t) = \begin{cases} K \cdot \dfrac{dG(t)}{dt} & \text{if} \quad \dfrac{dG(t)}{dt} > 0 \quad \text{and} \quad G(t) > G_b \\ 0 & \text{otherwise} \end{cases}
\qquad\qquad 5.23
$$

thus given the definition of Φ_s and Φ_d, (equations 4.8 and 4.9) one can write:

$$\Delta SR(t) = SR_s(t) + SR_d(t) = \begin{cases} \Phi_s \cdot Y(t) + \Phi_d \cdot \dfrac{dG(t)}{dt} & \text{if } \dfrac{dG(t)}{dt} \geq 0 \\ \\ \Phi_s \cdot Y(t) & \text{if } \dfrac{dG(t)}{dt} < 0 \end{cases} \qquad 5.24$$

Moreover, under GLP1 stimulus, considering as example equations of *Model 6*, one obtains:

$$\Delta SR^{GLP1}(t) = \begin{cases} \Delta SR(t) \cdot \left(a \cdot GLP1(t) + b \cdot \dfrac{dGLP1(t)}{dt} + 1 \right) & \text{if } \dfrac{dGLP1(t)}{dt} \geq 0 \\ \\ \Delta SR(t) \cdot \left(a \cdot GLP1(t) + 1 \right) & \text{otherwise} \end{cases} \qquad 5.25$$

since:

$$\Delta SR^{GLP1}(t) = SR_s^{GLP1}(t) + SR_d^{GLP1}(t) \qquad 5.26$$

where for static secretion one has:

$$SR_s^{GLP1}(t) = \Phi_s^{GLP1} \cdot Y(t) \qquad 5.27$$

with

$$\Phi_s^{GLP1} = \begin{cases} \Phi_s \cdot \left(a \cdot GLP1(t) + b \cdot \dfrac{dGLP1(t)}{dt} + 1 \right) & \text{if } \dfrac{dGLP1(t)}{dt} \geq 0 \\ \\ \Phi_s \cdot \left(a \cdot GLP1(t) + 1 \right) & \text{otherwise} \end{cases} \qquad 5.28$$

thus

$$SR_s^{GLP1}(t) = \begin{cases} (\Phi_s \cdot Y(t)) \cdot \left(a \cdot GLP1(t) + b \cdot \dfrac{dGLP1(t)}{dt} + 1 \right) & \text{if} \quad \dfrac{dGLP1(t)}{dt} \geq 0 \\ (\Phi_s \cdot Y(t)) \cdot (a \cdot GLP1(t) + 1) & \text{otherwise} \end{cases} \qquad 5.29$$

Similarly for the dynamic secretion one has:

$$SR_d^{GLP1}(t) = \begin{cases} \Phi_d^{GLP1} \cdot \dfrac{dG(t)}{dt} & \text{if} \quad \dfrac{dG(t)}{dt} > 0 \quad \text{and} \quad G(t) > G_b \\ 0 & \text{otherwise} \end{cases} \qquad 5.30$$

with

$$\Phi_d^{GLP1} = \begin{cases} \Phi_d \cdot \left(a \cdot GLP1(t) + b \cdot \dfrac{dGLP1(t)}{dt} + 1 \right) & \text{if} \quad \dfrac{dGLP1(t)}{dt} \geq 0 \\ \Phi_d \cdot (a \cdot GLP1(t) + 1) & \text{otherwise} \end{cases} \qquad 5.31$$

thus

$$SR_d^{GLP1}(t) = \begin{cases} \text{if } \dfrac{dG(t)}{dt} \geq 0 \\ \quad \begin{cases} \left(\Phi_d \cdot \dfrac{dG(t)}{dt} \right) \cdot \left(a \cdot GLP1(t) + b \cdot \dfrac{dGLP1(t)}{dt} + 1 \right) & \text{if } \dfrac{dGLP1(t)}{dt} \geq 0 \\ \left(\Phi_d \cdot \dfrac{dG(t)}{dt} \right) \cdot (a \cdot GLP1(t) + 1) & \text{otherwise} \end{cases} \\ \text{if } \dfrac{dG(t)}{dt} < 0 \\ \quad 0 \end{cases} \qquad 5.32$$

and in conclusion one obtains:

$$\Delta SR^{GLP1}(t) = SR_s^{GLP1}(t) + SR_d^{GLP1}(t) =$$

$$
= \begin{cases}
\text{if } \dfrac{dG(t)}{dt} \geq 0 \\[2ex]
\begin{cases}
\left[\left(\Phi_s \cdot Y(t) + \Phi_d \cdot \dfrac{dG(t)}{dt}\right) \cdot \left(a \cdot GLP1(t) + b \cdot \dfrac{dGLP1(t)}{dt} + 1\right)\right] \text{if } \dfrac{dGLP1(t)}{dt} \geq 0 \\[3ex]
\left[\left(\Phi_s \cdot Y(t) + \Phi_d \cdot \dfrac{dG(t)}{dt}\right) \cdot \left(a \cdot GLP1(t) + 1\right)\right] \qquad \text{otherwise}
\end{cases} \\[5ex]
\text{if } \dfrac{dG(t)}{dt} < 0 \\[2ex]
\begin{cases}
\left(\Phi_s \cdot Y(t)\right) \cdot \left(a \cdot GLP1(t) + b \cdot \dfrac{dGLP1(t)}{dt} + 1\right) \quad \text{if } \dfrac{dGLP1(t)}{dt} \geq 0 \\[3ex]
\left(\Phi_s \cdot Y(t)\right) \cdot \left(a \cdot GLP1(t) + 1\right) \qquad\qquad \text{otherwise}
\end{cases}
\end{cases}
$$

5.33

Given the equivalence of the two representations of *Model 6*, it is possible to present the formulation of the model with GLP-1 modulating above basal insulin secretion, which provides a much more straight connection of the effect of GLP-1 on insulin secretion. For sake of brevity the equivalence of the two representations of GLP-1 action is reported in details only for *Model 6*, since one can easily apply the same procedure to the other models.

Then the action of GLP-1 on over basal insulin secretion of *Model 5, 6, 7* and *8* can be rewritten as follows:

Model 5:

$$\Delta SR^{GLP1}(t) = \Delta SR(t) \cdot \left(a \cdot GLP1(t) + 1\right)$$

5.34

with $\Delta SR(t)$ the glucose-dependent secretion rate before GLP-1 infusion, $\Delta SR^{GLP-1}(t)$ the glucose-dependent secretion rate after GLP-1 infusion, GLP1(t) the over-basal hormone concentration, and a model parameter.

*Model 6***:**

$$\Delta SR^{GLP1}(t) = \begin{cases} \Delta SR(t) \cdot \left(a \cdot GLP1(t) + b \cdot \dfrac{dGLP1(t)}{dt} + 1 \right) & \text{if} \quad \dfrac{dGLP1(t)}{dt} \geq 0 \\ \Delta SR(t) \cdot \left(a \cdot GLP1(t) + 1 \right) & \text{otherwise} \end{cases} \qquad 5.35$$

with a and b model parameters representing the percentage increase of ΔSR due to the GLP-1 and GLP-1 rate of change, respectively.

Model 7:

$$\Delta SR^{GLP1}(t) = \Delta SR(t) \cdot \left(1 + \frac{c \cdot GLP1(t)}{d + GLP1(t)} \right) \qquad 5.36$$

with c and d model parameters representing, respectively, the maximum percentage increase of ΔSR due to GLP-1 and the value of the above basal GLP-1 concentration at which the half-maximum percentage increase is obtained.

Model 8:

$$\Delta SR^{GLP1}(t) = \begin{cases} \Delta SR(t) \cdot \left(1 + \dfrac{c \cdot GLP1(t)}{d + GLP1(t)} + b \cdot \dfrac{dGLP1(t)}{dt} \right) & \text{if } \dfrac{dGLP1(t)}{dt} \geq 0 \\ \Delta SR(t) \cdot \left(1 + \dfrac{c \cdot GLP1(t)}{d + GLP1(t)} \right) & \text{otherwise} \end{cases} \qquad 5.37$$

with b, c and d as defined above.

5.2.2 GLP-1 potentiation index

GLP-1 potentiation index Π, can be redefined as the ratio between the average percentage increase in over-basal insulin secretion and average plasma GLP-1 concentration. With this definition, Π (% per pmol/l) can be derived for all the above models by adopting the same method employed in paragraph 5.5.1.

For *Model 5,* one has:

$$\Pi = a \cdot 100 \qquad\qquad 5.38$$

For *Model 6*:

$$\Pi = \left(a + b \cdot \frac{GLP1_{max}}{AUC[GLP1(t)]} \right) \cdot 100 \qquad\qquad 5.39$$

with AUC denoting the area under the curve and $GLP1_{max}$ the peak value of over-basal GLP-1 concentration.

With *Model 7* two potentiation indexes can be defined, as with *Model 3*:
for t < 180 min, where GLP-1 is infused to achieve physiological over basal GLP-1 concentrations ($GLP1_p$):

$$\Pi_p = \frac{\int_0^{180} f(GLP1) \cdot dt}{\int_0^{180} GLP1 \cdot dt} \cdot 100 \cong$$

$$\cong \frac{\dfrac{c \cdot GLP1_p^2}{\left(d + GLP1_p\right)^2} \cdot (180 - 120) + \dfrac{c \cdot d}{\left(d + GLP1_p\right)^2} \cdot AUC[GLP1(t)]_{120}^{180}}{AUC[GLP1(t)]} \cdot 100 =$$

$$= \left(\frac{c \cdot GLP1_p^2 \cdot (180 - 120)}{\left(d + GLP1_p\right)^2 \cdot AUC[GLP1(t)]_{120}^{180}} + \frac{c \cdot d}{\left(d + GLP1_p\right)^2} \right) \cdot 100 \qquad 5.40$$

and

$$\Pi_{sp} = \frac{\Pi_p \cdot AUC[GLP1(t)]_{120}^{180}}{AUC[GLP1(t)]_{120}^{240}} \cdot 100 +$$

$$+ \frac{\dfrac{c \cdot GLP1_{sp}^2 \cdot (240 - 180)}{(d + GLP1s_{op})^2} + \dfrac{c \cdot d}{(d + GLP1_{sp})^2} \cdot AUC[GLP1(t)]_{180}^{240}}{\cdot AUC[GLP1(t)]_{120}^{240}} \cdot 100 \qquad 5.41$$

Similarly potentiation indexes with *Model 8* are:

$$\Pi_p = \frac{c \cdot GLP1_p^2 \cdot (180 - 120)}{\left(d + GLP1_p\right)^2 \cdot AUC[GLP1(t)]_{120}^{180}} \cdot 100 +$$

$$+ \frac{c \cdot d}{\left(d + GLP1_p\right)^2} \cdot 100 + \qquad 5.42$$

$$+ b \cdot \frac{GLP1_{MAX}}{AUC[GLP1(t)]}$$

and

$$\Pi_{sp} = \frac{\Pi_p \cdot AUC[GLP1(t)]_{120}^{180}}{AUC[GLP1(t)]_{120}^{240}} \cdot 100 +$$

$$+ \frac{\dfrac{c \cdot GLP1_{sp}^2 \cdot (240 - 180)}{(d + GLP1_{sp})^2} + \dfrac{c \cdot d}{(d + GLP1_{sp})^2} \cdot AUC[GLP1(t)]_{180}^{240}}{\cdot AUC[GLP1(t)]_{120}^{240}} \cdot 100 +$$

$$+ b \cdot \frac{GLP1_{MAX}}{AUC[GLP1(t)]} \cdot 100$$

5.43

CHAPTER 6

IDENTIFICATION

6.1 INTRODUCTION

In this chapter identification of the C-peptide minimal model (described in Chapter 4) and *Models 1-8* (described in Chapter 5) against data of database 1 (described in Chapter 3, paragraph 3.2) is presented. Results on database 2 (described in Chapter 3, paragraph 3.3) prove the capability of the model to fit the data of oral test. Results on database 3 (described in Chapter 3, paragraph 3.4) will be discussed in the next chapter where model validation is tackled.

6.2 NUMERICAL IDENTIFICATION

Models parameters were estimated for each subject in each database, together with a measure of their precision, by applying weighted nonlinear least square methods [13] to plasma C-peptide concentration, as implemented in

SAAM II (Simulation Analysis and Modeling software) [4]. If some parameters are estimated with poor precision, Maximum A Posteriori (MAP) Bayesian estimator approach was adopted. Weights were chosen optimally, i.e. equal to the inverse of the variance of the C-peptide measurement errors, which was assumed to be independent, Gaussian, and with zero mean and known variance, equal to:

$$\sigma^2(Cp) = 2000 + 0.001 \cdot Cp(t)^2 \qquad\qquad 6.1$$

as proposed by Toffolo et al. in [84].

Plasma glucose and glucose rate of change, for the C-peptide model, together with plasma GLP-1, for *Models 1, 3, 5,* and 7, and GLP-1 rate of change for *Models 2, 4, 6,* and 8 were the models forcing functions assumed to be known without error. Of note, for database 2 and 3, total instead of active GLP-1 concentration was used. The choice of use total GLP-1 instead of active plasma GLP-1 concentration as forcing function is due to the extensive degradation of plasma active GLP-1 exerted by DPP-IV inhibitors; thus active GLP-1 may not show a response to small meals, hence, the sum of the intact hormone and its metabolite (i.e. total GLP-1) represents a better measure for estimation of GLP-1 effect on insulin secretion [40].

 Glucose, and GLP-1 concentrations were linearly interpolated between data. Since cost and blood volume considerations limited the number of glucose and GLP-1 data points available, time derivative were calculated on virtually continuous signals reconstructed by stochastic deconvolution [17]. Briefly, the method can be described as follows.

Let c(t) and u(t) being two continuous-time signals where

$$u(t) = \dot{c}(t) \qquad\qquad 6.2$$

for a generic t_0, one has the following integral:

$$c(t) = c(t_0) + \int_{t_0}^{t} u(\tau)d\tau \qquad\qquad 6.3$$

Assuming, for simplicity, $t_0 = 0$ and $c(0) = 0$, one can rewrite equation 6.3 as:

$$c(t) = \int_{0}^{t} g(t - \tau)u(\tau)d\tau = g(t) * u(t) \qquad\qquad 6.4$$

where g(t) is the step function, i.e. g(t) = 0 for t < 0 and g(t) = 1 for t ≥ 0, and the symbol '*' denotes convolution, thus equation 6.4 could be interpreted as a convolution integral (Figure 6. 1).

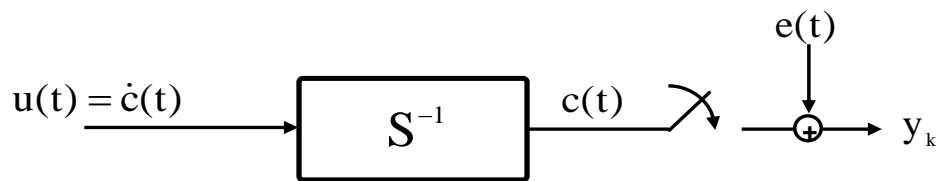**Figure 6. 1 – Deconvolution problem scheme**

The problem of recovering u(t) from the time-series {yk}, k=1, …n, of the noisy samples of c(t) is known as a deconvolution problem. It is well known that the deconvolution problem is ill-conditioned [17], [77]. However, regularization mwthod can be adopted to overcome this issue by taking into account the expectation on the smoothness of the unknown input signal.

The model numerical identification requires the knowledge of C-peptide kinetics parameters, k_{01} (min^{-1}), k_{21} (min^{-1}), k_{12} (min^{-1}). Estimation of kinetics parameters requires an additional experiment on the same subject, consisting of a bolus of C-peptide and a concomitant infusion of somatostatin to inhibit endogenous C-peptide secretion; however it is possible to eliminate the need for a separate experiment to assess kinetics parameters by adopting the method proposed by Van Cauter et al. in [86] to derive C-peptide kinetic parameters in an individual based

on anthropometric data: age, weight, height and gender. Thus kinetics parameters were fixed to standard population values:

$$k_{12} = FRA \cdot b_1 + (1 - FRA) \cdot a_1$$
$$k_{01} = \frac{a_1 \cdot b_1}{k_{12}} \qquad\qquad 6.5$$
$$k_{21} = a_1 \cdot b_1 - k_{12} - k_{01}$$

where

$$a_1 = 0.14$$
$$FRA = 0.76 \qquad\qquad 6.6$$
$$b_1 = \frac{\ln 2}{0.14 \cdot Age \cdot 29.16}$$

6.3 STATISTICAL ANALYSIS

Data are presented as mean ± SE, if not differently indicated. Two sample comparisons were done by Wilcoxon Signed Rank test (significance level set to 5%). Pearson's correlation was used to evaluate univariate correlation.

6.4 DATABASE 1: C-PEPTIDE MINIMAL MODEL

The experiment design of database 1 is described in detail in Chapter 3 paragraph 3.2. It can be divided into two parts based on the intravenous infusion of GLP-1. In fact from 0 to 120 min there is no GLP-1 infusion thus the protocol

is the same of a hyperglycemic clamp with plasma glucose clamped at 150 mg/dl; on the other hand from 121 to 240 min an intravenous GLP-1 infusion is started inducing a rise in the plasma C-peptide concentrations despite plasma glucose was kept steady at 150 mg/dl by varying the rate of intravenous glucose infusion:

Phase I *(0 – 120 min)*:   no GLP-1 infusion. The experiment design is the same of an hyperglycaemic clamp whit plasma glucose concentration level constant at value 150 mg/dl.

Phase II *(121 – 240 min)*:   The intravenous infusion of GLP-1 starts at rate of 0.75 pmol/Kg/min from minutes 121 to minutes 180; subsequently increasing to value 1.5 pmol/Kg/min from minutes 181 to minutes 240 min.

The C-peptide model was identified, as described in paragraph 6.2, using data of *Phase I*. Then, C-peptide model parameters were fixed and used to simulate *Phase II* plasma C-peptide concentrations. As expected, the C-peptide model is able to fit well the data of *Phase I*, as shown in Figure 6. 2, and provided a good precision of the parameters estimates:

$$K = 15.7 \ 10^{-9}, CV = 4\%$$
$$\alpha = 0.039 \ min^{-1}, CV = 18\%$$
$$\beta = 1.37 \ min^{-1}, CV = 6\%$$
$$h = 92 \ mg/dl, CV = 5\%$$

However, the C-peptide model is not able to predict plasma C-peptide data of *Phase II,* as shown in Figure 6. 2, since from 121 to 240 min the GLP-1 intravenous infusion induced a rise in the plasma C-peptide concentration levels despite plasma glucose concentration is kept at a steady concentration of 150

77

mg/dl. It would have been possible to *a priori* assume that the model would have not been able to predict *Phase II* data since it does not take in account the effect of GLP-1 on insulin secretion; Figure 6. 2 clearly points out the goodness of the C-peptide model prediction during *Phase I* and its inadequacy to simulate plasma C-peptide data of *Phase II*.

To further prove the inadequacy of the C-peptide minimal model to fit *Phase II*, the model was identified on plasma C-peptide data of both *Phase I* and *Phase II* (from 0 to 240 min). As expected, model fit of the data were clearly not satisfactory.

In conclusion it is possible to state that the C-peptide model proposed in [83] it is not able to adequately describe plasma C-peptide in presence of over-basal GLP-1 concentrations, since the model lacks of a mathematical description of the ability of the GLP-1 to enhance the secretion of insulin. Therefore a novel model is required to properly describe insulin secretion in presence of incretin hormone such as the GLP-1, which takes into account the so called incretin effect.

6.5 DATABASE 1: MODELS OF GLP-1 ACTION ON STATIC β-CELLS RESPONSIVITY

The models were numerically identified on C-peptide data by nonlinear least squares as described in detail in paragraph 6.2. *Model 1, 2, 3* and *4* fitted the data well as confirmed by inspection of visual predictive check (VPC) of models prediction vs plasma C-peptide data and the relative weighted residuals, which are shown in Figure 6. 3, Figure 6. 4, Figure 6. 5, Figure 6. 6. For all models weighted residuals presents zero mean and are sufficiently random.

The tested models provided precise estimates of models parameters, which are reported in Table 6. 1
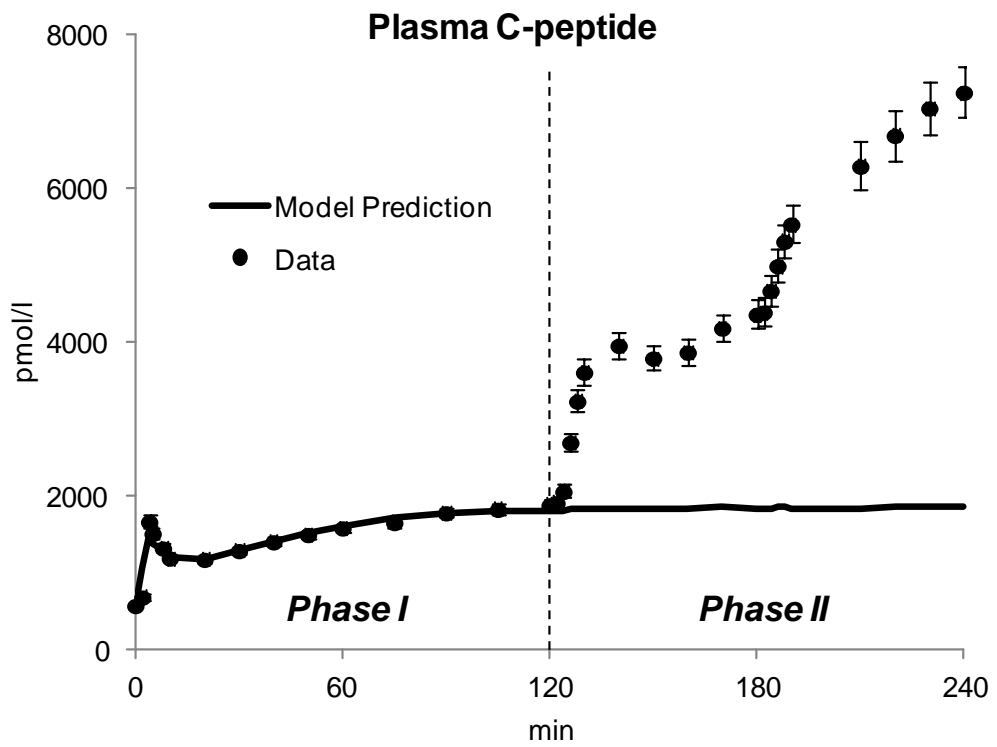
Figure 6. 2 – Average plasma C-peptide concentration data (black dots) vs average C-peptide model prediction (black line) of the average subject: model was identified on data of *Phase I* and then used to simulate data of *Phase II*

	Model 1	Model 2	Model 3	Model 4
α *[min⁻¹]*	0.035 ± 0.002 (10)	0.046 ± 0.001 (11)	0.039 ± 0.002 (10)	0.046 ± 0.001 (10)
h *[mg/dl]*	89.46 ± 1.20 (4)	90.69 ± 1.14 (4)	92.45 ± 1.19 (4)	92.96 ± 1.24 (4)
$K=\Phi_d$ *[10⁻⁹]*	260.347 ± 16.2393 (5)	259.8 ± 16.0 (5)	261.21 ± 17.15 (5)	247.63 ± 16.25 (5)
$\beta=\Phi_s$ *[10⁻⁹ min⁻¹]*	29.2 ± 2.00 (8)	21.5 ± 1.0 (8)	27.8 ± 1.67 (8)	24.1 ± 1.49 (8)
a *[l/pmol]*	0.13 ± 0.01 (7)	0.16 ± 0.01 (7)	-	-
b *[l×min/pmol]*	-	0.64 ± 0.07 (30)	-	0.46 ± 0.06 (31)
c *[dimensionless]*	-	-	7.21 ± 0.87 (17)	5.24 ± 0.97 (13)
d *[pmol/l]*	-	-	57.96 ± 10.19 (37)	60.94 ± 10.93 (39)

Table 6. 1 - Estimates of model parameters (mean±SE). Numbers between parenthesis represent CV%
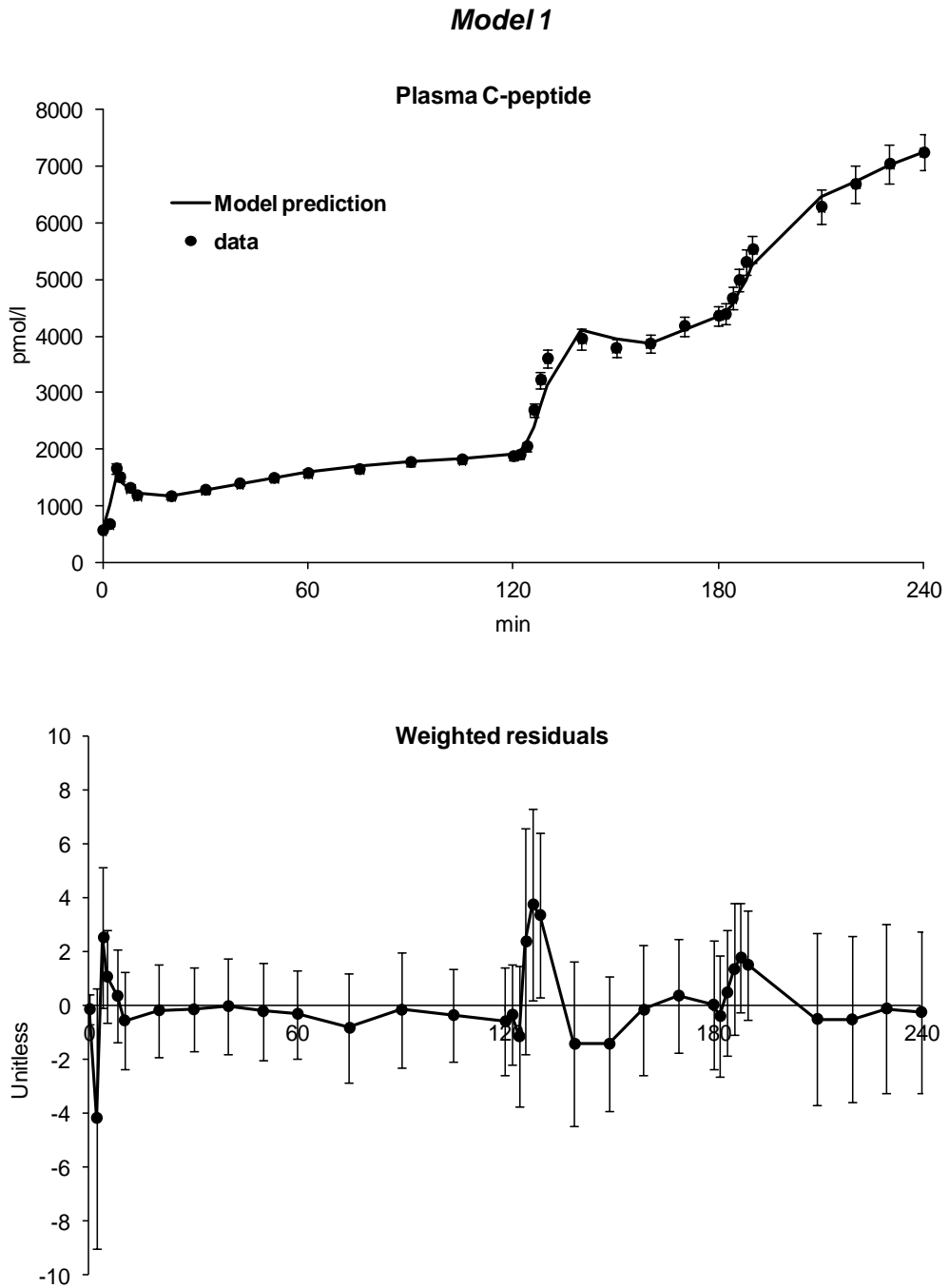
Model 1

Figure 6. 3 – Average (N = 88) model prediction vs C-peptide concentration data (upper panel) and weighted residuals (lower panel) of *Model 1*. Vertical bars represent SE for model prediction data and SD for weighted residuals
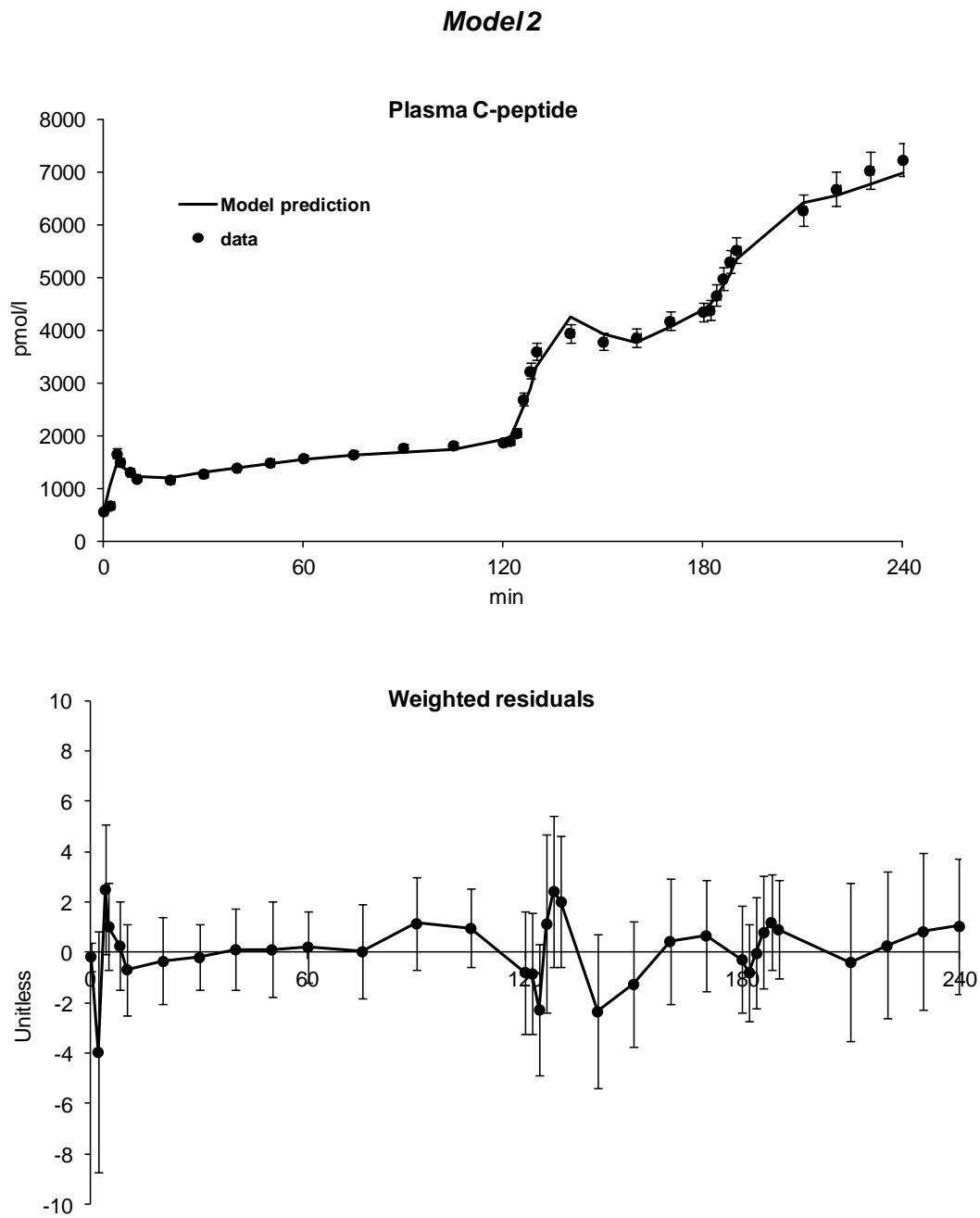
Model 2

Figure 6. 4 – Average (N = 88) model prediction vs C-peptide concentration data (upper panel) and weighted residuals (lower panel) of *Model 2*. Vertical bars represent SE for model prediction data and SD for weighted residuals
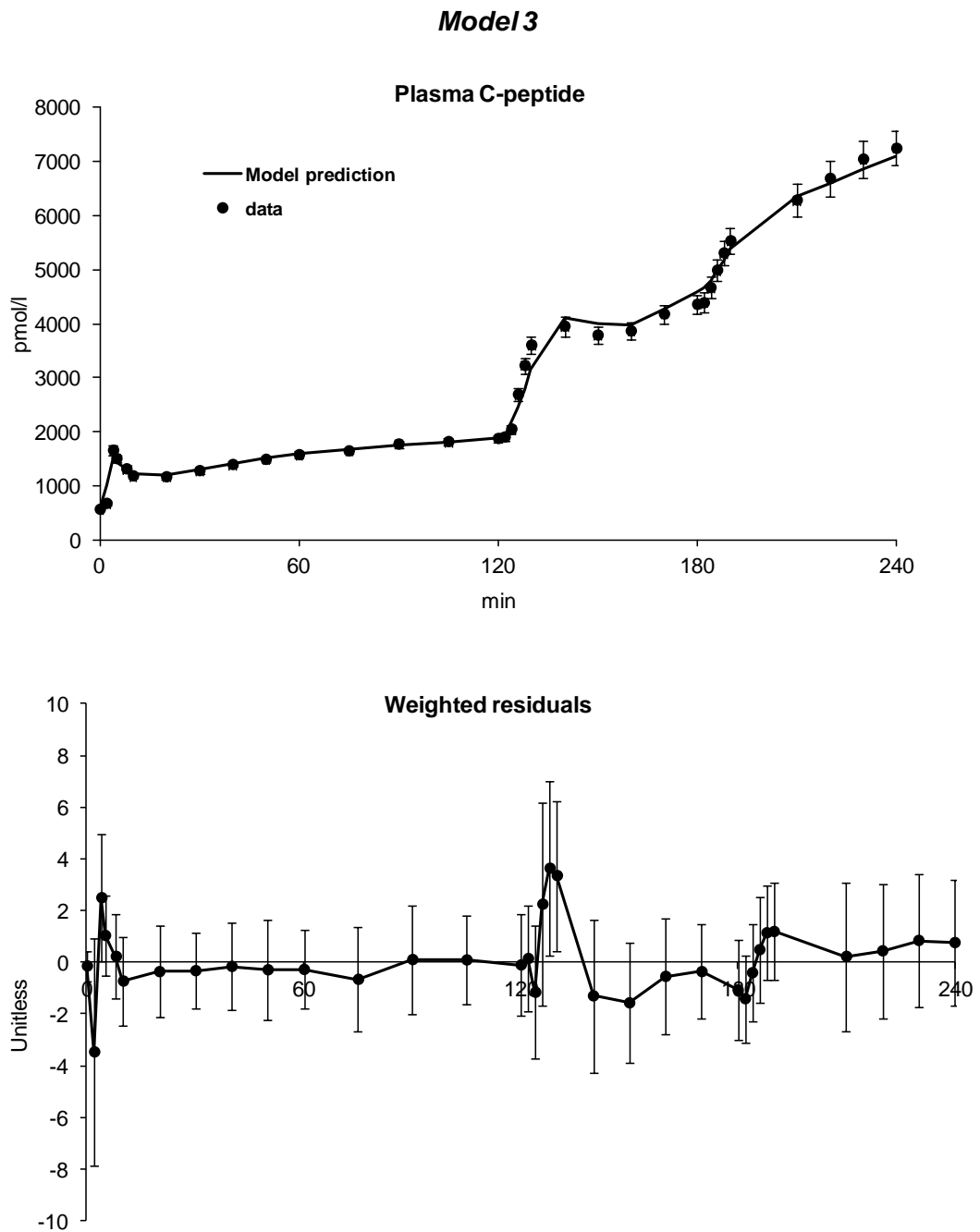
Model 3

Figure 6. 5 – Average (N = 88) model prediction vs C-peptide concentration data (upper panel) and weighted residuals (lower panel) of *Model 3*. Vertical bars represent SE for model prediction data and SD for weighted residuals
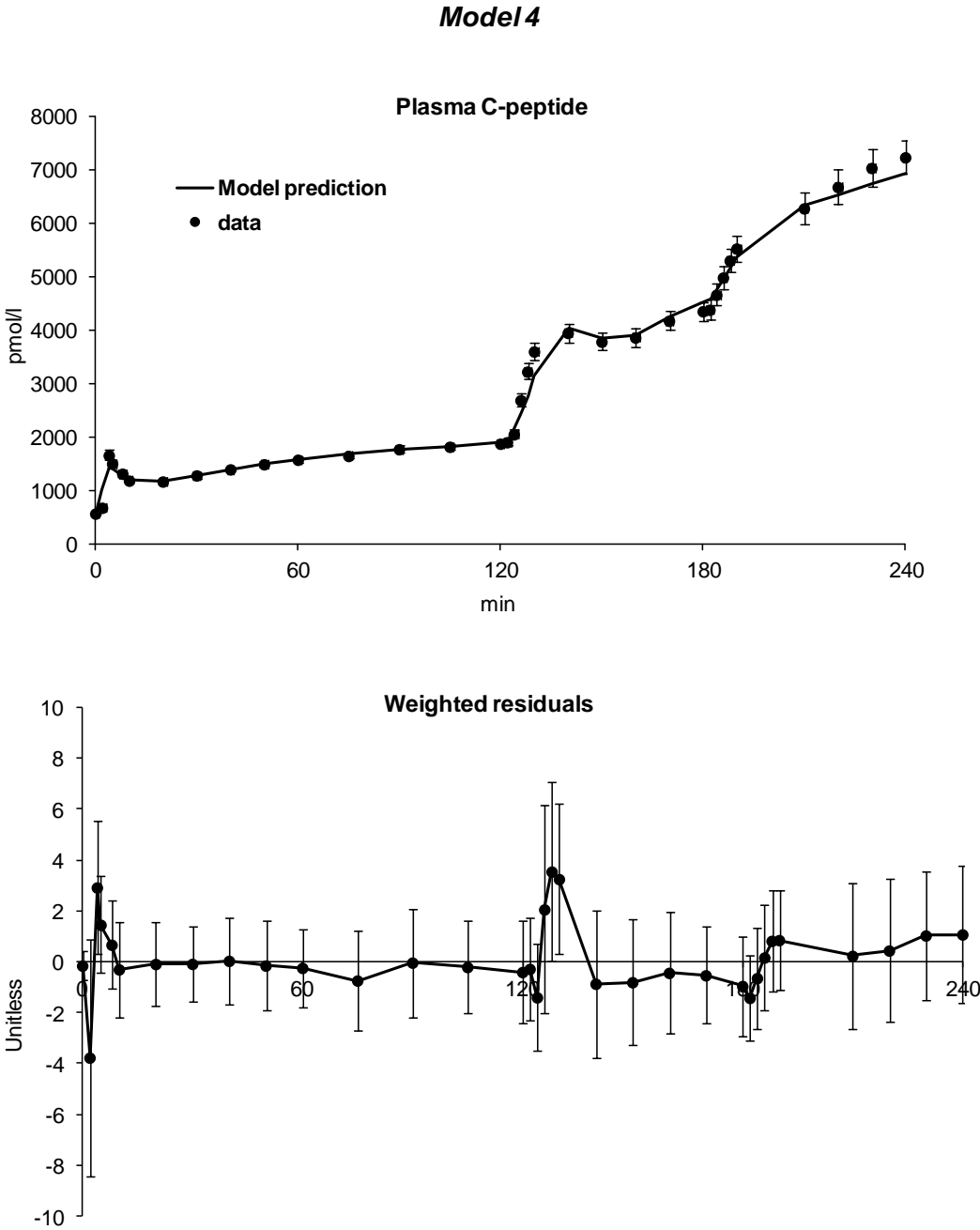
Model 4

Plasma C-peptide

Weighted residuals

Figure 6. 6 – Average (N = 88) model prediction vs C-peptide concentration data (upper panel) and weighted residuals (lower panel) of *Model 4*. Vertical bars represent SE for model prediction data and SD for weighted residuals

6.6 DATABASE 1: MODELS OF GLP-1 ACTION ON STATIC AND DYNAMIC β-CELLS RESPONSIVITY

The models were numerically identified on C-peptide data by nonlinear least squares as described in detail in paragraph 6.2. *Models 5, 6, 7,* and *8* fitted the data well; model predictions of plasma C-peptide vs data and time courses of weighted residuals obtained with the four models are shown in Figure 6. 7, Figure 6. 8, Figure 6. 9 and Figure 6. 10. *Model 8* provided on average the best fit. Model parameters are reported in Table 6. 2 together with their precision.

		Model 5	Model 6	Model 7	Model 8
α	$[min^{-1}]$	0.036 ± 0.002 (10)	0.042 ± 0.002 (10)	0.038 ± 0.002 (10)	0.043 ± 0.002 (10)
h	$[mg/dl]$	90.15 ± 1.20 (4)	90.25 ± 1.11 (4)	93.25 ± 1.17 (4)	91.84 ± 1.07 (4)
$K=\Phi_d$	$[10^{-9}]$	249.51 ± 16.18 (5)	245.7 ± 15.6 (5)	253.35 ± 16.28 (5)	246.72 ± 15.60 (5)
$\beta=\Phi_s$	$[10^{-9}\ min^{-1}]$	29.9 ± 2.00 (8)	25.25 ± 1.4 (8)	29.75 ± 1.87 (8)	25.77 ± 1.50 (8)
a	$[l/pmol]$	0.11 ± 0.01 (7)	0.12 ± 0.01 (6)	-	-
b	$[l\times min/pmol]$	-	0.62 ± 0.06 (21)	-	0.56 ± 0.06 (25)
c	$[dimensionless]$	-	-	6.4 ± 0.93 (16)	4.09 ± 0.86 (11)
d	$[pmol/l]$	-	-	60.73 ± 9.89 (36)	54.75 ± 10.76 (33)

Table 6. 2 – Estimates of model parameters (mean±SE). Numbers between parenthesis represent CV%

Model 5

Plasma C-peptide
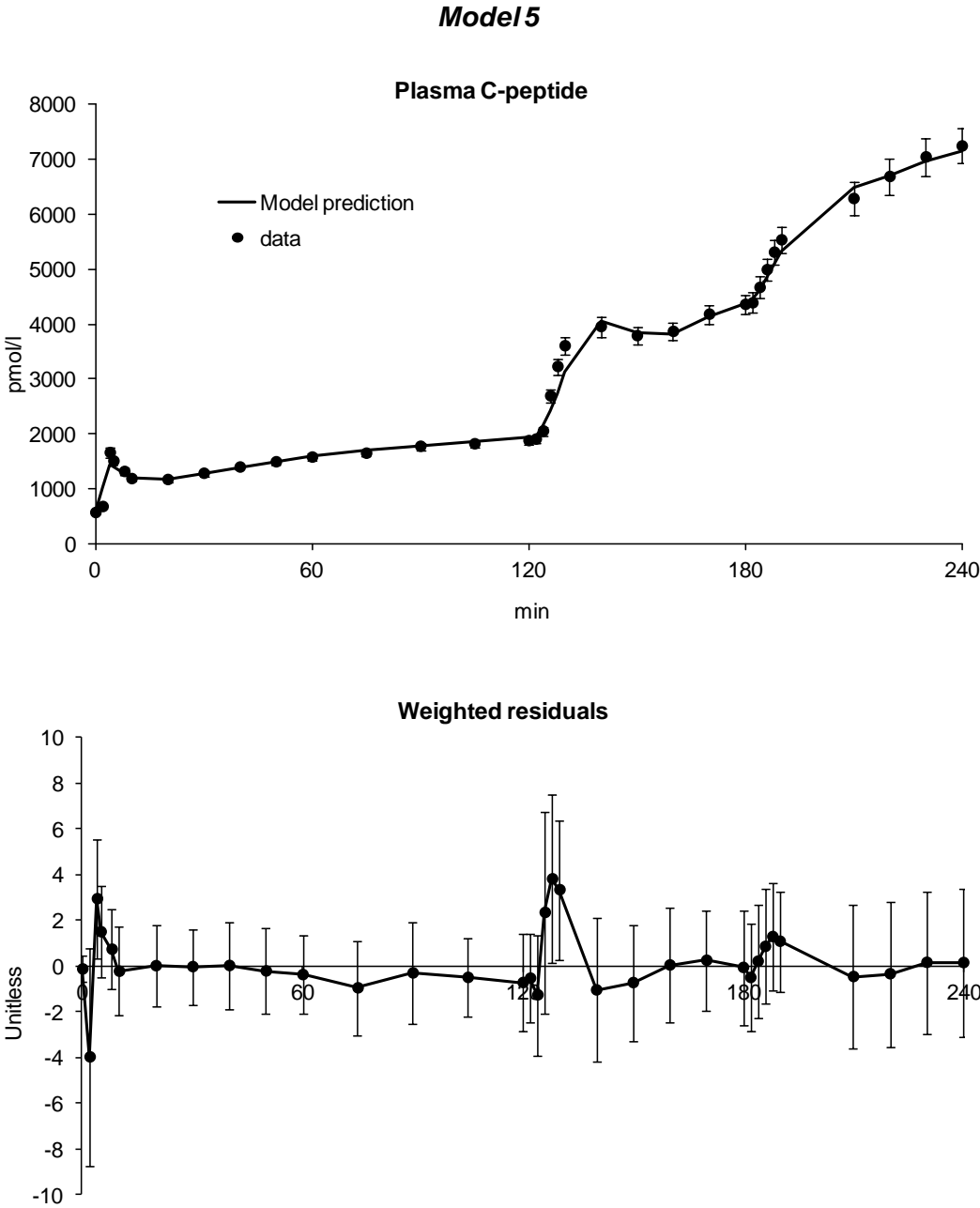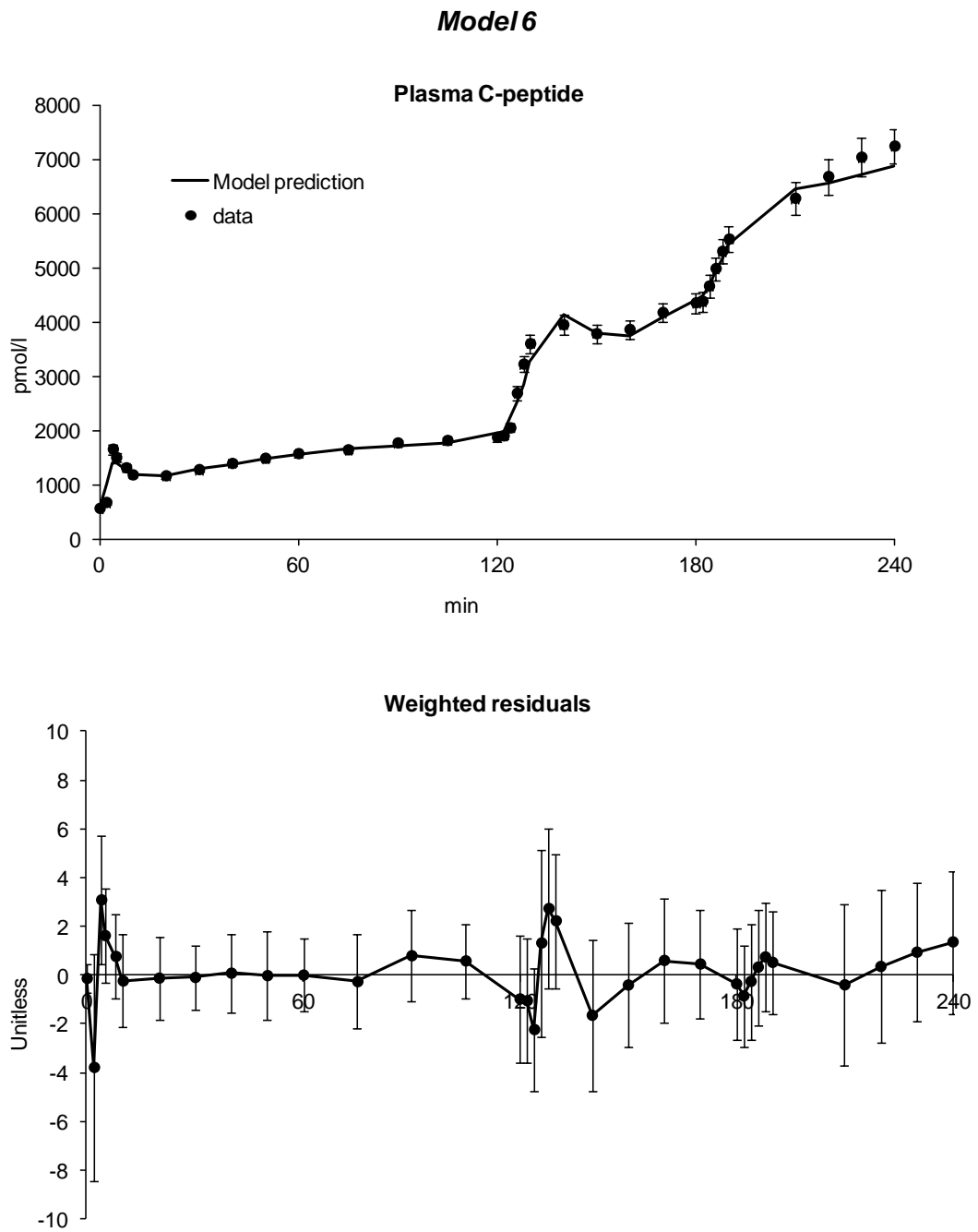

Weighted residuals

Figure 6. 7 – Average (N = 88) model prediction vs C-peptide concentration data (upper panel) and weighted residuals (lower panel) of *Model 5*. Vertical bars represent SE for model prediction data and SD for weighted residuals

Model 6

Plasma C-peptide

Weighted residuals

Figure 6. 8 – Average (N = 88) model prediction vs C-peptide concentration data (upper panel) and weighted residuals (lower panel) of *Model 6*. Vertical bars represent SE for model prediction data and SD for weighted residuals
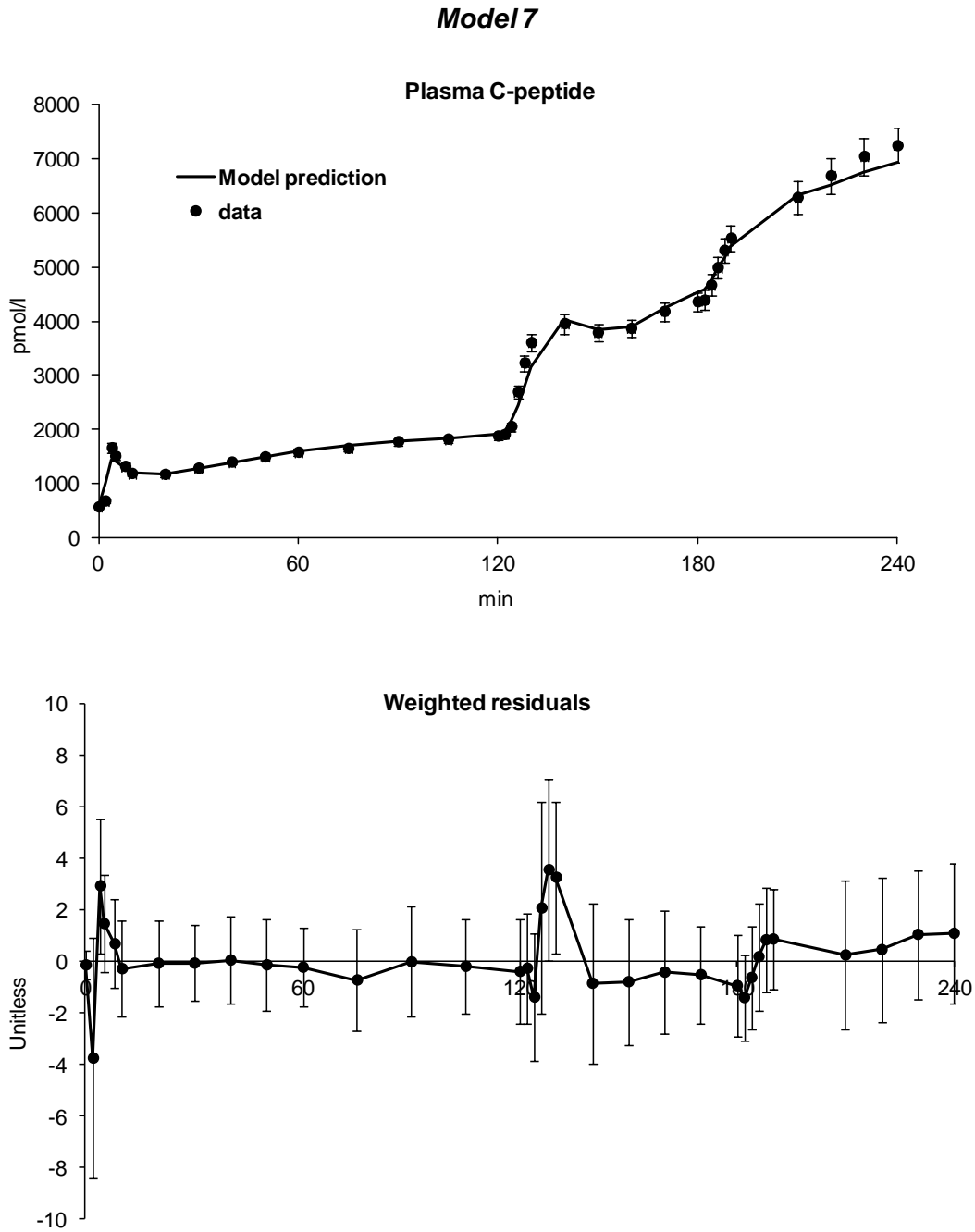
Model 7

Figure 6. 9 – Average (N = 88) model prediction vs C-peptide concentration data (upper panel) and weighted residuals (lower panel) of *Model 7*. Vertical bars represent SE for model prediction data and SD for weighted residuals

Model 8
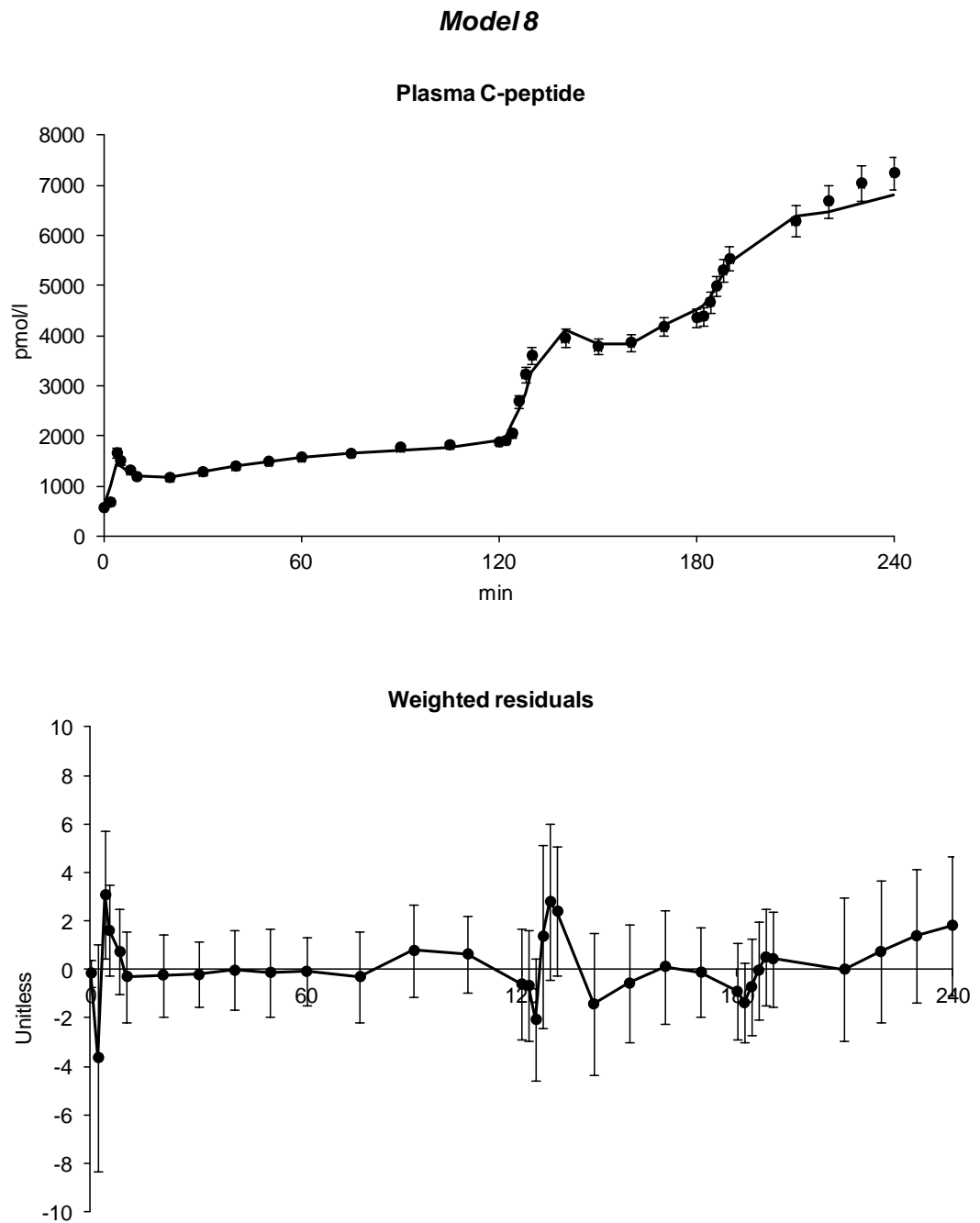
Plasma C-peptide

Weighted residuals

Figure 6. 10 – Average (N = 88) model prediction vs C-peptide concentration data (upper panel) and weighted residuals (lower panel) of *Model 8*. Vertical bars represent SE for model prediction data and SD for weighted residuals

6.7 MODEL SELECTION

Models were compared on the basis of standard criteria criteria [12]:

- ability to describe the data (Weighted Residual Square Sum, WRSS),
- precision of parameter estimates (expressed as CV),
- model parsimony (Akaike Information Criterion, AIC)
- residual independence (Anderson Run Test)

Table 6. 3 shows the quantitative criteria used for model selection. All the tested models fit the data sufficiently well as confirmed by the Run Test, which supported randomness of residuals in 65% of the subjects for the first set of models (*Model 1, 2, 3* and *4*) and 70% for the second set of models(*Model 5, 6, 7* and *8*). As expected, increasing the complexity of the model (and the number of parameters), worsens the precision of parameter estimates (increased CV). Among the models of GLP-1 action on static insulin secretion*Model 3* provided in average the best fit (lower Weighted Residual Sum of Squares, WRSS), with lower parsimonious index. Moreover it is of interest to note that *Model 4* reduces to simpler models in some cases: it collapsed to *Model 3* in 11% of the subjects, since parameter *b* tends to zero, to *Model 2* in 45% of the subject, since parameter d was very high, and even to *Model 1* in 22% of the subjects, since both changes in parameters b and d occurred. Similarly *Model 3* reduces to *Model 2* in 39% of the subjects since parameter d was very high, and *Model 2* reduces in *Model 1* in 10% of the subjects since parameter b goes to zero. From the analysis of the four models of GLP-1 action models on static β-cell insulin secretion, *Model 3* results the best able to reliably predict the C-peptide pattern during hyperglycemic clamp with exogenous GLP-1 infusion.

In overall the parsimony criterion indicates *Model 8* as the most parsimonious (lowest AIC). However, for *Model 4*, *Model 8* collapsed into simpler models in most cases: e.g. to *Model 7* in 11 subjects, since parameter b was zero, to *Model 6*

in 43 subjects, since parameter d was very high, and even to *Model 5* in 17 subjects, since both changes in parameters b and d occurred. Even if in the remaining 21 subjects *Model 8* was superior to the other models, it seems to be a better choice to select *Model 6* as the best model since it is the most parsimonious to adequately fit the data in most cases. Before GLP-1 infusion, beta-cell responsivity indexes in *Model 6*, were: $\Phi_s=25.2\pm1.4$ 10^{-9} min^{-1} and $\Phi_d=245.7\pm15.6$ 10^{-9}. Under GLP-1 stimulus, the potentiation index estimated with *Model 6* was $\Pi=12.6\pm0.7$ % per pmol/l. In addition, it provides estimates of the potentiation index only modestly different from that of *Model 8*, which is the most complex among the proposed models. In fact, if potentiation index was estimated with more complex models, similar results would have been obtained, e.g. with *Model 8* $\Pi=15.5\pm1.1$ % per pmol/l (correlation with *Model 6* index: R=0.95 p<0.001). This confirms that *Model 6*, despite being less accurate than *Model 8* in some cases, it still provides good estimates of the efficiency of the GLP-1 control on over-basal insulin secretion.

	Residual Independence (Run Test)	Data Fit (WRSS)	Precision (CV)	Parsimony Criterion (AIC)	N° Parameters	nonzero parameters %
Model 1	60%	284	7%	286	1	100%
Model 2	68%	250	30%	254	2	90%
Model 3	64%	243	37%	247	2	61%
Model 4	59%	246	39%	252	3	22%
Model 5	68%	192	7%	194	1	100%
Model 6	75%	145	13%	149	2	77%
Model 7	70%	163	28%	167	2	44%
Model 8	71%	109	28%	115	3	19%

Table 6. 3 – Models of GLP-1 action on insulin secretion comparison

In conclusion *Model 6* provides the better fit of C-peptide data and precise parameter estimates in the largest number of subjects. Moreover, it provides a precise estimate of the potentiation index measuring the ability of GLP-1 to promote the above-basal insulin secretion. To appreciate the meaning of this index consider that during hyperglycemic conditions (~150mg/dl): an increase of 5 pmol/l in peripheral GLP-1 concentrations, similar to that occurring after a meal, is predicted to induce a 63% increase in glucose-stimulated insulin secretion. This finding is comparable with the results reported in [11] for an OGTT, although the levels of GLP-1 were not reported.

Models 4-8 and their results have been published in [16].

6.8 DATABASE 2: ORAL GLP-1 MODEL

The ability to quantify the incretin effect could provide an important tool to better understand the pathophysiology of type 2 diabetes and measure response to specific therapy [8], [15], [62]. Model 6 was proved useful to assess GLP-1 potentiation in very challenging conditions, using data of hyperglycemic clamp with a concomitant exogenous GLP-1 intravenous infusion of database 1. However, such experimental design is not physiological and widely applicable. For this reason, it was investigated whether it were possible to identify Model 6 on C-peptide data measured during an oral test, such as a meal, in order to quantify GLP-1 action in a more physiological experimental condition.

To this purpose, we used database 2 glucose, C-peptide and GLP-1 concentrations measured in 22 subjects who underwent a mixed meal study [8], which is described in detail in Chapter 3, paragraph 3.3.

The model was numerically identified on C-peptide data by nonlinear least squares as described in detail in paragraph 6.2. However it was not possible to estimate with good precision all the parameters of *Model 6*, since parameter b

tends to zero, thus model derivative control of GLP-1 on insulin secretion was neglected, with the result that *Model 6* collapsed into *Model 5* in all the subjects. In fact, during the more physiological condition of a mixed meal C-peptide dynamics can be properly described with a simpler model, since signals dynamics of an oral glucose challenge result slower if compared to intravenous ones [9].

Model 5 was identified on data of baseline and treatment meal study in the 22 IFG subjects. Thus results are shown for each group of study subjects: placebo baseline (N = 11), sitagliptin baseline (N = 11), placebo treatment (N = 11) and sitagliptin treatment (N = 11).

Figure 6. 11, Figure 6. 12, Figure 6. 13 and Figure 6. 14 show the average model prediction against average C-peptide concentration for placebo baseline, sitagliptin baseline, placebo treatment and sitagliptin treatment. *Model 5* well described C-peptide data in all subjects. Indexes of β-cells responsivity and potentiation index Π were estimated with good precision for all subjects together with α and h. Average values are reported in Table 6. 4 and Table 6. 5.

The model allows to assess the profiles of the insulin secretion rate (SR) at basal GLP-1 concentration and the potentiated insulin secretion rate due to GLP-1 (SR^{GLP-1}), moreover it is possible to reconstruct the time course of incretin effect, Π(t). Profiles are shown in Figure 6. 15 and Figure 6. 16 only for placebo and sitagliptin baseline group, since as reported in detail in Chapter 8, there are no significant difference between baseline and treatment study. Maximum of potentiation is reached at 30 min with an increase of 74% and 49% of insulin secretion rate for placebo and sitagliptin subjects group respectively.

		Placebo					
		Baseline			Treatment		
α	$[min^{-1}]$	0.047 (10)	$\pm$	0.005	0.061 (11)	$\pm$	0.014
h	$[mg/dl]$	94 (2)	$\pm$	2	95 (2)	$\pm$	2
$K=\Phi_d$	$[10^{-9}]$	501 (13)	$\pm$	72	637 (14)	$\pm$	163
$\beta=\Phi_s$	$[10^{-9}\ min^{-1}]$	32.8 (6)	$\pm$	3.44	35.6 (6)	$\pm$	3.08
Π	$[\%]$	8.22 (35)	$\pm$	3.49	7.09 (33)	$\pm$	2.40

Table 6. 4 – Average values of estimated parameters for placebo subjects. CVs are reported between brackets.

		Sitagliptin					
		Baseline			Treatment		
α	$[min^{-1}]$	0.055 (11)	$\pm$	0.009	0.11 (13)	$\pm$	0.026
h	$[mg/dl]$	97 (3)	$\pm$	3	95 (2)	$\pm$	2
$K=\Phi_d$	$[10^{-9}]$	532 (16)	$\pm$	136	376 (30)	$\pm$	87
$\beta=\Phi_s$	$[10^{-9}\ min^{-1}]$	33.76 (6)	$\pm$	5.88	36.5 (5)	$\pm$	4.05
Π	$[\%]$	7.16 (23)	$\pm$	1.92	7.98 (25)	$\pm$	0.20

Table 6. 5 – Average values of estimated parameters for sitagliptin subjects. CVs are reported between brackets.
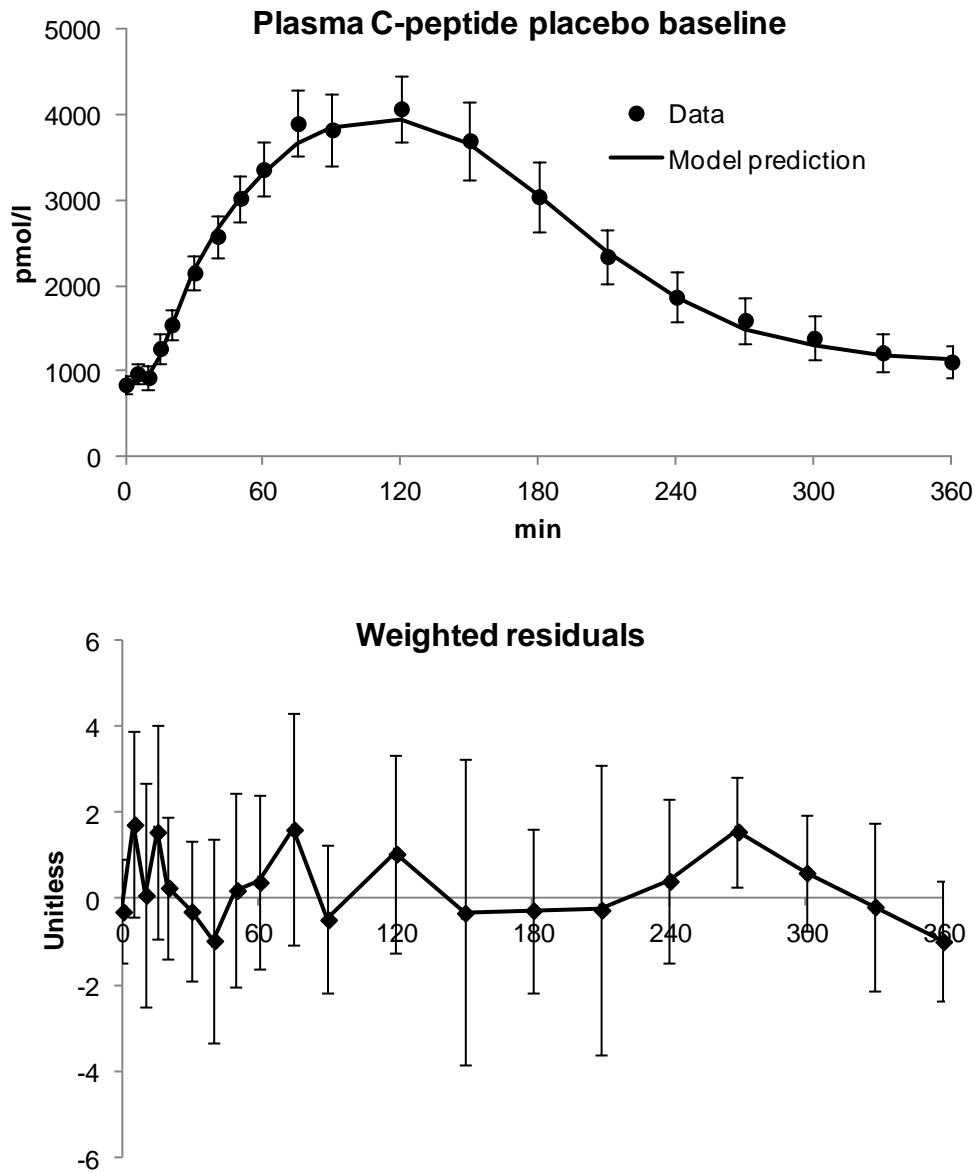
Figure 6. 11 – Average (N = 11) model prediction vs C-peptide concentration data (upper panel) and weighted residuals (lower panel) for placebo baseline group. Vertical bars represent SE for model prediction data and SD for weighted residuals
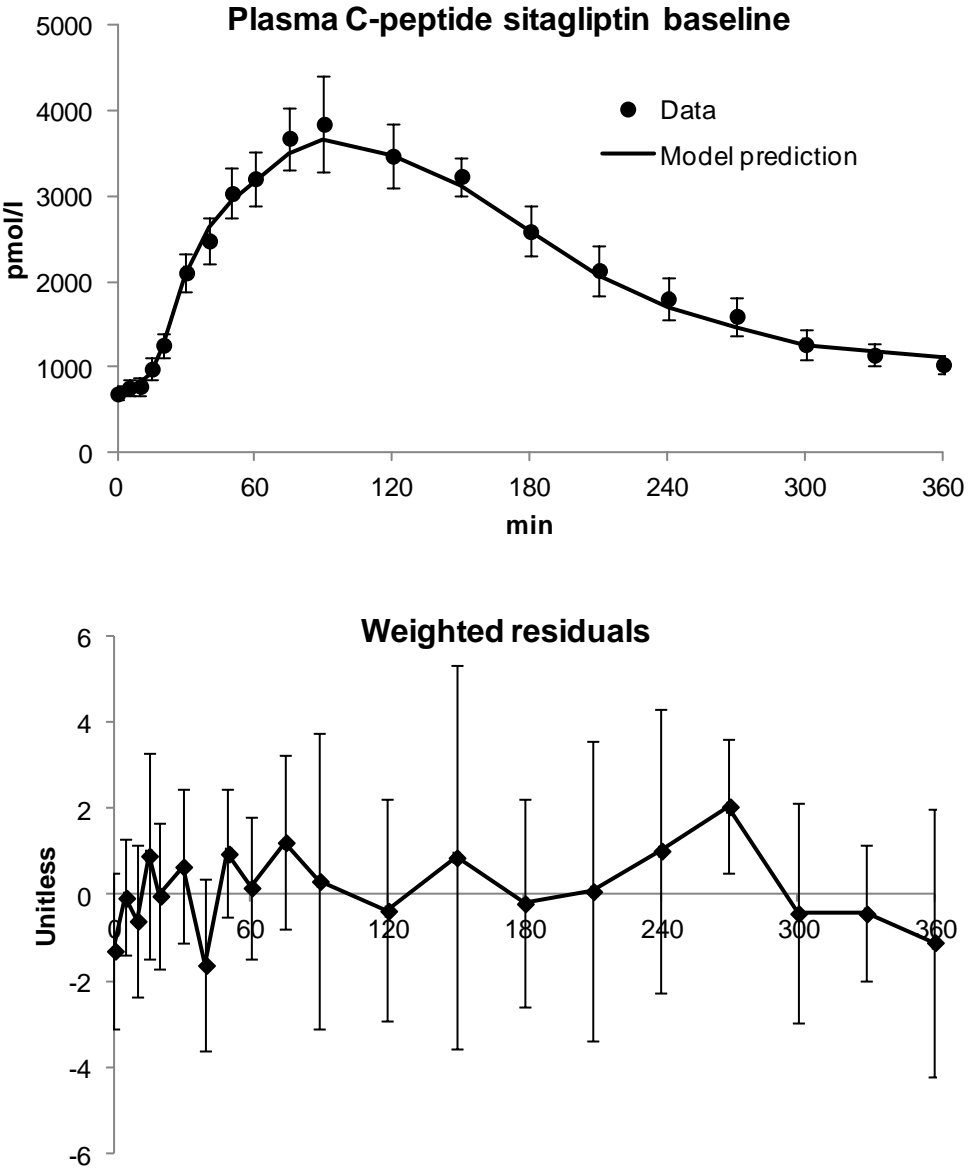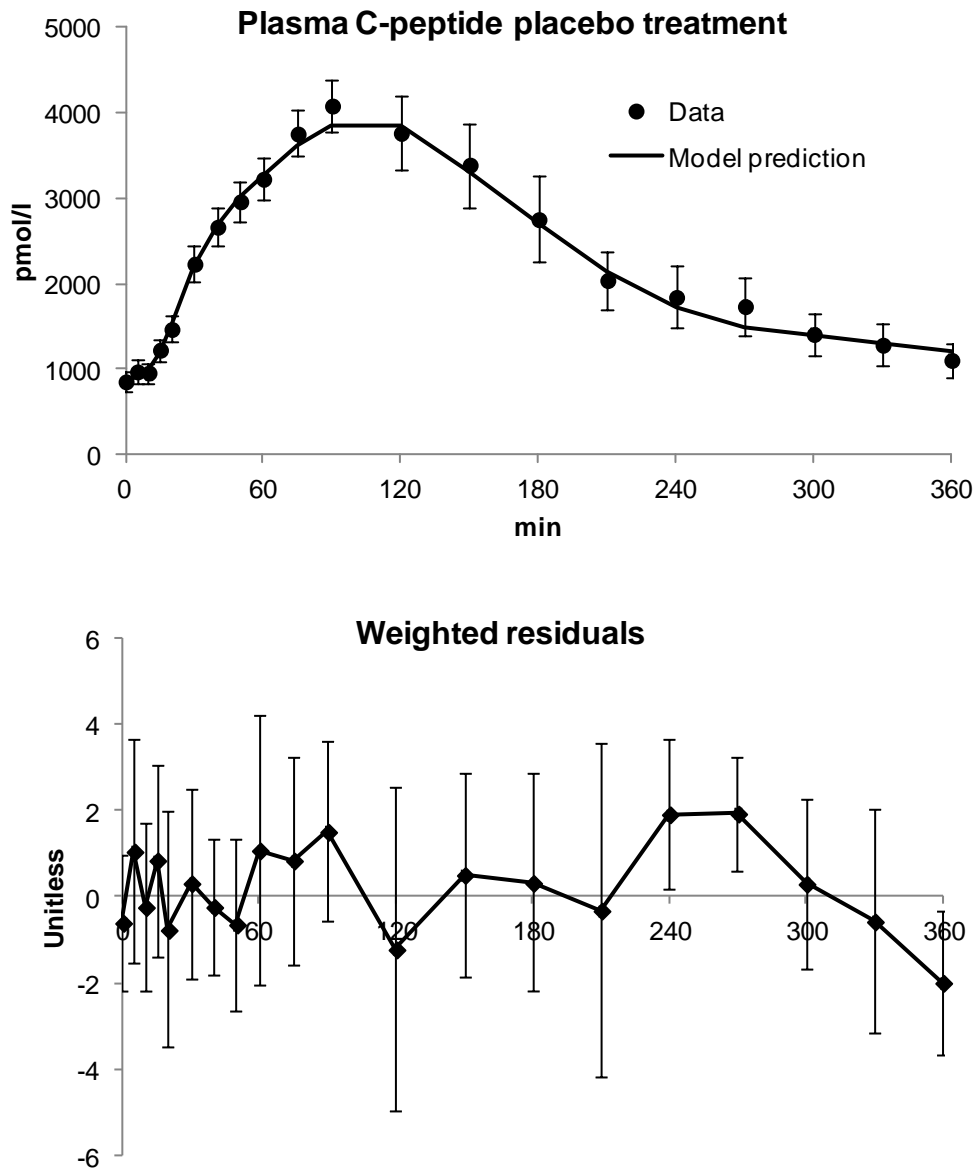
Figure 6. 12 – Average (N = 11) model prediction vs C-peptide concentration data (upper panel) and weighted residuals (lower panel) for sitagliptin baseline group. Vertical bars represent SE for model prediction data and SD for weighted residuals

Figure 6. 13 – Average (N = 11) model prediction vs C-peptide concentration data (upper panel) and weighted residuals (lower panel) for placebo treatment group. Vertical bars represent SE for model prediction data and SD for weighted residuals
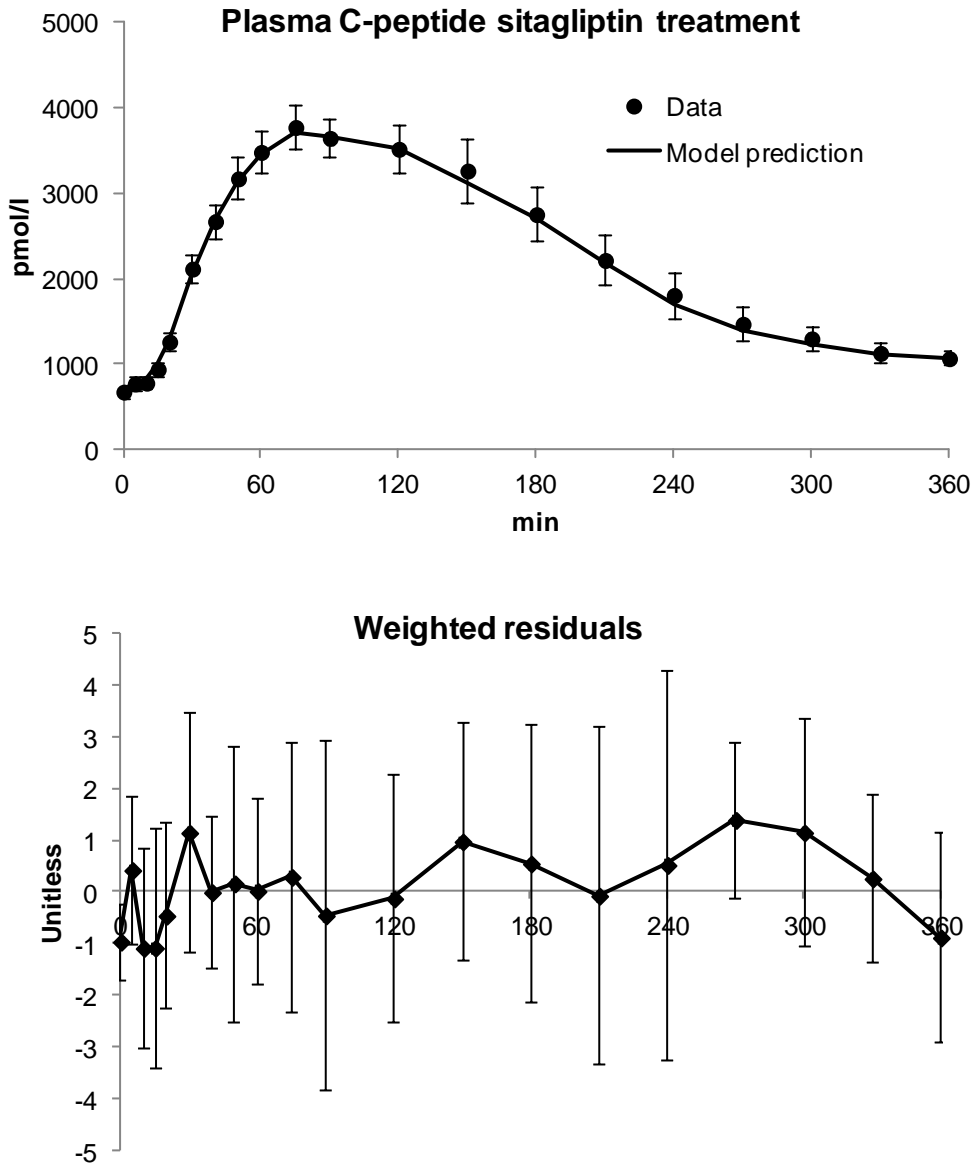
Figure 6. 14 – Average (N = 11) model prediction vs C-peptide concentration data (upper panel) and weighted residuals (lower panel) for sitagliptin treatment group. Vertical bars represent SE for model prediction data and SD for weighted residuals
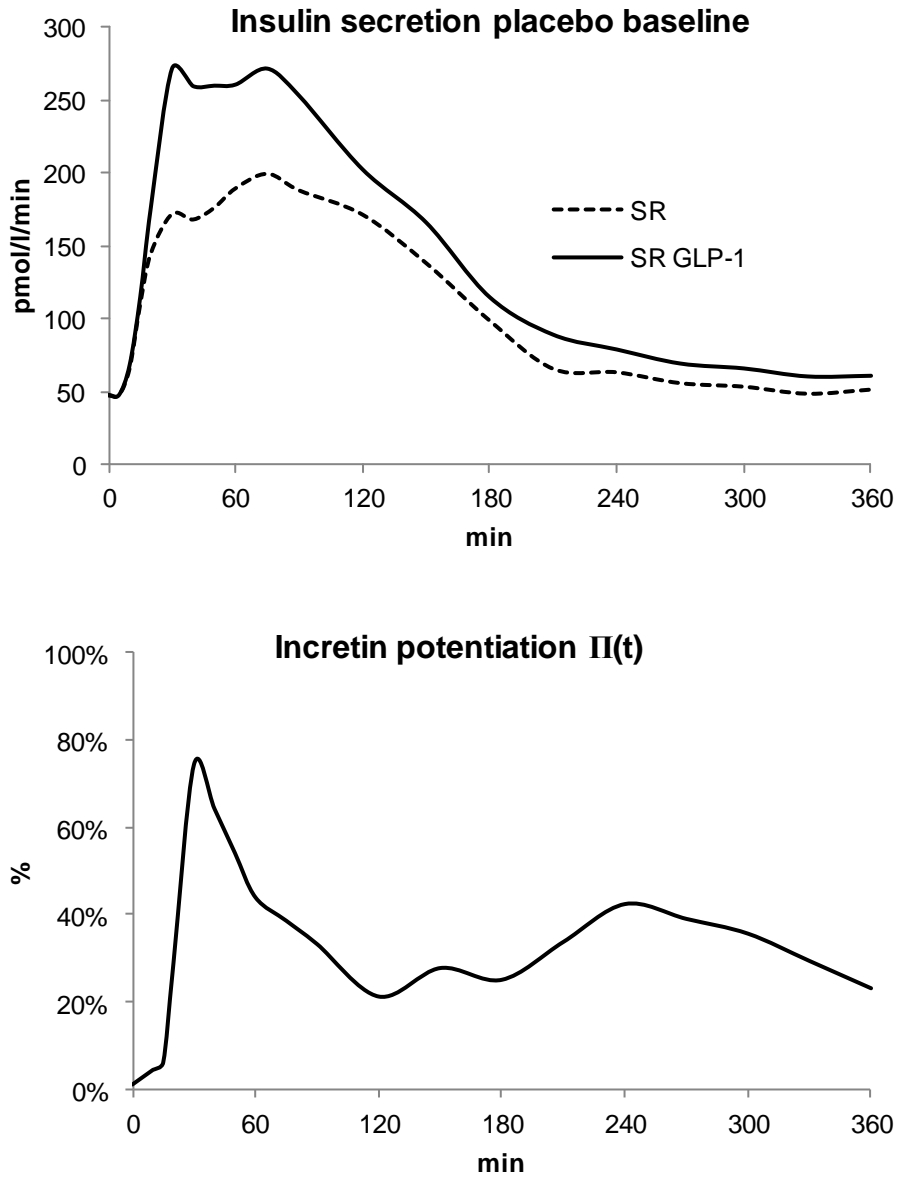
Figure 6. 15 – Average (N = 11) Insulin secretion (SR) vs potentiated insulin secretion due to GLP-1 (SR GLP-1) (upper panel) and incretin potentiation profile estimated in the placebo baseline group (lower panel)

Insulin secretion sitagliptin baseline
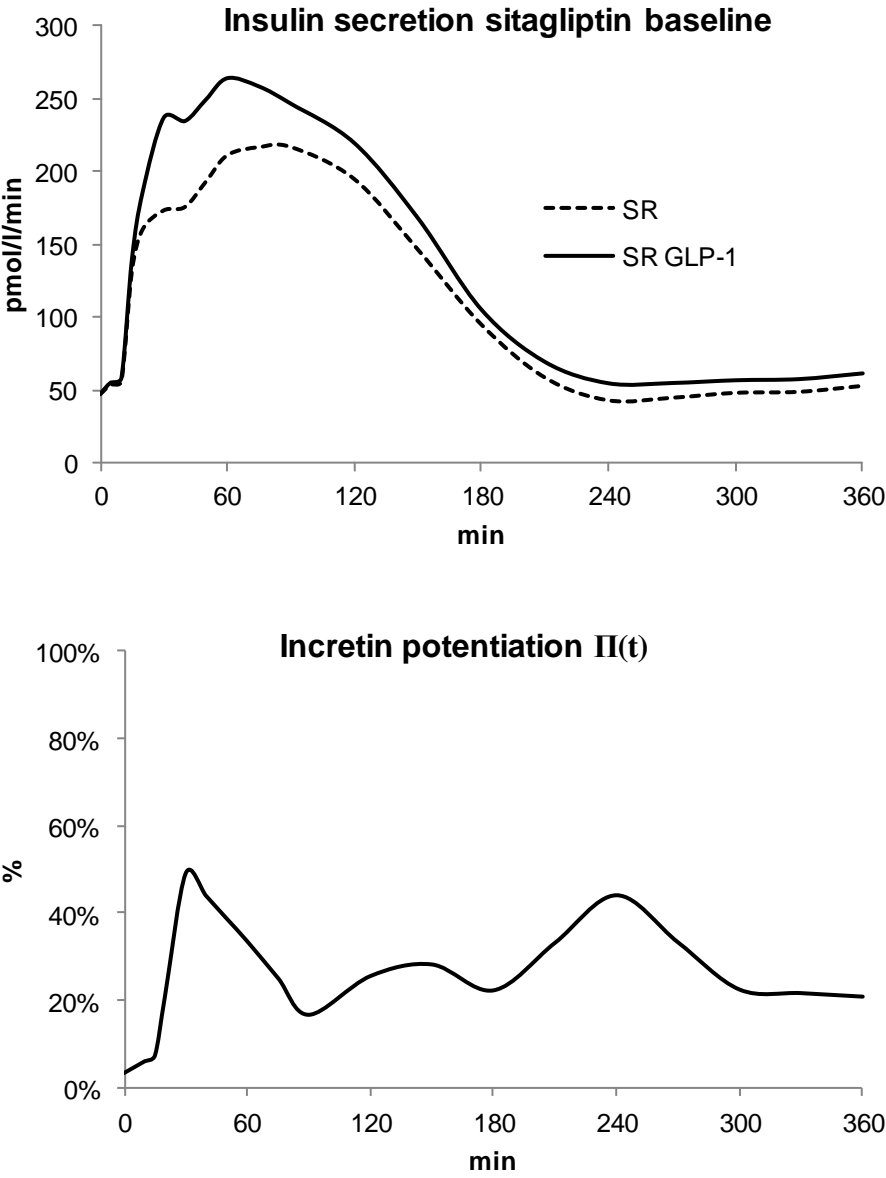
Incretin potentiation Π(t)

Figure 6. 16 – Average (N = 11) Insulin secretion (SR) vs potentiated insulin secretion due to GLP-1 (SR GLP-1) (upper panel) and incretin potentiation profile estimated in the sitagliptin baseline group (lower panel)

6.9 DATABASE 3: C-PEPTIDE MODEL

C-peptide model was identified on OGTT and I-IVG data of database 3 as described in paragraph 6.2. The model of C-peptide well describes both OGTT and I-IVG data, as shown by average model predictions vs average C-peptide in Figure 6. 17 and Figure 6. 18. Model parameters were estimated with good precision for all subjects and are reported in Table 6. 6. Results showed an increase of both static and dynamic β-cell responsivity indexes during the OGTT with respect to I-IVG; the mean increase was 68% for the static, Φ_s, (P=0.001) and 146% for the dynamic, Φ_d, (P=0.001) responsivity indexes, (Figure 6. 19). Time course of incretin effect P(t) was calculated as described in detail in paragraph 4.3, and shown in Figure 6. 20. Using equation 4.12 it was possible to assess potentiation index PI.

		OGTT			I-IVG		
α	$[min^{-1}]$	0.15	±	0.01	0.13	±	0.03
			(22)			(19)	
h	$[mg/dl]$	92	±	2	93	±	3
			(2)			(2)	
$K=\Phi_d$	$[10^{-9}]$	915	±	166	372	±	61
			(10)			(12)	
$\beta=\Phi_s$	$[10^{-9}\ min^{-1}]$	40.7	±	4.78	24.2	±	2.91
			(5)			(5)	
PI	$[\%\cdot pmol/l]$		1.93	±		0.53	

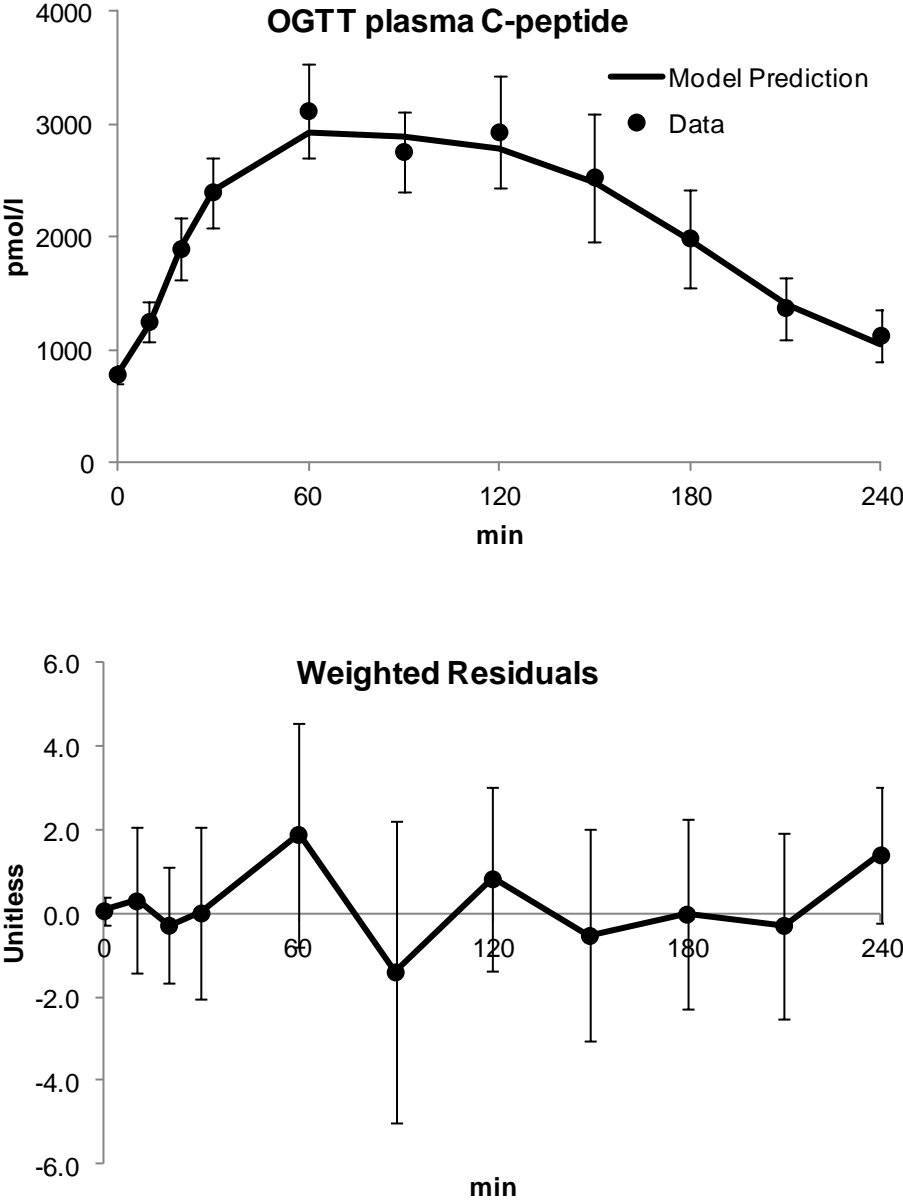**Table 6. 6 – C-peptide model parameters estimates**

Figure 6. 17 – Average (N=10) C-peptide model prediction vs data (top panel) and weighted residuals (bottom panel) in OGTT study. Vertical bars represents SE for model prediction data and SD for weighted residuals
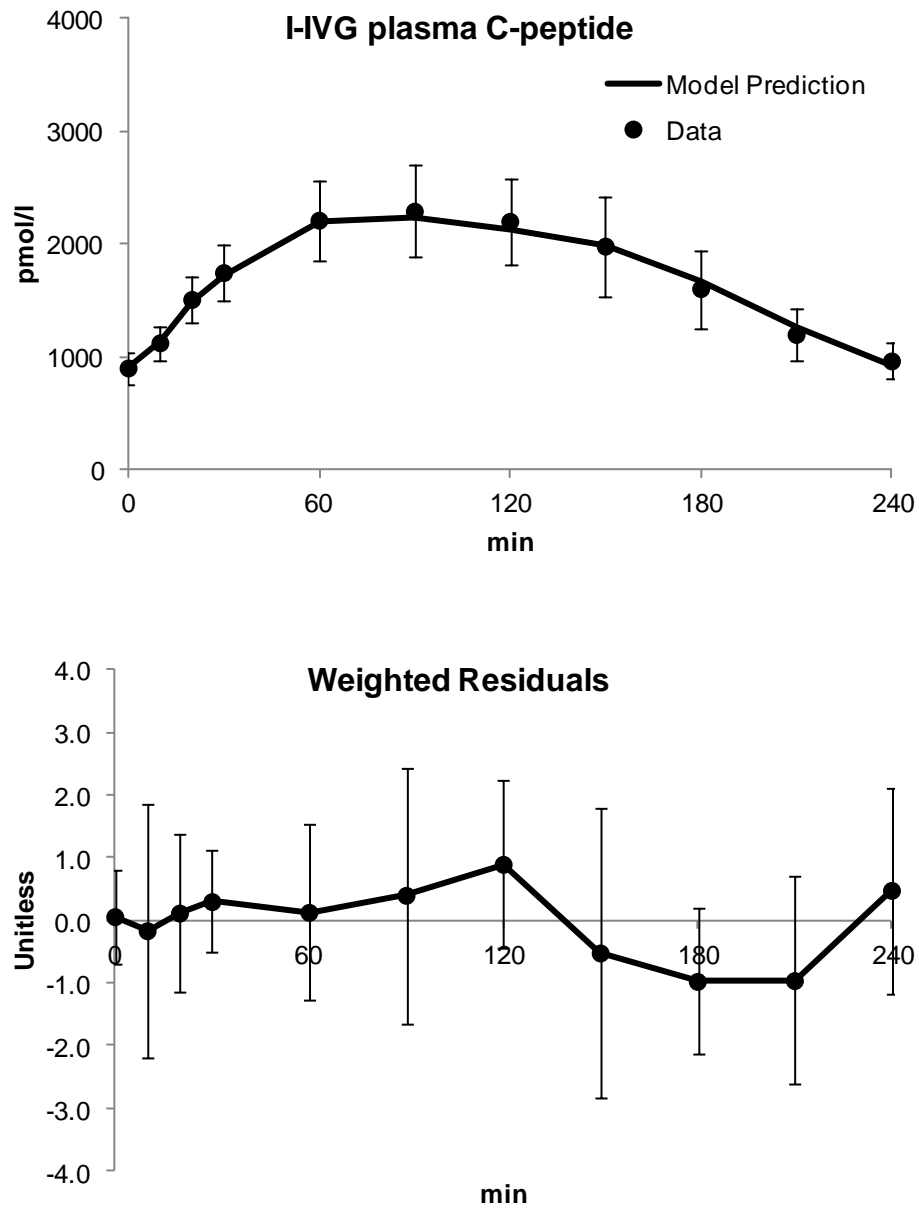
Figure 6. 18-– Average (N=10) C-peptide model prediction vs data (top panel) and weighted residuals (bottom panel) in I-IVG study. Vertical bars represents SE for model prediction data and SD for weighted residuals
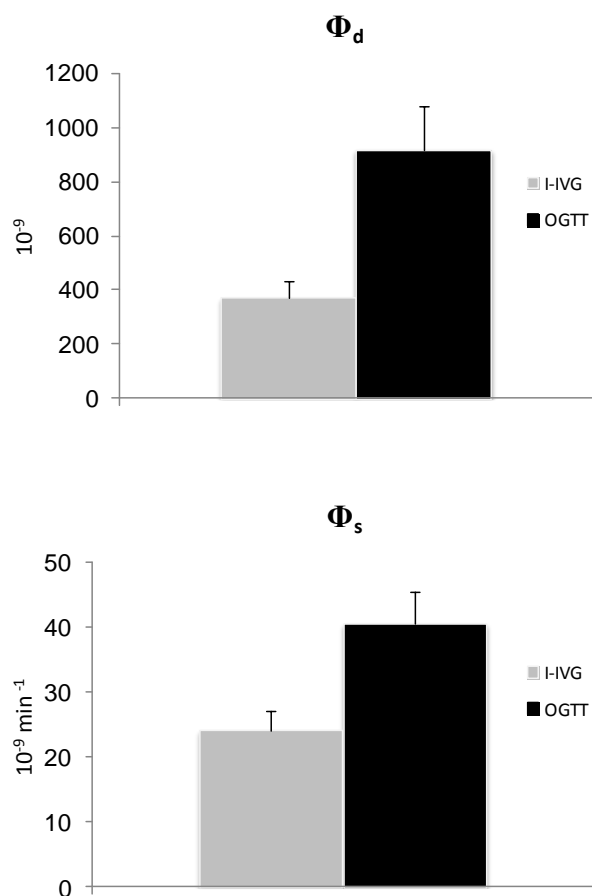
$$\Phi_d$$

Figure 6. 19 – Average (N=10) Φ_d (top panel) and Φ_s (bottom panel) estimated from OGTT and I-IVG study. Vertical bars represent SE
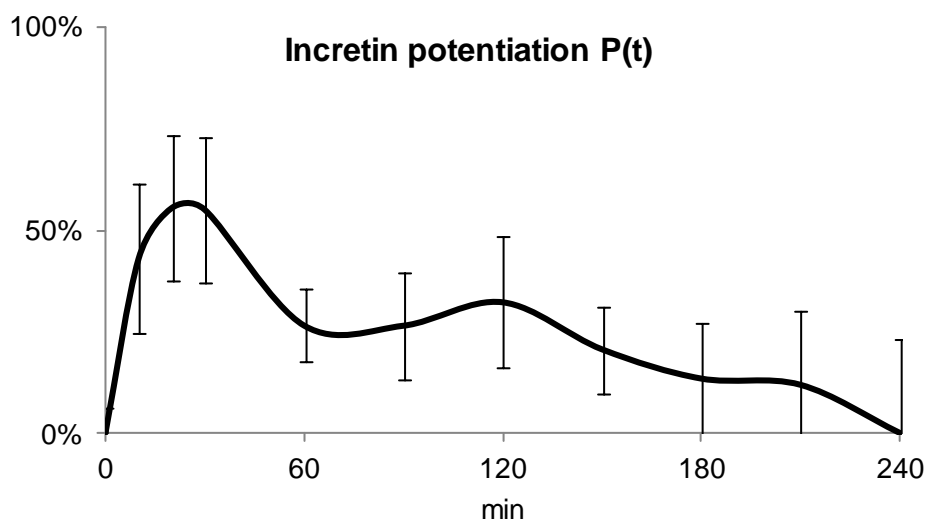

Figure 6. 20 – Average (N=10) time course of incretin potentiation. Vertical bars represent SE

6.10 DATABASE 3: ORAL GLP-1 MODEL

Oral GLP-1 model was identified on OGTT data as described in paragraph 6.2. The model well describes plasma C-peptide concentrations during OGTT, as shown by average model prediction vs average C-peptide in Figure 6. 21. Model parameters were estimated with good precision for all subjects and are reported in Table 6. 7. It is possible to compare β-cells responsivity indexes, Φ_s and Φ_d, assessed with the C-peptide model during I-IVG study vs those calculated with the *oral GLP-1 model* in the OGTT study; Φ_s and Φ_d calculated with *oral GLP-1 model* are on average 31% and 45% higher than their i.v. counterparts. However only the difference in the the dynamic is statistically significant (P = 0.015, Figure 6. 22). The model allows to assess the profiles of the insulin secretion rate (SR) at basal GLP-1 concentration and the potentiated insulin secretion rate due to GLP-1 (SR^{GLP-1}). It is also possible to reconstruct the time course of incretin effect, $\Pi(t)$, (Figure 6. 23, upper panel), using equation 4.1 and substituting insulin secretion profiles SR^{OGTT} and SR^{I-IVG} with SR^{GLP-1} and SR respectively (Figure 6. 23, lower panel).

		OGTT		
α	*[min^{-1}]*	0.14	$\pm$ (22)	0.01
h	*[mg/dl]*	97	$\pm$ (4)	2
$K=\Phi_d$	*[10^{-9}]*	539	$\pm$ (35)	98
$\beta=\Phi_s$	*[10^{-9} min^{-1}]*	31.6	$\pm$ (17)	4.40
Π	*[% · pmol/l]*	1.70	$\pm$ (67)	0.39

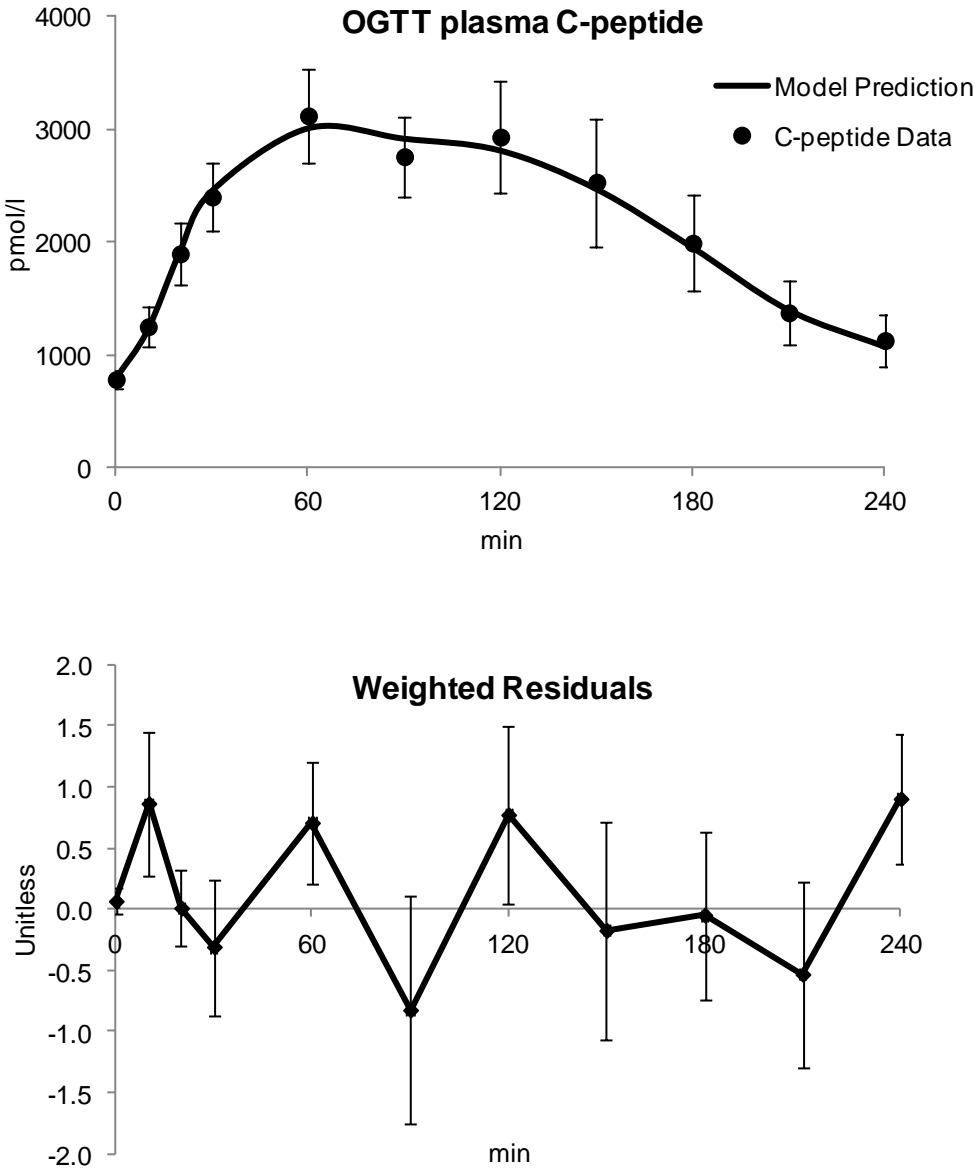**Table 6. 7 – Estimates of the *oral GLP-1 model* parameters**

Figure 6. 21 – Average (N=10) *oral GLP-1 model* prediction vs data (top panel) and weighted residuals (bottom panel) in OGTT study. Vertical bars represents SE for model prediction data and SD for weighted residuals
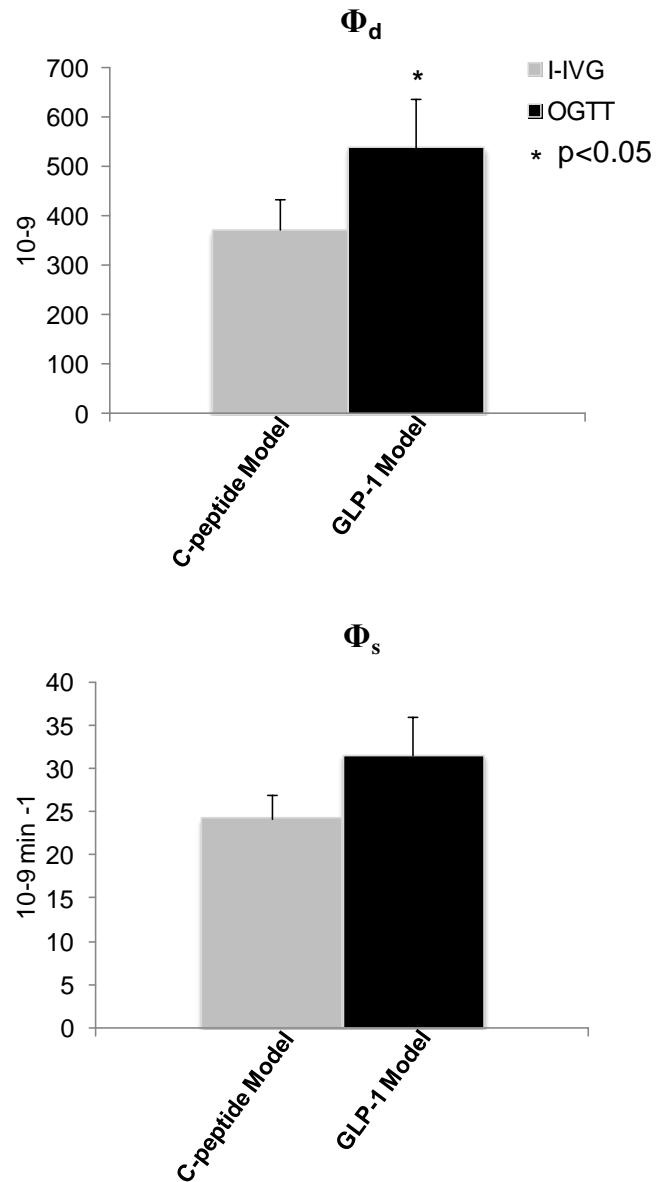
Figure 6. 22 – Average (N=10) Φ_s (bottom panel) and Φ_d (top panel) responsivity indexes in the OGTT assessed with *oral GLP-1 model* vs those assessed with C-peptide model in the I-IVG study. Vertical bars represent SE
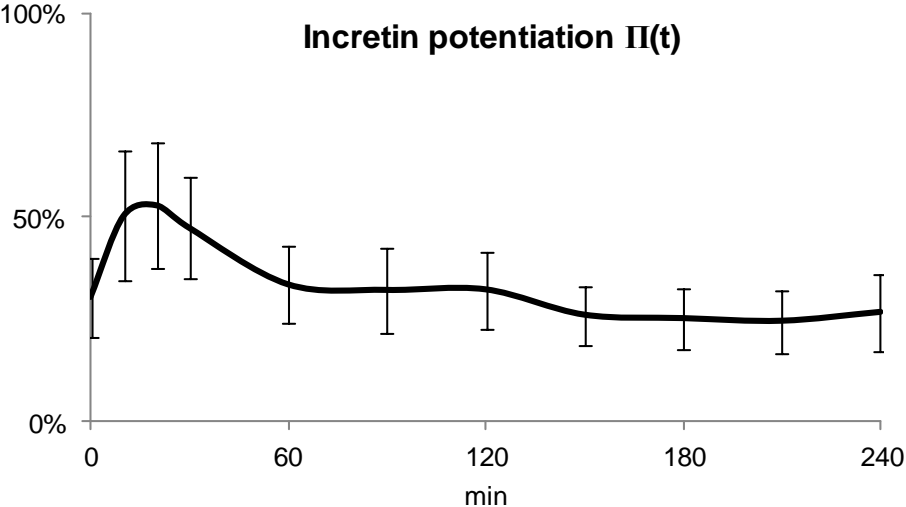
Figure 6. 23 – Average (N=10) time course of incretin potentiation calculated with *oral GLP-1 model* from OGTT data. Vertical bars represent SE

CHAPTER 7

GLP-1 MODEL VALIDATION

7.1 INTRODUCTION

In the previous chapters, a model of GLP-1 action on insulin secretion was developed by adopting standard modeling methodology. A number of models were tested against data, beginning with the simplest one and systematically increasing the complexity. Each of the model was then numerically identified from experimental data, both in a very challenging experimental condition, such as a hyperglycemic clamp with concomitant GLP-1 intravenous infusion, and in a more physiological condition such as a meal. Quantitative criteria were used to select the most parsimonious model, including randomness of the residuals, parameter precision, parsimony criteria, and parameter plausibility. However, no model can have an absolute validity, since it is by definition an approximation of reality.

In this chapter model validation is tackled by comparing *oral GLP-1 model* ability to simultaneously quantify insulin secretion enhancement due to GLP-1, i.e. potentiation index Π, and β-cells responsivity indexes, i.e. Φ_s and Φ_d, from data of

an oral glucose test (OGTT) against those provided by the gold standard technique proposed by Campioni et al. in [11].

Data and protocol used in this chapter for validation purpose is described in detail in Chapter 3, paragraph 3.4.

7.2 POTENTIATION INDEXES COMPARISON

Model validation is tackled by comparing potentiation index Π calculated with the oral GLP-1 model from OGTT data with the incretin potentiation index PI calculated with gold standard method, using the C-peptide model on OGTT and I-IVG data.

A Naïve average data approach [25] has been adopted first. Average data are shown in Figure 7. 2. Then average subject was identified using both *oral GLP-1 model* on OGTT data to assess potentiation index Π, and with C-peptide model on OGTT and I-IVG data to assess incretin potentiation index PI. Both models well predicts average plasma C-peptide of the average subjects and provides precise estimates of the models parameters. Of interest, in the ideal case of a well matched plasma glucose, potentiation index Π and incretin potentiation index PI are virtual the same (Π = 6.55, CV = 65%; PI = 6.15 % · pmol/l, Figure 7. 1) Unfortunately, this is not always the case at single individual level in the 10 subjects of the study. Figure 7. 3 and Figure 7. 4 show a comparison between PI and Π. Potentiation indexes are similar in subjects where I-IVG plasma glucose is well matched with OGTT plasma glucose (subject #1, #3, #6, and #8). For instance Figure 7. 5 shows glucose, C-peptide and GLP-1 concentration of subject #6, where plasma glucose of the OGTT is virtually the superimposable with the i.v. one. In this case Π and PI were similar (Π = 1.47 vs PI = 1.57 % · pmol/l). Conversely in Figure 7. 6 plasma glucose, C-peptide and GLP-1 of subject #4, is shown. I-IVG does not match OGTT glucose concentration, thus affecting the assessment of the

potentiation indexes Π and PI (Π = 4.07 vs PI = 1.49 % · pmol/l). Likewise subject #4, also subject #2, #5, #7, #9 are characterized by unmatched plasma glucose, resulting in different estimates of the potentiation indexes Π and PI. In any case, the presence of glucose mismatch is not the only confounder. In fact, it is important to consider that other gut hormones contribute to the incretin effect, in particular GIP, which is released simultaneously with GLP-1 and has shown to have additive effect on insulin secretion [11]; thus incretin potentiation PI reflects the action of all incretin hormones on insulin secretion, whilst Π only accounts for GLP-1 action.

However, the fact that good match in plasma glucose profile was not obtained in all the subjects, precludes to assess model ability to segregate glucose vs GLP-1 stimulus with a single experiment.

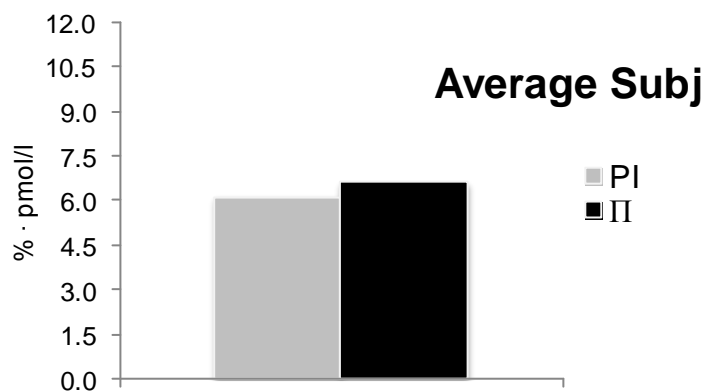To overcome this limitation we resorted to in silico simulation.

Figure 7. 1 – Comparison between Π estimated with the *oral GLP-1 model* (black) vs PI estimated with the standard method (light grey) in subject in the average subject
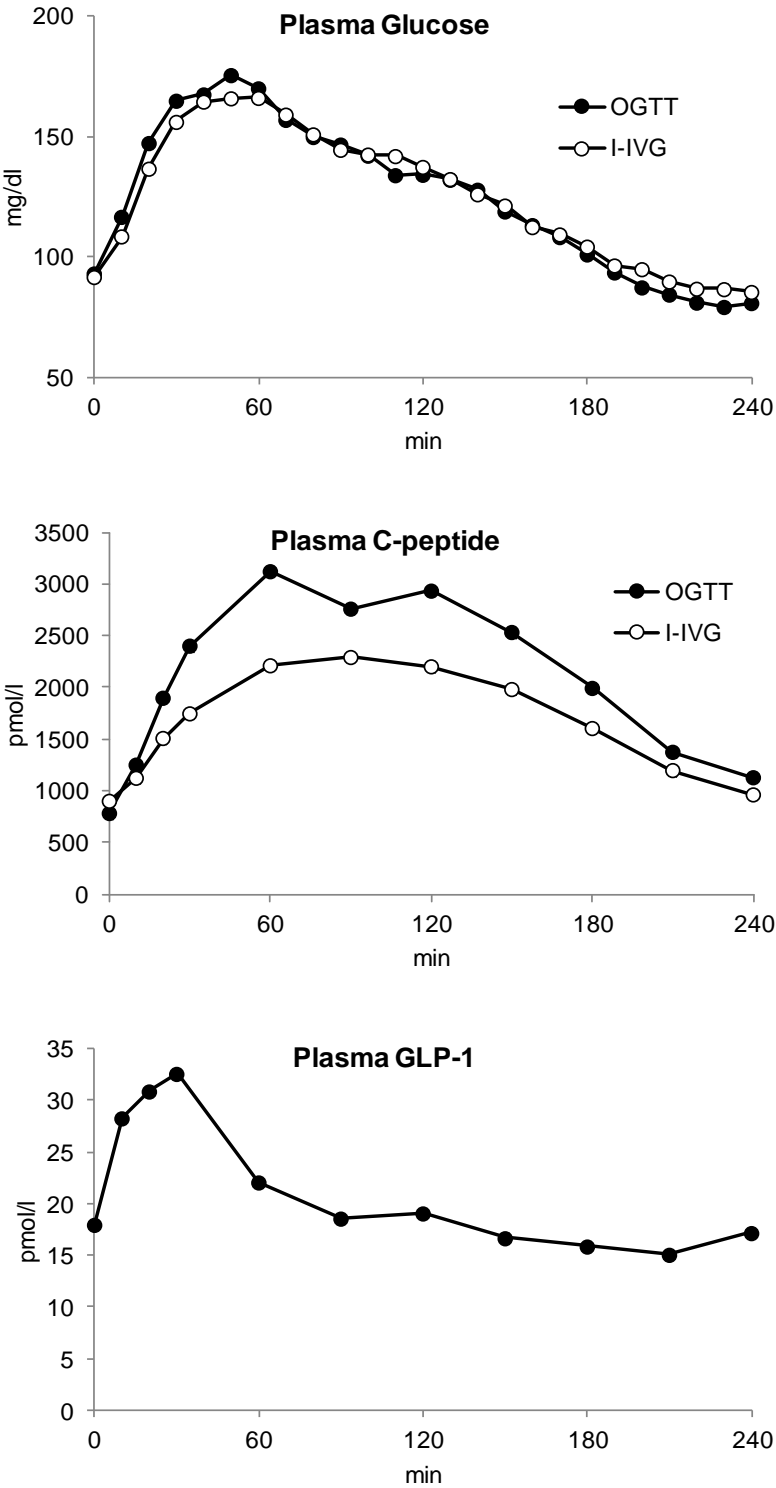
Figure 7. 2 – Average (N = 10) plasma glucose (top), C-peptide (middle) and GLP-1 (bottom) in OGTT and I-IVG study of the average subject.

Figure 7. 3 – Comparison between Π estimated with the *oral GLP-1 model* (black) vs PI estimated with the standard method (light grey) in subject #1, #2, #3, #4, #5, #6
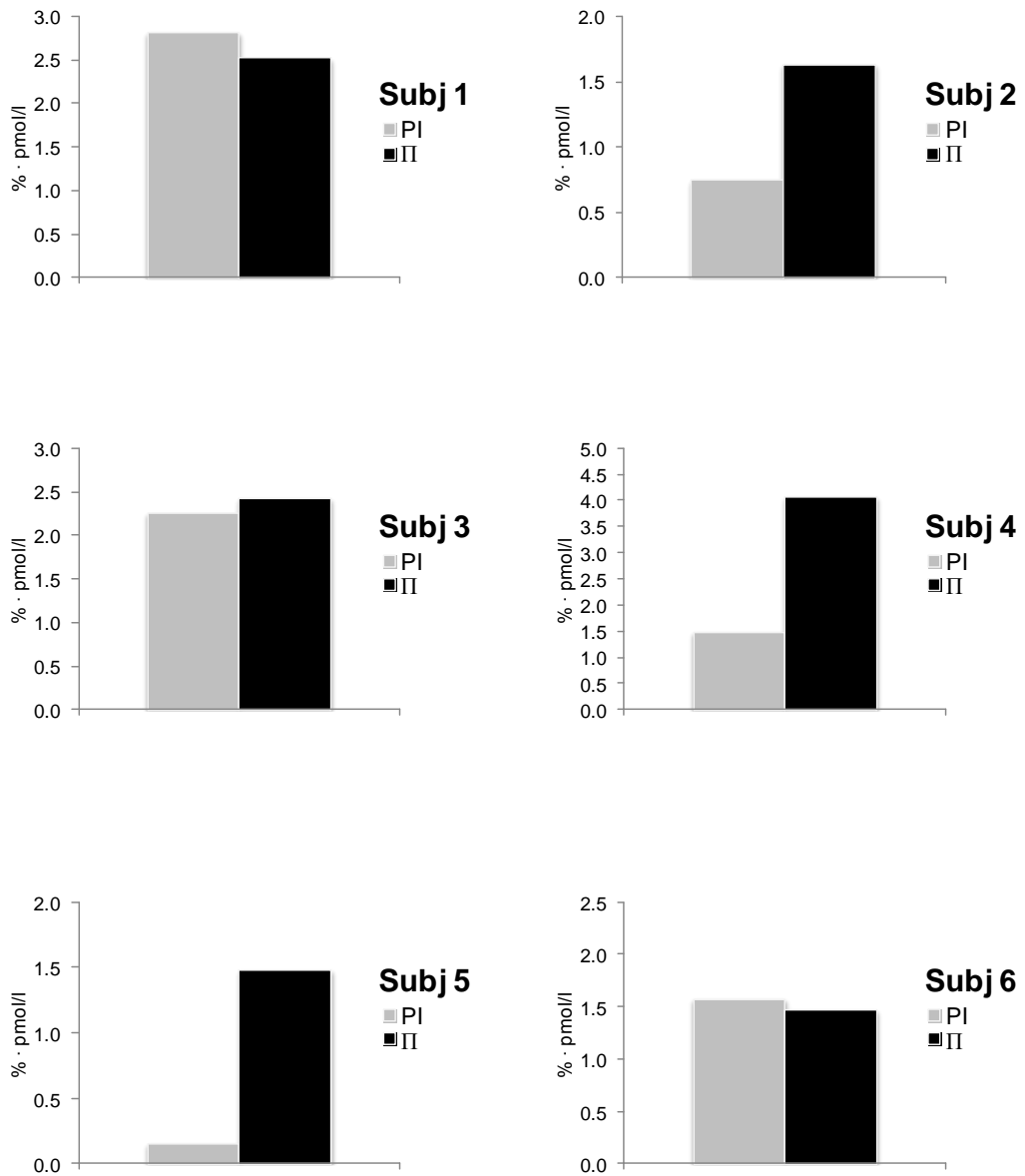
Figure 7. 4 – Comparison between Π estimated with the *oral GLP-1 model* (black) vs PI estimated with the standard method (light grey) in subject #7, #8, #9, #10

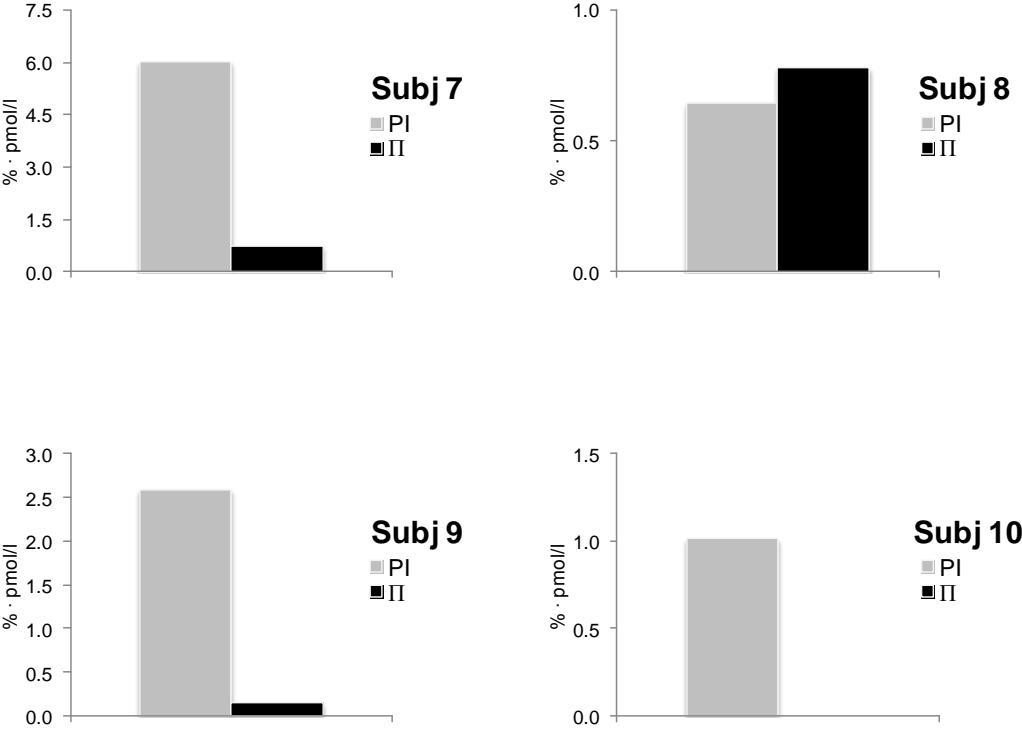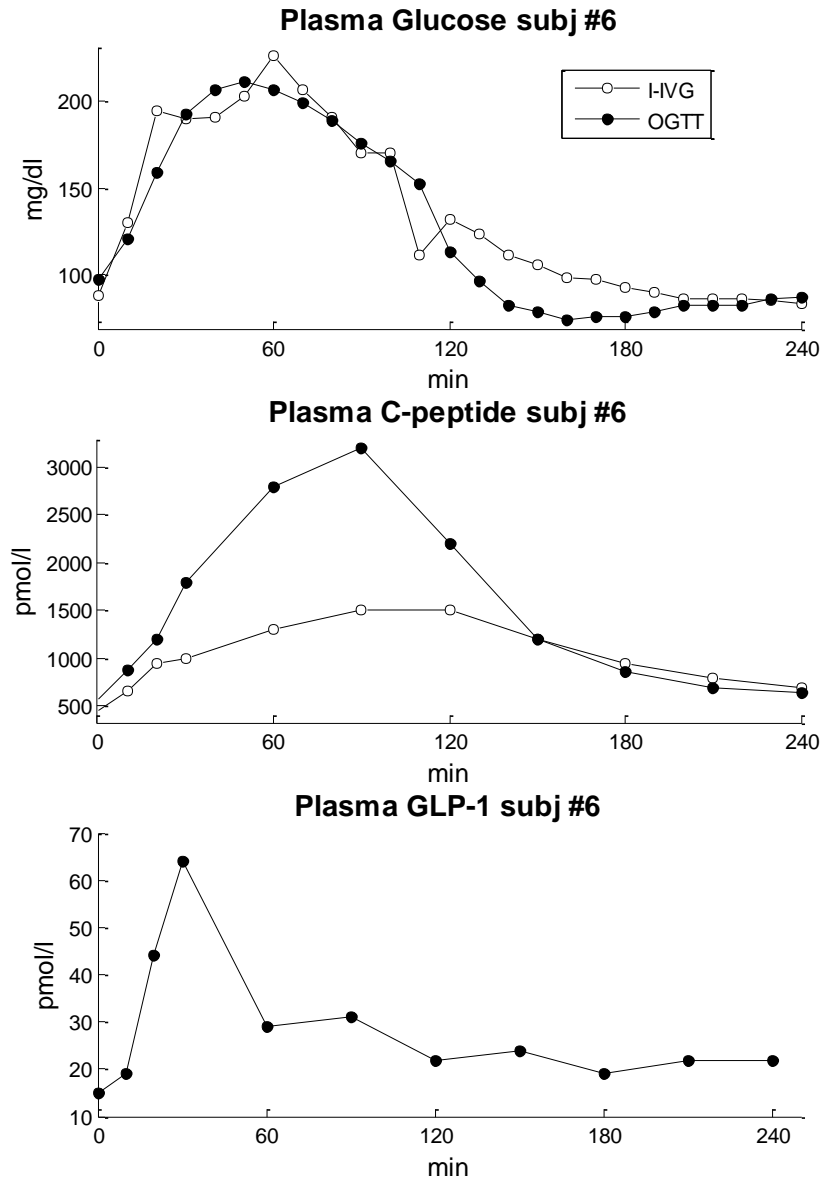**Figure 7. 5 – Plasma glucose (top), C-peptide (middle) and GLP-1 (bottom) in OGTT and I-IVG study measured in subject #6**
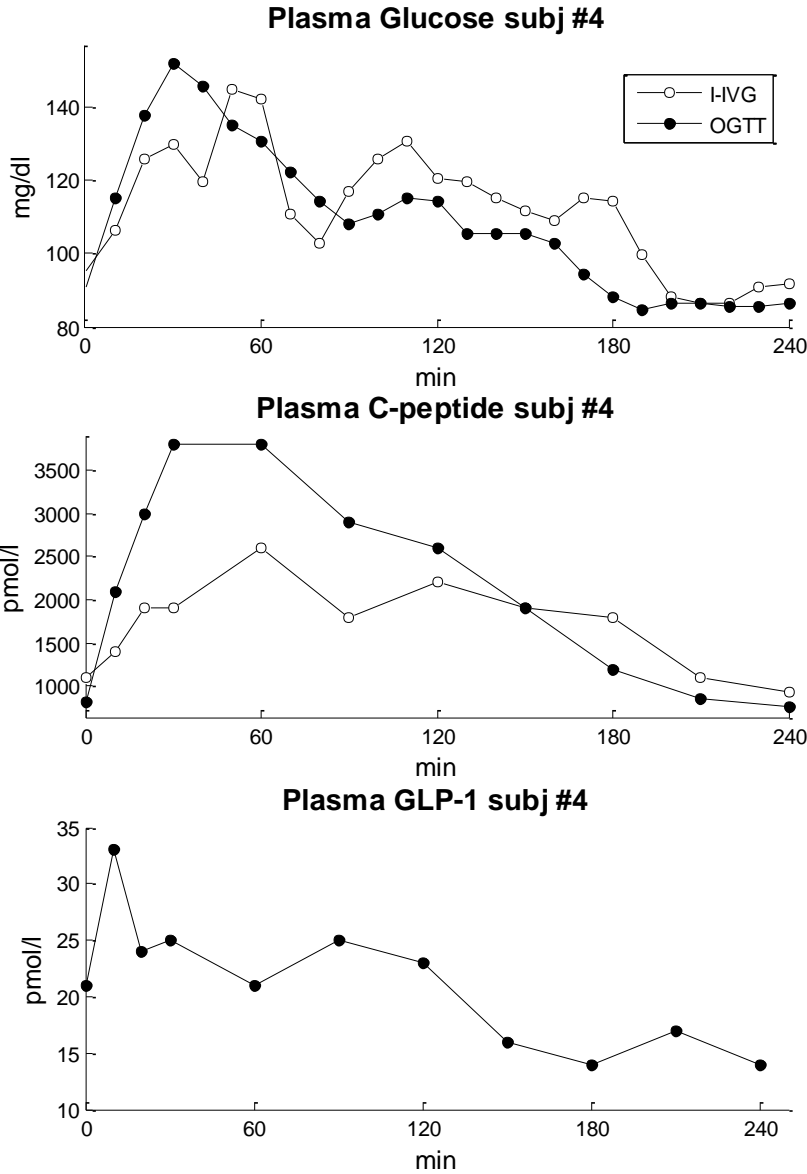
Figure 7. 6 – Plasma glucose (top), C-peptide (middle) and GLP-1 (bottom) in OGTT and I-IVG study measured in subject #4

7.3 IN SILICO VALIDATION OF *ORAL GLP-1 MODEL*

7.3.1 Generating in silico data for model validation

The use of in silico simulation for validation purpose eliminates the need of expensive experiments and allows to test the model in a controlled scenario [87].

Thus using methodology which is typical of the engineering field, the *oral GLP-1 model* has been further and intensively tested trough in silico simulations and validated by comparing results with those obtained with Campioni method.

Validation dataset, described in detail in Chapter 3, paragraph 3.4, is affected by unmatched plasma glucose in the OGTT and I-IVG study in subject #2, #4, #5, #7, #9, which leads to different estimates of the potentiation indexes Π and PI. Moreover in this particular study design, other gut hormones contribute to the incretin effect, thus incretin potentiation PI calculated with Campioni method may reflects the action of all incretin hormones on insulin secretion, whilst potentiation index Π, estimated with the oral GLP-1 model, quantifies the effect of GLP-1 on insulin secretion.

Thus in order to test the performance of the model on an ideal dataset which is not affected by plasma glucose mismatch and for which GLP-1 is the only incretin hormone, in silico data were generated as described below. For each real subject, 100 profile C-peptide concentrations of the OGTT are simulated by as follow (Figure 7. 7):

- model parameters α, Φ_s, Φ_d, and h were fixed to those estimated with the C-peptide model from the I-IVG data;
- 100 different values of potentiation index Π were generated for each subject in the range [0.01 0.45] with a constant step of 0.0044 % · pmol/l.

This range was chosen in order to span from the minimum to the maximum value of potentiation observed in real subjects;

- GLP-1 model was solved, using I-IVG glucose and OGTT GLP-1 concentrations as the model-forcing functions, with fixed α, Φ_s, Φ_d, h and varying Π, thus generating for each subject 100 plasma C-peptide profiles. In this way, we could assess the model at the limits of its domain validity, since plasma C-peptide concentrations reached in some case supraphysiological levels;

- Measurement error (assumed to be independent, Gaussian, with zero mean and known variance, equal to: $\sigma^2(Cp) = 2000 + 0.001 \cdot Cp(t)^2$ as proposed by Toffolo et al. in [84]) was then superimposed to the simulated C-peptide profiles.
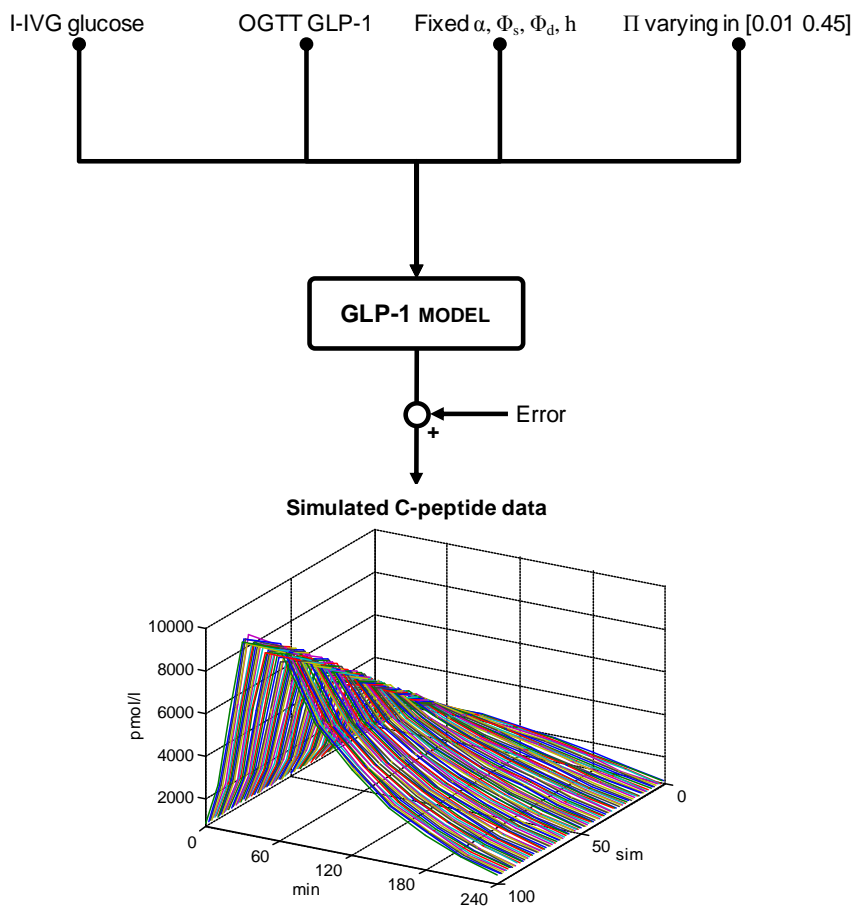
Figure 7. 7 – Generation of simulated OGTT plasma C-peptide concentration

7.3.2 Identification results

Oral GLP-1 model was identified on simulated OGTT data as described in Chapter 4, paragraph 4.4 and 4.5.2. The model well describes simulated plasma C-peptide concentrations, as shown in Figure 7. 8 and Figure 7. 9. Weighted residuals are random pattern and lie in the range [-1 +1]. Model parameters are estimated with good precision for all simulated profiles.

Figure 7. 8 – Weighted residuals in subject #1, #2, #3 and #4

Figure 7. 9 – Weighted residuals of subject #5, #6, #7, #8, #9 and #10

One of the great advantages of in silico validation is that one works with controlled conditions and knows the true value of Π. Thus it is possible to compare the estimated Π (Π^*) value from simulated data with the true value of Π used to generate them. Since parameter estimation provides, together with the value of the parameter, also its coeffi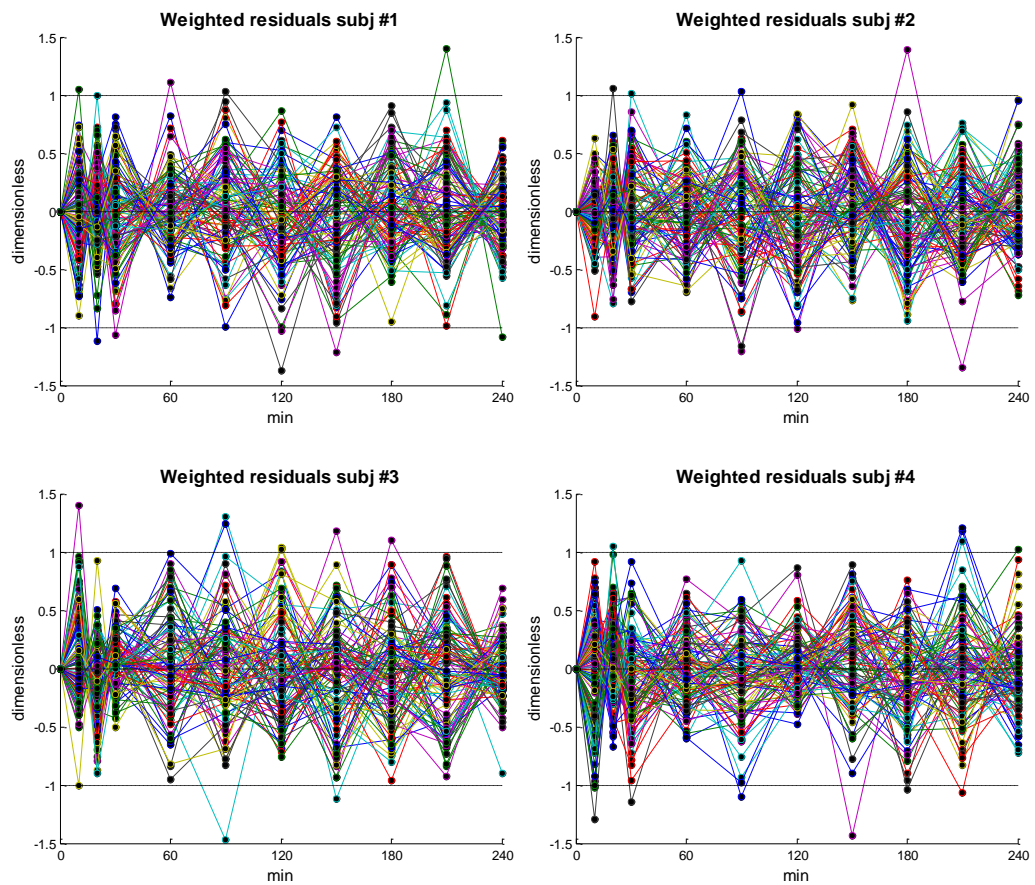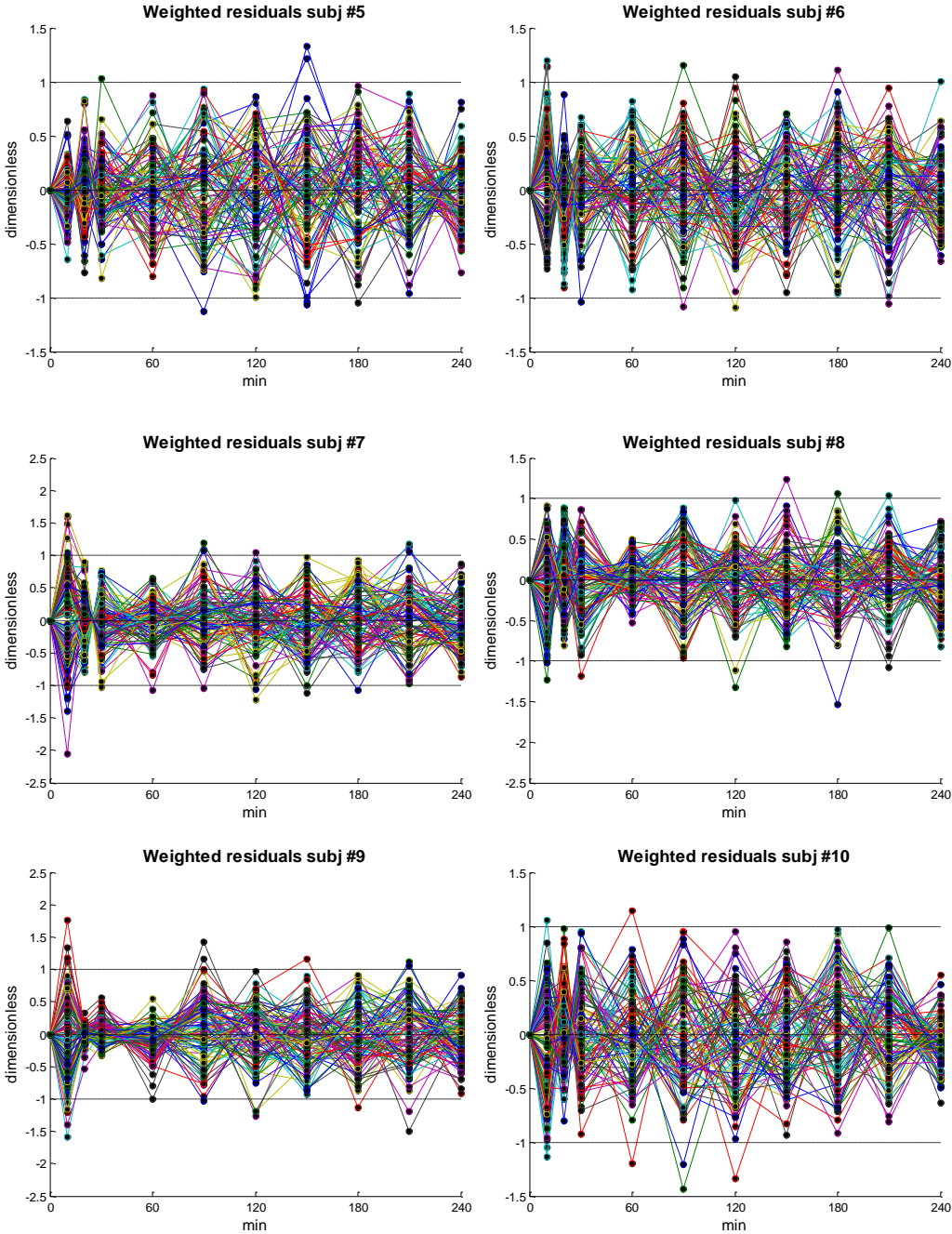cient of variation (CV), this information can also be used to assess model ability to estimate the true value of the potentiation index Π. In particular, if the true Π falls in the 66% confidence interval of estimated Π^*, we can consider the estimate accurate. Accuracy is then defined as the percentage of accurate estimates.

Results are reported in Table 7. 1. On average *oral GLP-1 model* has an accuracy of 93 $\pm$ 1 % in estimating the true potentiation due to GLP-1. No statistical difference in any subject is reported between true Π and Π^*. Correlation of true Π vs Π^* are shown in Figure 7. 10 and Figure 7. 11. On average estimated Π are well correlated with true Π (r = 0.96 $\pm$ 0.01). Slope of linear regression results on average 1.06 $\pm$ 0.03, thus estimated potentiation index Π is almost equivalent to true Π.

To note that at higher values of potentiation index, distance between true Π and Π^* increases. One of the possible explanation is that the higher the potentiation index is the higher plasma C-peptide concentration. This make the model working near to the limits of its domain of validity, consequently affecting estimation of Π^*. However in real subjects it is uncommon that Π is greater than 20 % $\cdot$ pmol/l.

	Accuracy (%)	Correlation	Slope
subj1	96	0.96	0.99
subj2	97	0.89	1.20
subj3	93	1.00	0.99
subj4	95	0.98	1.00
subj5	98	0.98	1.00
subj6	95	0.99	0.99
subj7	89	0.97	1.10
subj8	94	0.99	1.00
subj9	90	0.93	1.10
subj10	87	0.88	1.20
mean	93	0.96	1.06
SD	4	0.04	0.09
SE	1	0.01	0.03

Table 7. 1 – Accuracy, correlation and slope of the regression between true and estimated Π
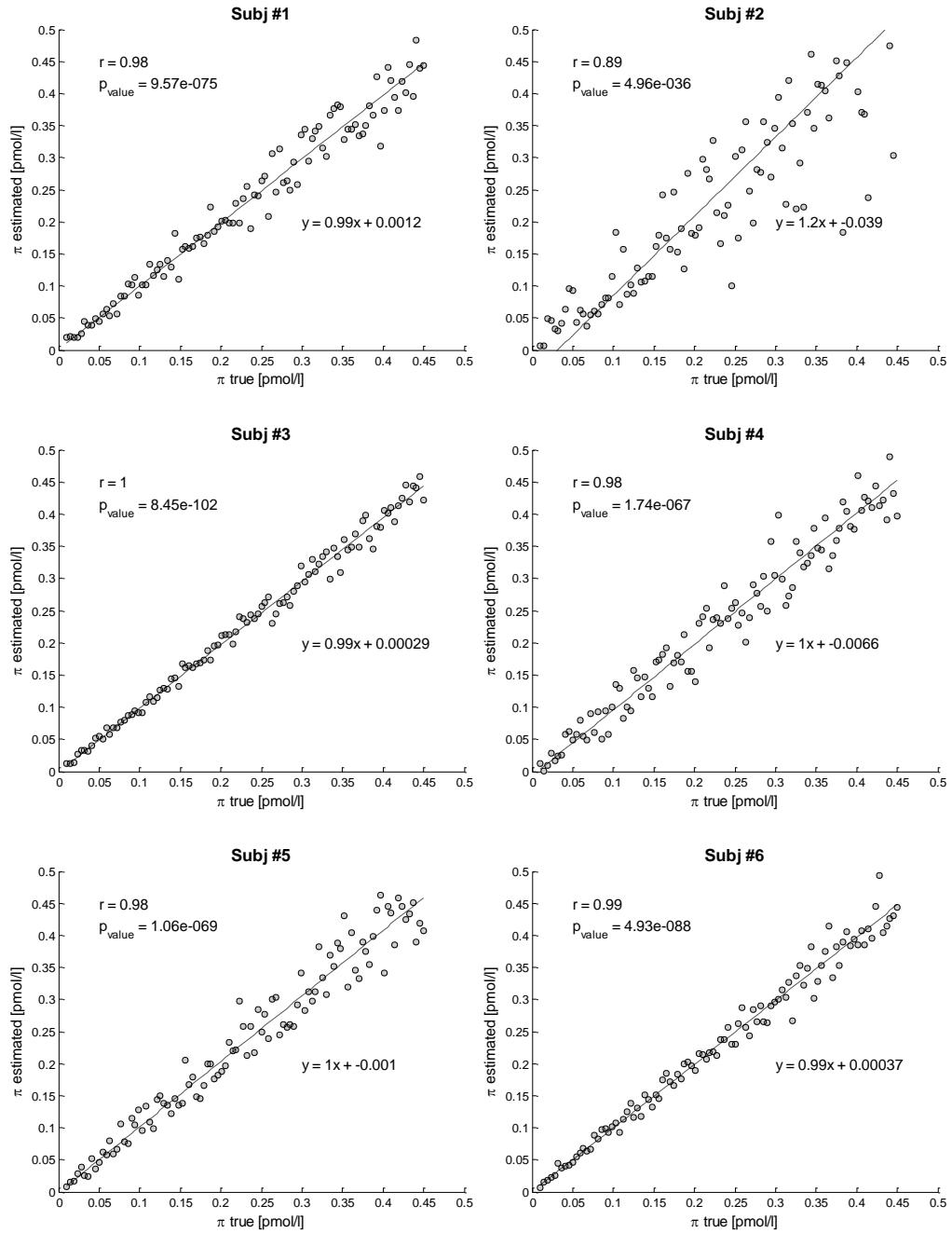
Figure 7. 10 – Correlation between true vs estimated Π in subject #1, #2, #3, #4, #5, #6
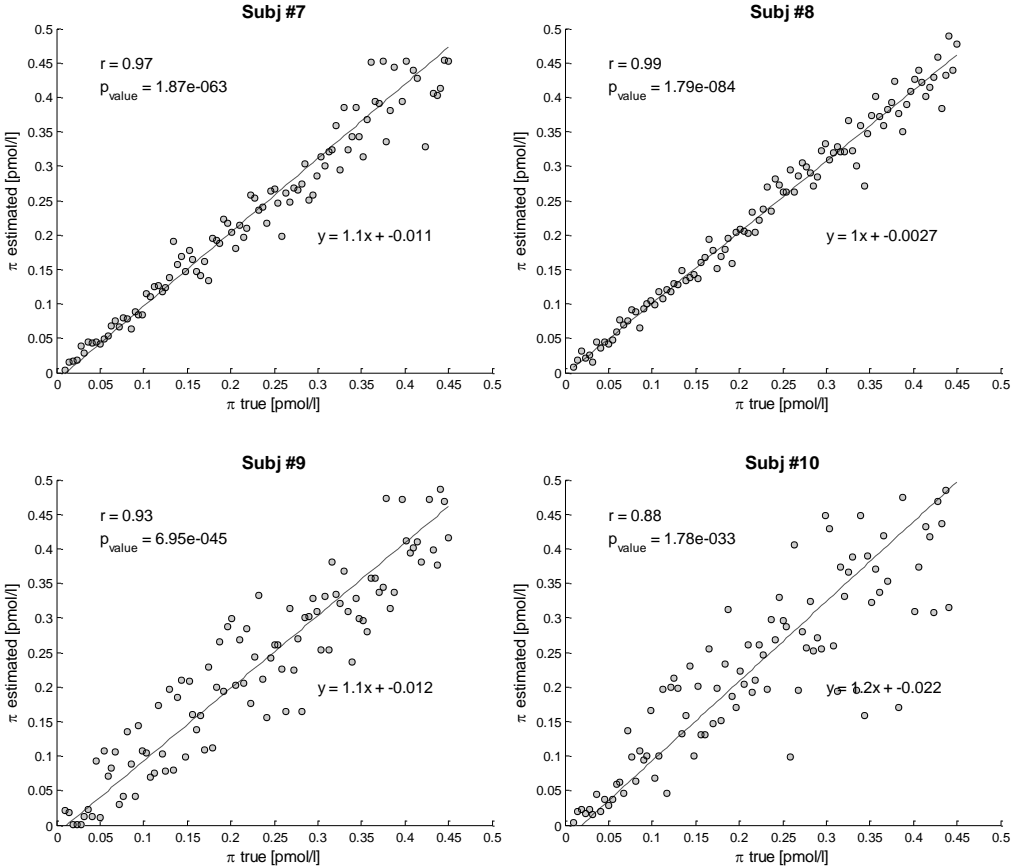
Figure 7. 11 – Correlation between true vs estimated Π in subject #7, #8, #9, #10

7.3.3 Comparison of oral GLP-1 potentiation index Π vs standard method

C-peptide model was identified on real I-IVG and simulated OGTT data as described in detail in Chapter 6, paragraph 6.9, and PI of the standard method was calculated using equation 4.12. Correlation between the two indexes is shown for each subject in Figure 7. 12 and Figure 7. 13. Potentiation index Π is well correlated with PI, on average r = 0.96 ± 0.01 as reported in Table 7. 2. On average, slope of the linear regression results 1.16 ± 0.05, pointing out that Campioni index PI tends to slightly underestimate true potentiation.

Thus in silico validation leads to conclude that under the hypothesis of exact model and perfectly matched glucose data in OGTT and I-IVG, *oral GLP-1 model* allows to correctly estimate the action of GLP-1 on insulin secretion using data of a single oral glucose test.

	Correlation	Slope
subj1	0.98	1.30
subj2	0.89	1.10
subj3	0.99	1.20
subj4	0.98	1.20
subj5	0.98	1.10
subj6	0.99	1.10
subj7	0.97	1.40
subj8	0.99	1.30
subj9	0.93	1.10
subj10	0.88	0.83
mean	0.96	1.16
SD	0.04	0.16
SE	0.01	0.05

Table 7. 2 – Accuracy, correlation and slope of the regression between true and estimated Π
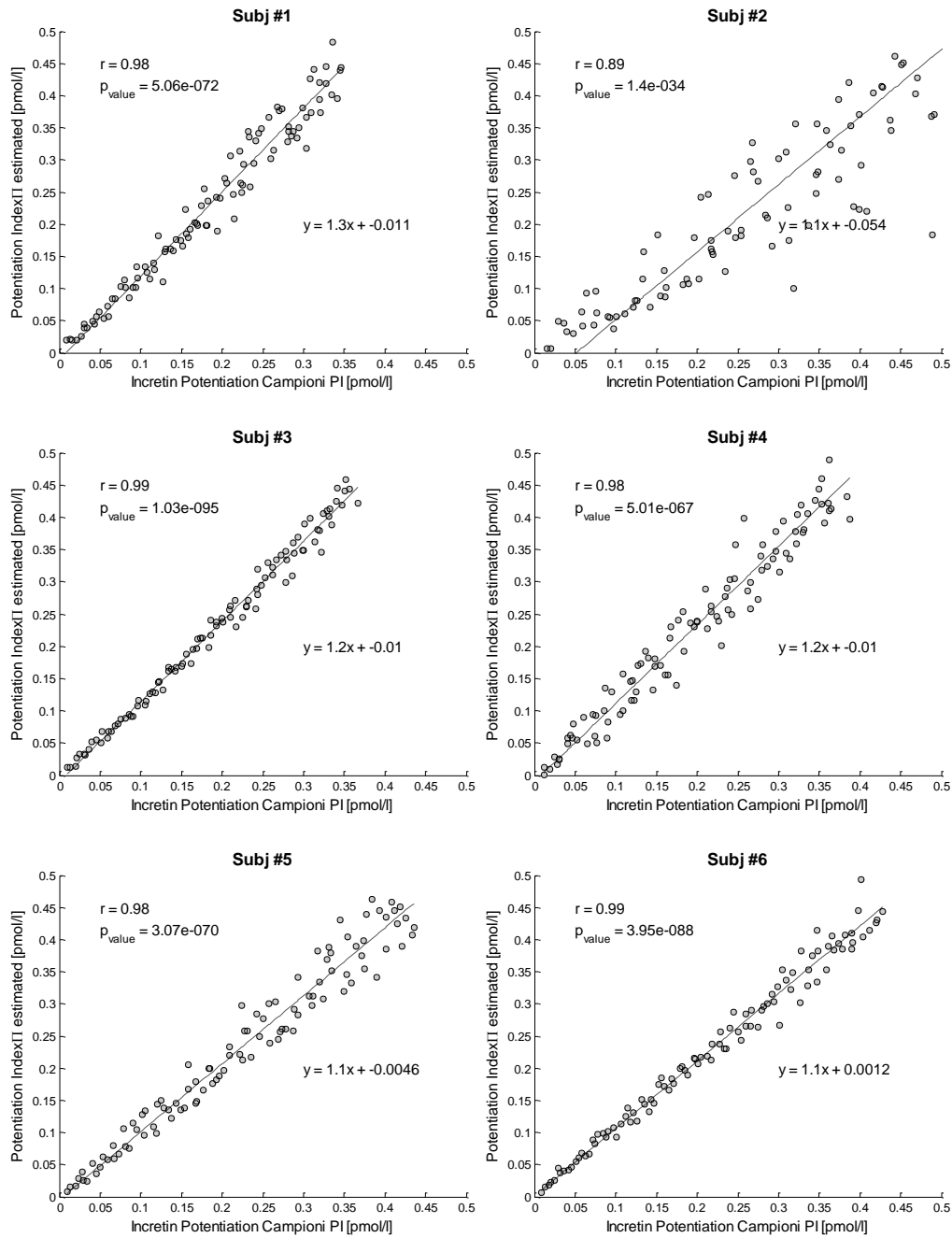
Figure 7. 12 – Correlation between PI vs Π in subject #1, #2, #3, #4, #5, #6
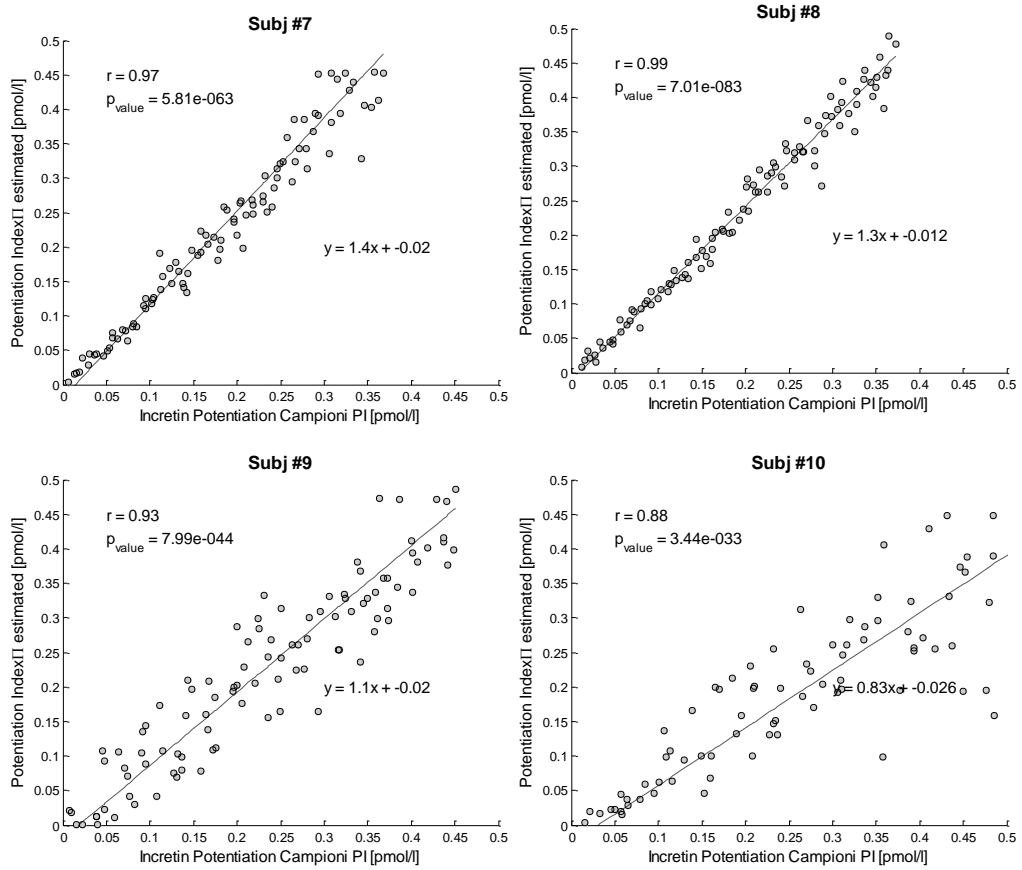
Figure 7. 13 – Correlation between PI vs Π in subject #7, #8, #9, #10

CHAPTER 8

USE OF GLP-1 MODELS

8.1 ASSESSMENT OF THE EFFECT OF DPP-4 INHIBITION WITH SITAGLIPTIN ON INCRETIN SECRETION USING ORAL GLP-1 MODEL

8.1.1   *Background*

Low GLP-1 concentrations have been observed in IFG. It is uncertain whether these abnormalities contribute directly to the pathogenesis of IFG and impaired glucose tolerance. DPP-4 inhibitors, such as sitagliptin, raise GLP-1 concentration possibly improving secretion and lowering postprandial glucose excursion.

The current experiments tested this hypothesis by measuring insulin secretion and action and fasting and postprandial glucose turnover before and after 8 weeks of therapy with a DPP-4 inhibitor. Data and protocol are described in detail in Chapter 3 paragraph 3.3 and are shown, for reader convenience, in Figure 8. 1.

8.1.2 Results

After 8 weeks of sitagliptin treatment, sitagliptin decreased postprandial total GLP-1 concentrations (5652 ± 357 vs 5034 ± 257 pmol/l per 6 h, P = 0.02). Intriguingly, total GLP-1 concentrations were almost unchanged (5008 ± 428 vs 5560 ± 446 pmol/l per 6 h, P = 0.11) by placebo as shown in Figure 8. 1 panel D and Figure 8. 2 panel C.

After 8 weeks of sitagliptin treatment, total GLP-1 concentrations were also almost unchanged (5008 ± 428 vs 5560 ± 446 pmol/l per 6 h, P = 0.11) as shown in Figure 8. 1 panel D and Figure 8. 1 panel C. Administration of sitagliptin or placebo did not alter fasting glucose prior to meal ingestion (102.78 ± 2.52 vs 104.04 ± 2.16 mg/dl, P = 0.60 and 105.66 ± 1.80 vs 104.94 ± 2.16 mg/dl, P = 0.68, Figure 8. 1 panel A). Glucose area under curve was unchanged by sitagliptin and placebo (47393.39 ± 2443.70 vs 45254.90 ± 1538.16 mg/dl per 6 h, P = 0.09; and 46328.93 ± 1361.29 vs 45578.36 ± 1765.55 mg/dl per 6 h, P = 0.28, Figure 8. 2 panel A). Baseline, peak or overall postprandial C-peptide concentrations did not differ after administration of sitagliptin or placebo (Figure 8. 1 panel C and Figure 8. 2 panel B).

Indexes of β-cells responsivity and potentiation index Π were estimated with oral GLP-1 model with good precision for all subjects both at baseline and treatment meal study. Table 8. 1 reports parameters estimates. Sitagliptin did not alter insulin secretion, indeed there are no significant changes in Φ_s or Φ_d. Π showed a slight increase after 8-week treatment with sitagliptin, but still there is no significant difference.

8.1.3 Conclusion

The present study indicates that use of DPP-4 inhibition to raise circulating concentrations of intact GLP-1 did not lower fasting or postprandial glucose concentrations in IFG. This would imply that circulating incretin concentrations play no role in the pathogenesis of IFG. Of note, the postprandial pattern of

change in insulin and C-peptide concentrations were virtually identical before and after treatment, indicating that increased circulating incretin concentrations had no effect on hepatic insulin clearance. Moreover the estimated effect of GLP-1 on insulin secretion, i.e. the incretin potentiation index Π, is mild (8 % per pmol/l on average). Thus one can speculate that the particular study cohort is composed by individuals that are not very responsive to a therapy which involves DPP-4 inhibitors. More encouraging results may be found with individuals who have an higher response of β-cells to GLP-1.

In summary, this study demonstrates that short-term DPP-4 inhibition in IFG does not alter glucose concentrations and glucose metabolism. This would suggest that incretin hormones play little role in the pathogenesis of IFG. In addition to raising concentrations of GLP-1 and GIP by inhibiting DPP-4 mediated degradation, sitagliptin lowered total GLP-1 and GIP, suggesting negative feedback inhibition of enteroendocrine secretion [8].
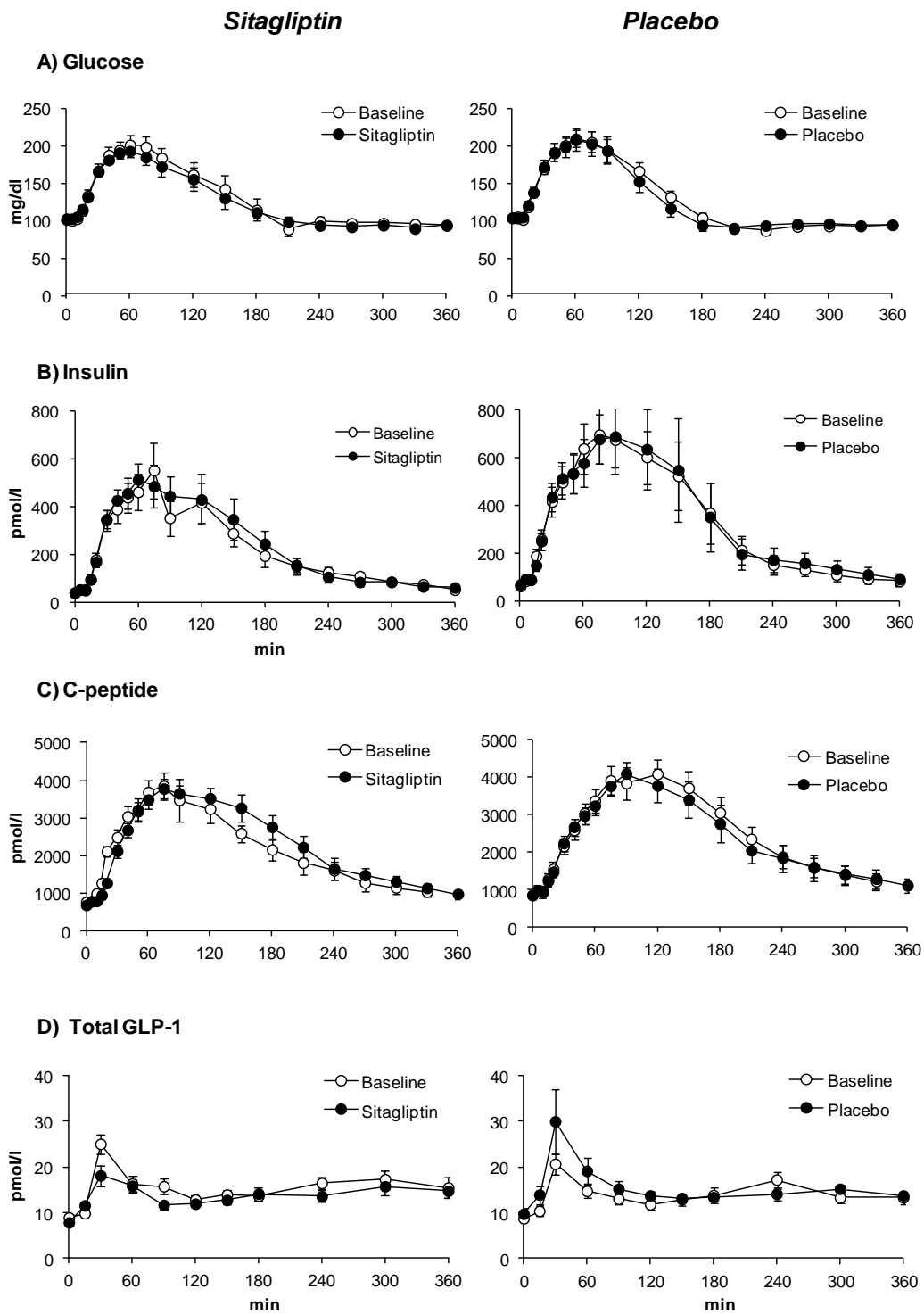
Figure 8. 1 – Average (N=22) measured concentrations of plasma glucose (A), C-peptide (B) and total GLP-1 (C) for baseline (white dots) and sitagliptin (black dots) mixed meal study. Vertical bars represents SE.

		Placebo					
		Baseline			**Treatment**		**P**
α	*[min⁻¹]*	0.047 (10)	±	0.005	0.061 (11)	±	0.014	*0.31*
h	*[mg/dl]*	94 (2)	±	2	95 (2)	±	2	*0.87*
$K=\Phi_d$	*[10⁻⁹]*	501 (13)	±	72	637 (14)	±	163	*0.45*
$\beta=\Phi_s$	*[10⁻⁹ min⁻¹]*	32.8 (6)	±	3.44	35.6 (6)	±	3.08	*0.42*
Π	*[%]*	8.22 (35)	±	3.49	7.09 (33)	±	2.40	*0.83*

		Sitagliptin					
		Baseline			**Treatment**		**P**
α	*[min⁻¹]*	0.055 (11)	±	0.009	0.11 (13)	±	0.026	*0.19*
h	*[mg/dl]*	97 (3)	±	3	95 (2)	±	2	*0.58*
$K=\Phi_d$	*[10⁻⁹]*	532 (16)	±	136	376 (30)	±	87	*0.20*
$\beta=\Phi_s$	*[10⁻⁹ min⁻¹]*	33.76 (6)	±	5.88	36.5 (5)	±	4.05	*0.56*
Π	*[%]*	7.16 (23)	±	1.92	7.98 (25)	±	0.20	*0.20*

Table 8. 1 – Oral GLP-1 model parameter estimates
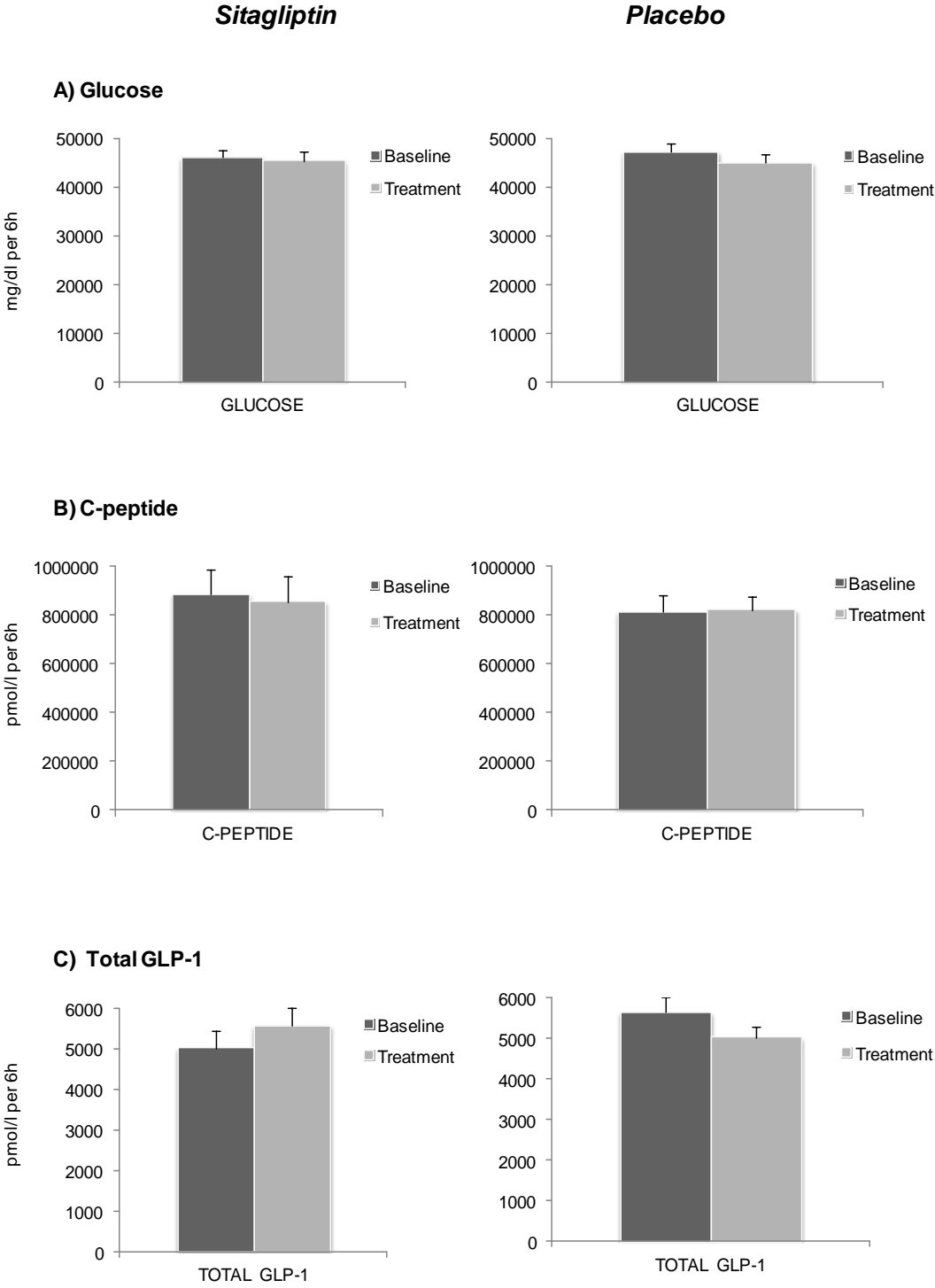
133

Figure 8. 2 – AUC of glucose, C-peptide and total GLP-1 concentrations in the presence (dull grey) and absence (light gray) of sitagliptin (left panels) and placebo (right panels).

CHAPTER 9

DISCUSSION

The prevalence of diabetes is increasing dramatically in populations of the world, due to a more sedentary lifestyle, an increased occurrence of obesity, population aging and genetic factor. Traditional medications for type 2 diabetes lower blood glucose through diverse mechanisms of action, however many of the oral hypoglycemic agents lose their efficacy over time, resulting in progressive deterioration in β-cells function and loss of glycemic control, since they cannot prevent β-cell death or re-establish β-cell mass. Consequently, there is an increasing interest in developing therapeutic agents that preserve or restore functional β-cells mass such as the incretin hormone GLP-1, which not only acutely lowers blood glucose but also engages signaling pathways in the islet β-cells that leads to stimulation of β-cell proliferation and neo-genesis and inhibition of β-cell apoptosis [2], [19], [21], [24], [40].

GLP-1 is a potent insulin secretagogue hormone, secreted by L-cells of ileum and colon in a glucose dependent manner, which stimulates insulin secretion and inhibits glucagon release. When administered in pharmacological doses it also delays gastric emptying and promotes satiety leading to weight loss [2], [19], [21], [24], [40]. The actions of GLP-1 have thus generated a great deal of interest in using this peptide for the treatment of type 2 diabetes. However the active form of GLP-1 is rapidly degraded by the enzyme DPP-4 to its metabolite which does not

interact with the known GLP-1 receptor (GLP1R) [2], [21], [24]. Consequently GLP-1 based therapy for type 2 diabetes has required the development of GLP1R agonists that resist the action of DPP-4 [62] or compounds that inhibit DPP-4 which raise endogenous concentrations of GLP-1 [19]. However the gene coding for GLP1R is highly polymorphic and contains numerous non-synonymous SNPs which could potentially alter response to endogenous GLP-1 and GLP1R agonists. Thus the possibility to quantify the action of GLP-1 on insulin secretion due to inter-individual heterogeneity in response to GLP-1, is crucial to determine those individuals who may benefit more from such therapy than others earlier in the disease [74], [88]. Moreover impairment of insulin secretion and glucagon suppression suggests that decreased β-cell responsiveness to GLP-1 is part of the pathogenesis of type 2 diabetes [31]. Thus the ability to quantify the effect of GLP-1 on insulin secretion is a valuable tool to understand the pathogenesis of type 2 diabetes and to assess the efficacy of GLP-1 based therapy.

Several studies are available on GLP-1 action on insulin secretion [1], [2], [19], [26], [39], [56], however none of them has ever aimed to mechanistically model GLP-1 action on beta-cell. For instance, other investigators have previously utilized a hyperglycemic clamp to measure insulin secretion from deconvoluted C-peptide data. However such methodology does not take into account potential changes in glucose concentration during the hyperglycemic clamp or the changing GLP-1 concentrations prevailing during the experiment. The only model which indirectly accounts for a potentiation due to incretin is the one proposed by Mari and colleagues [55]. It introduced a potentiating factor, which modulates the dose-response relation between insulin secretion and plasma glucose, in order to better fit C-peptide data, but it did not explicitly describe incretins effect. Other studies, e.g. [1], also found a correlation between GLP-1 and the potentiating factor, or use the model to assess different hormone responses in morning vs afternoon [47]. However, in none of the above studies there was an attempt to mechanistically describe GLP-1 action on insulin secretion. At the state of the art, gold standard method to assess incretin effect has been proposed by Campioni et al. in [11], which allows to quantify the effect of incretin hormones on insulin secretion

together with the β-cells responsivity indexes to glucose by identifying C-peptide model on data of a specific protocol in which, each subject is studied twice, first with an OGTT, and second with an iso-glycemic intravenous infusion (I-IVG), the difference between oral and intravenous indexes provide an indirect measure of the incretin effect; in study [11] there was an approximately 60% difference between indexes, implying that the incretin effect is responsible for such potentiation.

The aim of this contribution is to develop a mathematical model which describes the mechanism of action of GLP-1 on insulin secretion, thus providing a direct measure of the magnitude of GLP-1 mediated increase in insulin secretion, together with β-cells responsivity indexes to glucose.

Different data set (database 1, database 2 and database 3) were used for model development and validation purpose:. Database 1 contains data of 88 subjects, which underwent a hyperglycemic clamp with concomitant GLP-1 intravenous were used to develop the model of GLP-1 action on insulin secretion. In fact, thanks to the fact that glucose is maintained almost constant, it was possible to single out the effect of GLP-1 on C-peptide secretion rate. However, the experimental conditions of such a protocol are very unphysiological. Thus data of 22 subjects studied with a mixed meal (database 2) were used to test the model performance in a more physiological condition. Database 3 consists of data of 10 healthy subjects studied twice with an OGTT and matched intravenous glucose challenge (I-IVG) and was used for model validation purpose.

Eight different models of increasing complexity were developed. All the models are based on the C-peptide model which is based on the common assumption that insulin secretion is made up of a basal component, a dynamic component, proportional to glucose rate of change through the dynamic responsivity index, Φ_d (10^{-9}), and a static index, proportional to glucose through the static responsivity, Φ_s (10^{-9} min^{-1}) [9]. The first set of models were developed taking into account the experimental condition of database 1, which is characterized by a plasma glucose maintained almost constant around a concentration of 150 mg/dl with an intravenous infusion when GLP-1 is infused intravenously, thus resulting in a

negligible dynamic insulin secretion. Therefore four different models (*Model 1, Model 2, Model 3* and *Model 4*) were developed assuming different description of GLP-1 action on static β-cells sensitivity index to glucose Φ_s. However several study which investigated the incretin effect on insulin secretion reported that the presence of GLP-1 could enhance both dynamic and static insulin secretion [1], [2], [11], [19], [26], [32], [37], [39], [42], [47], while it has no effect on basal secretion. Thus, in light of applicability of the model to different protocols designs, four models (*Model 5, Model 6, Model 7* and *Model 8*) were developed by incorporating these assumptions, hence the models assume that GLP-1 concentration enhances both dynamic and static β-cells responsivity indexes. In addition one of the advantages of *Models 5-8* is that models equations can be reformulated so that GLP-1 acts directly on the over-basal insulin secretion; in fact, describing GLP-1 secretagogue action on Φ_d and Φ_s is equivalent to assume that GLP-1 modulates the over-basal insulin secretion rate.

All the models provided a direct measure of the ability of GLP-1 to promote over-basal insulin secretion, the potentiation index Π (% per pmol/l), defined as the ratio between the average percent increase in over-basal insulin secretion and average plasma GLP-1 concentration.

All the developed models fit the data well, as confirmed by the run test, which supported randomness of residuals in 70% of the subjects. As expected, increasing the complexity of the models, worsens the precision of parameter estimates. Model selection was tackled by comparing the developed models on the basis of the following criteria: ability to describe the data (Weighted Residual Square Sum, WRSS), precision of parameter estimates (expressed as CV), model parsimony (Akaike Information Criterion, AIC) and residual independence (Anderson run test); moreover, since more complex models collapsed into simpler models when one or more parameters were estimated to be $\cong 0$, an additional criteria is the percentage of identifications for which all parameters are nonzero.

Model 6 results the most parsimonious, in fact, it better fit C-peptide data of database 1 and provided precise parameter estimates in the largest number of subjects. It also provides a potentiation index, $\Pi = 12.6 \pm 0.7$ % per pmol/l; thus,

during hyperglycemic conditions (~150mg/dl), an increase of 5 pmol/l in peripheral GLP-1 concentrations, similar to that occurring after a meal, is predicted to induce a 63% increase in glucose-stimulated insulin secretion. This finding is comparable with the results reported in [11] for an OGTT, although the levels of GLP-1were not reported.

As observed in Chapter 6, model selection criteria would have indicated *Model 8* as the most parsimonious one. However, *Model 8* reduces to *Model 7* in 11 subjects, since parameter b was zero, to *Model 6* in 43 subjects, since parameter d was very high, and to *Model 5* in 17 subjects, since both changes in parameters b and d occurred. One can thus speculate that *Model 8* is the most general model which is able to predict the C-peptide concentration, in very challenging conditions, such as during a hyperglycemic clamp with GLP-1 at physiological and supra-physiological concentration, while in most subjects or different experimental conditions, e.g. during a meal, a simpler model (but derived from *Model 8*) may be sufficient, e.g. Model 6 is a better candidate when plasma GLP-1 excursions are smaller, and thus the use of a nonlinear model may be not necessary. Of note the potentiation index provided by *Model 6* is virtually identical to that obtained with *Model 8* ($\Pi = 12.6 \pm 0.7$ % vs $\Pi = 15.5 \pm 1.1$ % per pmol/l, R = 0.95, p < 0.001). This supports that, even though simpler, *Model 6* is robust enough to adequately quantify the action of GLP-1 on glucose-dependent insulin secretion.

However it would be important to estimate β-cells responsivity and potentiation indexes from an oral test, since it offers several advantages with respect to intravenous tests: it is physiological, easy to perform, and applicable to large scale genetic and epidemiologic study. Therefore, *Model 6* was tested on database 2 in which of 22 subjects underwent an oral glucose load. The simpler experimental condition resulted in slower dynamics of plasma C-peptide and glucose concentrations [9], if compared with the hyperglycemic clamp ones. Thus the derivative control of GLP-1 on insulin secretion could be neglected and consequently Model 6 collapses into *Model 5*.

The model well predicts plasma C-peptide concentration and provides precise estimates of the parameters. It also provides the potentiation index which results actually lower than that calculated in database 1 using *Model 6* (7.8 vs 12.6 % per pmol/l); such difference can be explained with the fact that the subjects who have taken part in the study of database 2 are IFG while those of database 1 are healthy. The model also allows to determine the time course of the incretin effect by calculating the difference between the glucose-dependent secretion rate at basal GLP-1 level (SR) and the enhanced insulin secretion due to the action of the over-basal GLP-1 (SR^{GLP-1}); maximum of potentiation is reached at 30 min with an increase of 60% of insulin secretion rate. Of interest is that the magnitude and time course of the incretin effect predicted by *Model 5* is similar to that previously reported by Campioni et al. in [11]. Moreover at variance with Campioni methodology, which requires data from both oral and matched-intravenous glucose tests to measure the incretin potentiation, *Model 5* provides a precise measure of the incretin effect using data from a single oral glucose test.

Results obtained from database 1 and database 2 are consistent with the definition of models as an approximation of reality. A model in fact, can only be good enough in relation to its intended purpose. Indeed to describe complex systems, it may be appropriate to have of a set of models, where each of them would be the best in relation to its intended use [13]. *Model 6* results the best performing model in hyperglycemic clamp with exogenous GLP-1 infusion data, whilst in more physiological experimental condition such as a meal, *Model 5* is the optimal model.

Finally, model validation is tackled by comparing ability of Model 5 to measure GLP-1 induced potentiation on insulin secretion from oral glucose test (OGTT) data against that measured with the gold standard technique proposed by Campioni et al. in [11] using OGTT and matched intravenous glucose (I-IVG) data. However, due to some problems occurred with the protocol procedure, I-IVG plasma glucose in some subjects is not well matched with the OGTT one. This affected the calculation of incretin potentiation with Campioni method. As a matter of fact, comparison performed using average data, whose OGTT and I-IVG

plasma glucose are well matched, provided encouraging results In this ideal condition model potentiation index Π and Campioni incretin potentiation index PI were virtually the same (Π = 6.55, CV = 65%; PI = 6.15 % per pmol/l). It is worth noting that also in those subjects with a well matched plasma glucose concentration the model was in general able to assess a potentiation index Π similar to those calculated with Campioni technique. However glucose mismatch is not the only confounding effect. In fact other gut hormones, other than GLP-1, contribute to the incretin effect, in particular GIP, which is released simultaneously with GLP-1 and shown to have additive effect on insulin secretion [11]. PI estimated with the method proposed by Campioni reflects the action of all incretin hormones on insulin secretion, whilst potentiation index Π accounts only for GLP-1 action.

To overcome all these limitations, we used computer simulation to validate the model in a controlled scenario where, results are not affected by plasma glucose mismatching nor by incretin hormones other than GLP-1. In addition, simulation allowed to test model performance also for extremely high Π and consequently C-peptide concentration. The model was able to single out the effect of GLP-1 on insulin secretion and thus to correctly estimate Π in the 93 ± 1 % of the simulations. These results are encouraging but further studies, other than the in silico one, are needed to ultimately validate the model.

In conclusion in this study a model describing the mechanisms of GLP-1 action on insulin secretion was developed . It allows to measure the potentiation of insulin due to the hormone using data of a single oral glucose test. The model was applied successfully to different experimental protocols (hyperglycemic intravenous glucose with concomitant GLP-1 intravenous infusion, meal and OGTT) performed in healthy and impaired fasting glucose subjects, and in each case the model well describes the plasma C-peptide concentration and provides a precise estimate of model parameters. Validation of the model was performed both with real data and in silico simulations by comparing potentiation measured with the model against that calculated with the gold standard technique proposed by Campioni [11].

Moreover it is important to note that the model allows to measure the incretin potentiation specific of GLP-1, which despite playing a primary role in incretin effect, it is not the only hormone accountable for the enhancement of insulin secretion, since several other gut hormones contribute, such as GIP.

In conclusion the model is a valuable tool to measure insulin potentiation due to GLP-1 using data from an oral test, which thanks to its simplicity could be used in epidemiological and population studies, thus providing insights into the pathogenesis of diabetes and the efficacy of GLP-1 based therapies.

BIBLIOGRAPHY

[1]   Ahrén B, Holst JJ, Mari A. Characterization of GLP-1 effects on beta-cell function after meal ingestion in humans. Diabetes Care 26: 2860–2864, 2003.

[2]   Baggio LL, Drucker DJ. Biology of incretins: GLP-1 and GIP (Review).Gastroenterology 132: 2131–2157, 2007.

[3]   Ban K, Noyan-Ashraf MH, Hoefer J, Bolz SS, Drucker DJ, Husain M: Cardioprotective and vasodilatory actions of glucagon-like peptide 1 receptor are mediated through both glucagon-like peptide 1 receptor-dependent and -independent pathways. *Circulation* 117:2340-2350, 2008

[4]   Barrett PH, Bell BM, Cobelli C, Golde H, Schumitzky A, Vicini P, Foster DM. SAAM II: Simulation, Analysis, and Modeling Software for tracer and pharmacokinetic studies. Metabolism. Apr;47(4):484-92, 1998.

[5]   Bayliss WM, Starling EH: The mechanism of pancreatic secretion. *J Physiol* 28:325-353, 1902

[6]   Beinborn M, Worrall CI, McBride EW, Kopin AS. A human glucagon-like peptide-1 receptor polymorphism results in reduced agonist responsiveness. Regul Pept; 130:1–6, 2005.

[7]   Bell GI, Sanchez-Pescador R, Laybourn PJ, Najarian RC. Exon duplication and divergence in the human preproglucagon gene. Nature 304:368-371, 1983

[8]   Bock G, Dalla Man C, Micheletto F, Basu R, Giesler PD, Laugen J, Deacon CF, Holst JJ, Toffolo G, Cobelli C, Rizza RA, Vella A. The effect of DPP-4 inhibition with sitagliptin on incretin secretion and on fasting and postprandial glucose turnover in subjects with impaired fasting glucose. Clin Endocrinol (Oxf) 73:189-196, 2010.

[9]   Breda E, Cavaghan MK, Toffolo G, Polonsky KS, Cobelli C. Oral glucose tolerance test minimal model indexes of beta-cell function and insulin sensitivity. Diabetes 50: 150–158, 2001.

[10] Brubaker PL, Schloos J, Drucker DJ Regulation of glucagonlike peptide-1 synthesis and secretion in the GLUTag enteroendocrine cell line. Endocrinology 139:4108-4114, 1998.

[11] Campioni M, Toffolo G, Shuster LT, Service FJ, Rizza RA, Cobelli C. Incretin effect potentiates beta-cell responsivity to glucose as well as to its rate of change: OGTT and matched intravenous study. Am J Physiol Endocrinol Metab. 292:E54-60, 2007.

[12] Cobelli C, Foster D, Toffolo G. Tracer Kinetics in Biomedical Research: From Data to Model. Kluwer Academic/Plenum Publishers, New York, 2000.

[13] Cobelli C, Carson E: Introduction to Modelling in Physiology and Medicine. Academic Press, San Diego, 2008.

[14] Creutzfeldt W. The [pre-] history of the incretin concept. Regul Pept. Jun 15;128(2):87-91, 2005

[15] Dalla Man C, Bock G, Giesler PD, Serra DB, Ligueros Saylan M, Foley JE, Camilleri M, Toffolo G, Cobelli C, Rizza RA, Vella A. Dipeptidyl peptidase-4 inhibition by vildagliptin and the effect on insulin secretion and action in response to meal ingestion in type 2 diabetes. Diabetes Care. Jan;32(1):14-8, 2009.

[16] Dalla Man C, Micheletto F, Sathananthan A, Rizza R, Vella A, Cobelli C. A model of GLP-1 action on insulin secretion in nondiabetic subjetcs. Am J Physiol Endocrinol Metab, 298 1115-1121, 2010.

[17] De Nicolao G., Sparacino G., and Cobelli C. Nonparametric input estimation in physiological systems: problems, methods, and case studies. Automatica 33: 851-870, 1997.

[18] Drucker DJ, Mojsov S, Habener JF. Cell-specific post-translational processing of preproglucagon expressed from a metallothionine-glucagon fusion gene. J Biol Chem 261:9637-9643, 1986

[19] Drucker DJ. Therapeutic potential of dipeptidyl peptidase IV inhibitors for the treatment of type 2 diabetes. Expert Opin Investig Drugs 12: 87–100, 2003.

[20] Drucker DJ, Nauck MA. The incretin system: glucagon-like peptide-1 receptor agonists and dipeptidyl peptidase-4 inhibitors in type 2 diabetes. Lancet 368:1696-1705, 2006.

[21] Drucker DJ: The biology of incretin hormones. Cell Metab 3:153-165, 2006

[22] Eaton RP, Allen RC, Schade DS, et al: Prehepatic insulin production in man: Kinetic analysis using peripheral connecting peptide behavior. J Clin Endocrinol Metab 51:520-528, 1980.

[23] Efanova IB, Zaitsev SV, Zhivotovsky B, Kohler M, Efendic S, Orrenius S, Berggren PO: Glucose and tolbutamide induce apoptosis in pancreatic beta-

cells. A process dependent on intracellular Ca2+ concentration. J Biol Chem 273:33501-33507, 1998.

[24] Estall JL, Drucker DJ. Glucagon and glucagon-like peptide receptors as drug targets. Curr Pharm Des.; 12(14):1731-50, 2006.

[25] Ette EI, Williams PJ. Population pharmacokinetics II: estimation methods. Ann Pharmacother. Nov;38(11):1907-15, 2004.

[26] Farilla L, Bulotta A, Hirshberg B, Li Calzi S, Khoury N, Noushmehr H, Bertolotto C, Di Mario U, Harlan DM, Perfetti R. Glucagon-like peptide 1 inhibits cell apoptosis and improves glucose responsiveness of freshly isolated human islets. Endocrinology 144: 5149–5158, 2003.

[27] Ferrannini E, Cobelli C: The kinetics of insulin in man. II. Role of the liver. Diabetes Metab Rev 3:365-397, 1987.

[28] Flier JS. Clinical review 94: what's in a name? In search of leptin's physiologic role. J Clin Endocrinol Metab 83:1407-1413, 1998.

[29] Florez JC, Jablonski KA, Kahn SE, et al. Type 2 diabetes-associated missense polymorphisms KCNJ11 E23K and ABCC8 A1369S infl uence progression to diabetes and response to interventions in the Diabetes Prevention Program. Diabetes; 56 : 531 -6, 2007.

[30] Florez JC, Jablonski KA, Bayley N, et al. TCF7L2 polymorphisms and progression to diabetes in the Diabetes Prevention Program. N Engl J Med; 355 : 241 -50, 2006.

[31] Fritsche A, Stefan N, Hardt E, Haring H, Stumvoll M. Characterisation of beta-cell dysfunction of impaired glucose tolerance: evidence for impairment of incretin-induced insulin secretion. Diabetologia 43:852-858, 2000.

[32] Fujimoto W, Miki T, Ogura T, Zhang M, Seino Y, Satin LS, Nakaya H, Seino S. Niflumic acid-sensitive ion channels play an important role in the induction of glucose-stimulated insulin secretion by cyclic AMP in mice. Diabetologia 52: 863–872, 2009.

[33] Gloyn AL, Hashim Y, Ashcroft SJ, et al. Association studies of variants in promoter and coding regions of beta-cell ATPsensitive K-channel genes SUR1 and Kir6.2 with type 2 diabetes mellitus (UKPDS 53). Diabet Med; 18 : 206 -12, 2001.

[34] Gloyn AL, Weedon MN, Owen KR, et al. Large-scale association studies of variants in genes encoding the pancreatic beta-cell KATP channel subunits Kir6.2 (KCNJ11) and SUR1 (ABCC8) confi rm that the KCNJ11 E23K variant is associated with type 2 diabetes. Diabetes; 52 : 568 -72, 2003.

[35] Grant SF, Thorleifsson G, Reynisdottir I, et al. Variant of transcription factor 7-like 2(TCF7L2) gene confers risk of type 2 diabetes. Nat Genet; 38 : 320 -3, 2006.

[36] Grodsky G. A threshold distribution hypothesis for packet storage of insulin and its mathematical modeling. J Clin Invest 51: 2047–2059, 1972.

[37] Højberg PV, Zander M, Vilsbøll T, Knop FK, Krarup T, Vølund A, Holst JJ, Madsbad S. Near normalisation of blood glucose improves the potentiating effect of GLP-1 on glucose-induced insulin secretion in patients with type 2 diabetes. Diabetologia 51: 632–640, 2008.

[38] Hochberg Y, Benjamini Y. More powerful procedures for multiple significance testing. Stat Med; 9:811–818, 1990.

[39] Holst JJ, Toft-Nielsen MB, Orskov C, Nauck M, Willms B. On the effects of glucagon-like peptide-1 on blood glucose regulation in normal and diabetic subjects. Ann NY Acad Sci 805: 729–736, 1996.

[40] Holst JJ. The physiology of glucagon-like peptide 1. Physiol Rev. Oct;87(4):1409-39, 2007.

[41] Knudsen LB, Pridal L. Glucagon-like-peptide-1-(9-36)amide is a major metabolite of glucagon-like peptide-1-(7-36) amide after in vivo administration to dogs, and it acts as an antagonist on the pancreatic receptor. Eur J Pharmacol 318:429-435, 1996.

[42] Kwan EP, Gao X, Leung YM, Gaisano HY. Activation of exchange protein directly activated by cyclic adenosine monophosphate and protein kinase A regulate common and distinct steps in promoting plasma membrane exocytic and granule-to-granule fusions in rat islet beta cells. Pancreas 35: e45–e54, 2007.

[43] Layer P, Holst JJ, Grandt D, Goebell H. Ileal release of glucagon-like peptide-1 (GLP-1): association with inhibition of gastric acid secretion in humans. Dig Dis Sci 40:1074-1082, 1995.

[44] Licko V. Threshold secretory mechanism: a model of derivative element in biological control. Bull Math Biol 35: 51–58, 1973.

[45] Licinio-Paixao J, Polonsky KS, Given BD, et al: Ingestion of a mixed meal does not affect the metabolic clearance of biosynthetic human C-peptide. J Clin Endocrinol Metab 63:401-406, 1986.

[46] Lingohr MK, Buettner R, Rhodes CJ: Pancreatic beta-cell growth and survival--a role in obesity-linked type 2 diabetes? Trends Mol Med 8:375-384, 2002.

[47] Lindgren O, Mari A, Deacon CF, Carr RD, Winzell MS, Vikman J, Ahrén B. Differential islet and incretin hormone responses in morning versus afternoon after standardized meal in healthy men. J Clin Endocrinol Metab 94: 2887–2892, 2009.

[48] Lopez LC, Frazier ML, Su CJ, Kumar A, Saunders GF. Mammalian pancreatic preproglucagon contains three glucagon-related peptides. Proc Natl Acad Sci USA 80:5485-5489, 1983.

[49]   Lund PK, Goodman RH, Habener JF. Intestinal glucagons mRNAidentified by hybridization to a cloned islet cDNA encoding a precursor. Biochem Biophys Res Commun 100:1659-1666, 1981.

[50]   Lund PK, Goodman RH, Dee PC, Habener JF. Pancreatic preproglucagon cDNA contains two glucagon-related coding sequences arranged in tandem. Proc Natl Acad Sci USA 79:345-349, 1982.

[51]   Lund PK, Goodman RH, Montminy MR, Dee PC, Habener JF.Angler fish islet pre-proglucagon II. Nucleotide and corresponding amino acid sequence of the cDNA. J Biol Chem 258:3280-328, 1983.

[52]   Lyssenko V, Almgren P, Anevski D, et al. Genetic prediction of future type 2 diabetes. PLoS Med; 2 : e345, 2005.

[53]   Lyssenko V, Lupi R, Marchetti P, et al. Mechanisms by which common variants in the TCF7L2 gene increase risk of type 2 diabetes. J Clin Invest; 117 : 2155 -63, 2007.

[54]   Maida A, Lamont BJ, Cao X, Drucker DJ. Metformin regulates the incretin receptor axis via a pathway dependent on peroxisome proliferator-activated receptor-alpha in mice. Diabetologia 54:339-349, 2011.

[55]   Mari A, Schmitz O, Gastaldelli A, Oestergaard T, Nyholm B, Ferrannini E. Meal and oral glucose tests for assessment of beta -cell function: modeling analysis in normal subjects. Am J Physiol Endocrinol Metab. 283: E1159-66, 2002.

[56]   Møller JB, Jusko WJ, Gao W, Hansen T, Pedersen O, Holst JJ, Overgaard RV, Madsen H, Ingwersen SH. Mechanism-based population modelling for assessment of L-cell function based on total GLP-1 response following an oral glucose tolerance test. J Pharmacokinet Pharmacodyn. Dec;38(6):713-25. doi: 10.1007/s10928-011-9216-2, 2011.

[57]   Moore CX, Cooper GJ. Co-secretion of amylin and insulin from cultured islet beta-cells: modulation by nutrient secretagogues, islet hormones and hypoglycemic agents. Biochem Biophys Res Commun. Aug 30;179(1):1-9, 1991.

[58]   Mulholland DJ, Dedhar S, Coetzee GA, et al. Interaction of nuclear receptors with the Wnt/beta-catenin/Tcf signaling axis: Wnt you like to know? Endocr Rev; 26 : 898 -915, 2005.

[59]   Nauck MA, Heimestaat MM, Orskov C, Holst JJ, Ebert R, Creutzfeldt W. Preserved incretin activity of glucagon-like peptide 1 (7-36 amide), but not of synthetic human gastric inhibitory polypeptide in patients with type-2 diabetes mellitus. J Clin Invest 91:301-307, 1993.

[60]   Nauck MA, Niedereichholz U, Ettler R, Holst JJ, Ørskov C, Ritzel R, Schmiegel WH. Glucagon-like peptide 1 inhibition of gastric emptying

outweighs its insulinotropic effects in healthy humans. Am J Physiol 273:E981–E988, 1997.

[61] Nauck MA. Is glucagon-like peptide 1 an incretin hormone? Diabetologia 42:373-379, 1999.

[62] Nauck MA, Meier JJ. Glucagon-like peptide 1 and its derivatives in the treatment of diabetes. Regul Pept 128: 135–148, 2005.

[63] Pederson RA, White HA, Schlenzig D, Pauly RP, McIntosh CH, Demuth HU. Improved glucose tolerance in Zucker fatty rats by oral administration of the dipeptidyl peptidase IV inhibitor isoleucine thiazolidide. Diabetes 47:1253-1258, 1998.

[64] Pillonetto G, Sparacino G, Cobelli C. Reconstructing insulin secretion rate after a glucose stimulus by an improved stochastic deconvolution method. IEEE Trans Biomed Eng. Nov;48(11):1352-4, 2001.

[65] Polonsky KS, Licinio-Paizao J, Given BD, et al: Use of biosynthetic human C-peptide in the measurement of insulin secretion rates in normal volunteers and type I diabetic patients. J Clin Invest 77:98-105, 1986.

[66] Reimer RA, McBurney MI. Dietary fiber modulates intestinal proglucagon messenger ribonucleic acid and postprandial secretion of glucagon-like peptide-1 and insulin in rats. Endocrinology 137:3948-3956, 1996.

[67] Roberge JN, Brubaker PL. Secretion of proglucagon-derived peptides in response to intestinal luminal nutrients. Endocrinology 128:3169-3174, 1991

[68] Roberge JN, Brubaker PL. Regulation of intestinal proglucagon-derived peptide secretion by glucose-dependent insulinotropic peptide in a novel enteroendocrine loop. Endocrinology 133:233-240, 1993.

[69] Sathananthan A, Man CD, Micheletto F, Zinsmeister AR, Camilleri M, Giesler PD, Laugen JM, Toffolo G, Rizza RA, Cobelli C, Vella A. Common genetic variation in GLP1R and insulin secretion in response to exogenous GLP-1 in nondiabetic subjects: a pilot study. Diabetes Care. Sep;33(9):2074-6, 2010.

[70] Sathananthan A, Man CD, Zinsmeister AR, Camilleri M, Rodeheffer RJ, Toffolo G, Cobelli C, Rizza RA, Vella A. A concerted decline in insulin secretion and action occurs across the spectrum of fasting and postchallenge glucose concentrations. Clin Endocrinol (Oxf) 76:212-219, 2012.

[71] Schirra J, Katschinski M, Weidmann C, Scha¨fer T, Wank U, Arnold R, Go¨ke B. Gastric emptying and release of incretin hormones after glucose ingestion in humans. J Clin Invest 97:92-103, 1996.

[72] Schirra J, Leicht P, Hildebrand P, Beglinger C, Arnold R, Go¨ke B, Katschinski M. Mechanisms of the antidiabetic action of subcutaneous

glucagon-like peptide-1(7-36)amide in non-insulin dependent diabetes mellitus. J Endocrinol 156:177-186, 1998.

[73] Sesti G, Laratta E, Cardellini M, et al. The E23K variant of KCNJ11 encoding the pancreatic beta-cell adenosine 5 ′ -triphosphate-sensitive potassium channel subunit Kir6.2 is associated with an increased risk of secondary failure to sulfonylurea in patients with type 2 diabetes. J Clin Endocrinol Metab; 91 : 2334 -9, 2006.

[74] Schafer SA, Tschritter O, Machicao F, Thamer C, Stefan N, Gallwitz B, Holst JJ, Dekker JM, t Hart LM, Nijpels G, van Haeften TW, Haring HU, Fritsche A. Impaired glucagon-like peptide-1-induced insulin secretion in carriers of transcription factor 7-like 2 (TCF7L2) gene polymorphisms. Diabetologia 50:2443-2450, 2007.

[75] Shapiro ET, Tillil H, Rubenstein AH, et al: Peripheral insulin parallels changes in insulin secretion more closely than C-peptide after bolus intravenous glucose administration. J Clin Endocrinol Metab 67:1094-1099, 1988.

[76] Smushkin G, Sathananthan A, Dalla Man C, Zinsmeister AR, Camilleri M, Cobelli C, Rizza RA, Vella A. Defects in GLP-1 Response to an Oral Challenge Do Not Play a Significant Role in the Pathogenesis of Prediabetes. J Clin Endocrinol Metab 97:589-598, 2012.

[77] Sparacino G, Cobelli C. A stochastic deconvolution method to reconstruct insulin secretion rate after a glucose stimulus. IEEE Trans Biomed Eng. May;43(5):512-29, 1996.

[78] Steele, R., Bjerknes, C., Rathgeb, I. et al. Glucose uptake and production during the oral glucose tolerance test. Diabetes, 17, 415–421, 1968.

[79] Stoffel M, Espinoza R, LeBeau MM, Bell GI. Human glucagon-like peptide-1 receptor gene. Localization to chromosome 6p21 by fluorescence in situ hybridization and linkage of a highly polymorphic simple tandem repeatDNApolymorphism to other markers on chromosome 6. Diabetes 42:1215-1218, 1993.

[80] Stolerman ES, Florez JC. Genomics of type 2 diabetes mellitus: implications for the clinician. Nat Rev Endocrinol;5: 429–436, 2009.

[81] The DECODE Study Group, "Glucose tolerance and mortality: Comparison of WHO and American Diabetes Association diagnostic criteria," Lancet, vol. 354, pp. 617–621, 1999.

[82] Toffolo G, De Grandi F, and Cobelli C. Estimation of b-cell sensitivity from IVGTT C-peptide data. Knowledge of the kinetics avoids errors in modeling the secretion. Diabetes 44: 845–854, 1995.

[83] Toffolo G, Breda E, Cavaghan MK, Ehrmann DA, Polonsky KS, Cobelli C. Quantitative indexes of beta-cell function during graded up&down glucose

infusion from C-peptide minimal models. Am J Physiol Endocrinol Metab, 280: E2-E10, 2001.

[84] Toffolo G, Campioni M, Basu R, Rizza RA, Cobelli C. A minimal model of insulin secretion and kinetics to assess hepatic insulin extraction. Am J Physiol Endocrinol Metab 290: E169–E176, 2006.

[85] UK Prospective Diabetes Study (UKPDS) Group. Intensive blood-glucose control with sulphonylureas or insulin compared with conventional treatment and risk of complications in patients with type 2 diabetes (UKPDS 33).. Lancet 352:837-853, 1998.

[86] Van Cauter E, Mestrez F, Sturis J, and Polonsky KS. Estimation of insulin secretion rates from C-peptide levels. Comparison of individual and standard kinetic parameters for Cpeptide clearance. Diabetes 41: 368–377, 1992.

[87] Van De Waterbeemd H and Gifford E. ADMET In silico modelling: Towards prediction paradise? Nature Reviews: Drug Discovery, 2: 192-204, 2003.

[88] Vella A, Camilleri M. Pharmacogenetics: potential role in the treatment of diabetes and obesity. Expert Opin Pharmacother 9:1109-1119, 2008.

[89] Wei Y, Mojsov S. Tissue specific expression of the human receptor for glucagon-like peptide-1. Brain, heart and pancreatic forms have the same deduced amino acid sequences. FEBS Lett 358:219-224, 1995.

[90] Willms B, Werner J, Holst JJ, Ørskov C, Creutzfeld W, NauckMA. Gastric emptying, glucose responses and insulin secretion after a liquid test meal: effects of exogenous glucagon-like peptide-1 (GLP-1) (7-36)amide in type 2 (non-insulin-dependent) diabetic patients. J Clin Endocrinol Metab 81:327-332, 1996.

[91] Wolf G. Orexins: a newly discovered family of hypothalamic regulators of feed intake. Nutr Rev 56:172-173, 1998.

[92] www.diabetes.org

[93] www.easd.org

[94] www.idf.org

[95] Zimmet P, Alberti K G, and Shaw J, "Global and societal implications of the diabetes epidemic," Nature, vol. 414, pp. 782–787, 2001.